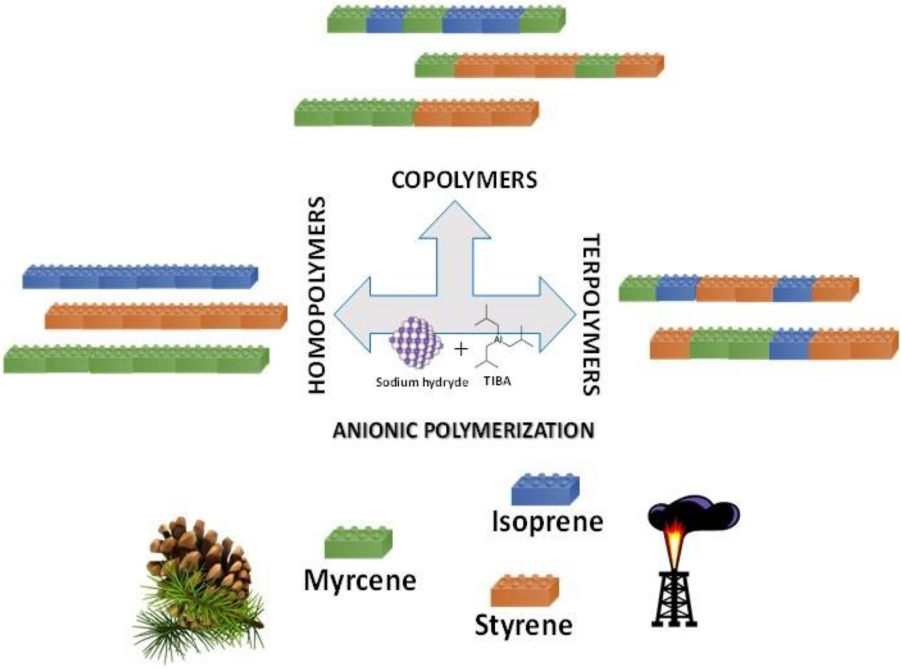

David Hermann Lamparelli, Magdalena Maria Kleybolte , Malte Winnacker and Carmine Capacchione

Sustainable myrcene-based elastomers via a convenient anionic polymerization

Sustainable myrcene-based elastomers via a convenient anionic polymerization

David Hermann Lamparelli[a], Magdalena Maria Kleybolte,[b] Malte Winnacker, *[b,c] and Carmine Capacchione *[b]

Abstract: Soluble heterocomplexes consisting of sodium hydride in combination with trialkylaluminum derivatives have been used as anionic initiating systems at 100 °C in toluene for convenient homo-, co- and ter-polymerization of myrcene with styrene and isoprene. In this way it has been possible to obtain elastomeric materials in a wide range of compositions with interesting thermal profiles and different polymeric architectures by simply modulating the alimentation feed and the [monomers]/[initiator systems] ratio. Especially, a complete study of the myrcene-styrene copolymers (PMS) was carried out, highlighting their tapered microstructures with high molecular weights (up to 159.8 KDa) and a single glass transition temperature. For PMS copolymer reactivity ratios, rmyr = 0.12 ± 0.003 and rsty =3.18 ± 0.65 and rmyr = 0.10 ± 0.004 and rsty = 3.32 ± 0.68 were determined according to the Kelen-Tudos (KT) and extended Kelen-Tudos (exKT) methods, respectively. Finally, this study showed an economic and alternative approach for the production of various elastomers by anionic copolymerization of renewable terpenes, such as myrcene, with commodities.

[a] Department of Chemistry and Biology "Adolfo Zambelli", University of Salerno, Giovanni Paolo II Str., 84084 Fisciano, Italy.
E-mail: ccapacchione@unisa.it
[b] WACKER-Chair of Macromolecular Chemistry, Technische Universität München Lichtenbergstraße 4 Str., 85747 Garching bei München, Germany.
[c] Catalysis Research Center (CRC) Ernst-Otto-Fischer-Straße 1, Garching bei München 85748, Germany.
E-mail: malte.winnacker@tum.de

Contents

1. Analysis of polymer compositions [1–6]

1.1 Determination of $M^{3,4}$ and $M^{1,4}$ contents in PM and PMS copolymers by ^1H NMR (TCE-d_2, 25 °C)

- $M^{3,4}(mol\%) = \frac{A_B}{A_A+\frac{A_B}{2}+A_C} \cdot 100$ **Equation E1**

Where: A_A is the area of the signals $\mathbf{M}^{1,4}{}_3$, $\mathbf{M}^{1,4}{}_7$, $\mathbf{M}^{1,2}{}_7$ and $\mathbf{M}^{3,4}{}_7$ (δ = 5.12 ppm); A_B is the area of the signal $\mathbf{M}^{3,4}{}_1$ (δ = 4.77 ppm); A_C is the area of the signal $\mathbf{M}^{1,2}{}_3$ (δ = 5.63 ppm);

- $M^{1,4}(mol\%) = \frac{A_A-(\frac{A_B}{2}+A_C)}{A_A+\frac{A_B}{2}+A_C} \cdot 100$ **Equations E2**

- $M^{1,2}(mol\%) = 100 - (M^{3,4}(mol\%) + M^{1,4}(mol\%))$

1.2 Determination of M and S contents in PSM copolymers by ^1H NMR (TCE-d_2, 25 °C)

- $M(mol\%) = \frac{\frac{1}{2}\cdot(A_A+\frac{A_B}{2})}{\frac{1}{2}\left(A_A+\frac{A_B}{2}\right)+\frac{A_C}{5}} \cdot 100$ **Equation E3**

Where: A_A is the area of the signals $\mathbf{M}^{1,4}{}_3$, $\mathbf{M}^{1,4}{}_7$ and $\mathbf{M}^{3,4}{}_7$ (δ=5.12 ppm); A_B is the area of the signal $\mathbf{M}^{3,4}{}_1$ (δ=4.77 ppm); A_C is the area of the signals S_4, S_5 and S_6 (δ=6.45-7.45 ppm)

- $S\ (mol\%) = 100 - M(mol\%)$ **Equation E4**

1.3 Determination of $I^{3,4}$, $I^{1,4}$ and $I^{1,2}$ contents in PI by ^1H NMR ($CDCl_3$ or TCE-$d2$, 25 °C)

- $I^{3,4}(mol\%) = \frac{\frac{B_A}{2}}{\frac{B_A}{2}+(B_B-2B_C)+B_c} \cdot 100$ **Equation E5**

Where: B_A is the area of the signals $\mathbf{I}^{3,4}{}_1$ (δ = 4.60-4.80 ppm); B_B is the area of the signal $\mathbf{I}^{1,2}{}_4$ and $\mathbf{I}^{1,4(cis+trans)}{}_3$ (δ = 4.80-5.40 ppm) and B_C is the area of the signal $I^{1,2}{}_3$ (δ = 5.75-5.90 ppm)

- $I^{1,4}(mol\%) = \frac{(B_B-2B_C)}{\frac{B_A}{2}+(B_B-2B_C)+B_c} \cdot 100$ **Equation E6**

- $I^{1,2}(mol\%) = 100 - I^{3,4}(mol\%) - I^{1,4}(mol\%)$ **Equation E7**

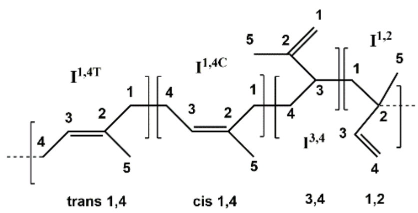

1.4 Determination of $I^{1,4\ cis}$ and $I^{1,4\ trans}$ contents in PI by ^{13}C NMR ($CDCl_3$, 25 °C)

- $I^{1,4}\ cis\ (mol\%) = \frac{C_A}{C_A+C_B} \cdot 100$ **Equation E8**

Where: C_A is the area of the signal $\mathbf{I}^{1,4\ CIS}{}_5$ (δ=23.5 ppm); C_B is the area of the signal $\mathbf{I}^{1,4\ TRANS}{}_5$ (δ=16.3 ppm)

- $I^{1,4}\ trans\ (mol\%) = 100 - I^{1,4}\ cis\ (mol\%)$ **Equation E9**

1.5 Determination of M and I contents in PMI copolymers by ^{13}C NMR ($CDCl_3$, 25 °C)

- $M(mol\%) = \frac{C_A}{C_A+C_B+C_C} \cdot 100$ **Equation E10**

where: C_A is the sum of the areas related to the signals $\mathbf{M}^{1,4\ (cis+trans)}{}_2$ (δ=139.3 ppm) and $\mathbf{M}^{3,4}{}_{2'}$ (δ=151.6 ppm); C_B is the area of the signals $\mathbf{I}^{3,4}{}_1$ and $\mathbf{I}^{1,2}{}_4$ (δ=111.4 ppm); C_c is the area of the signals $\mathbf{I}^{1,4}{}_2$ (δ=135.6 ppm)

- $I(mol\%) = 100 - M(mol\%)$ **Equation E11**

1.6 Determination of $M^{3,4}$ and $M^{1,4}$ contents in PMI copolymers by ^{13}C NMR ($CDCl_3$, 25 °C)

- $M^{3,4}(mol\%) = \frac{C_D}{C_A} \cdot 100$ **Equation E12**

where: C_A is the sum of the areas related to the signals $\mathbf{M}^{1,4\ (cis+trans)}{}_2$ (δ=139.3 ppm) and $M^{3,4}{}_{2'}$ (δ=151.6 ppm); C_D is the area of the signals $\mathbf{M}^{3,4}{}_{2'}$ (δ=151.6 ppm)

- $M^{1,4}(mol\%) = 100 - M^{3,4}(mol\%)$ **Equation S13**

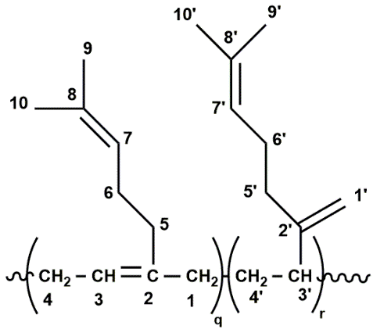

1.5 Determination of M and I contents in PMI copolymers by ^{13}C NMR (TCE-*d*2, 25 °C)

- $M(mol\%) = \frac{C_A}{C_A+C_B+C_C+C_E} \cdot 100$ **Equation E14**

where: C_A is the sum of the areas related to the signals $\mathbf{M}^{1,4\ (cis+trans)}{}_2$ (δ=139.3 ppm) and $\mathbf{M}^{3,4}{}_{2'}$ (δ=151.6 ppm); C_B is the area of the signals $\mathbf{I}^{3,4}{}_1$ and $\mathbf{I}^{1,2}{}_4$ (δ=111.4 ppm); C_c is the area of the signals $\mathbf{I}^{1,4}{}_2$ (δ=135.6 ppm); C_E is the area of the signals $\mathbf{S}_{3''}$ (δ=145.5 ppm) (see **Fig. S6**)

- $I(mol\%) = \frac{C_B+C_C}{C_A+C_B+C_C+C_E} \cdot 100$ **Equation E15**

- $S(mol\%) = \frac{C_E}{C_A+C_B+C_C+C_E} \cdot 100$ **Equation E16**

2 Determination of Reactivity Ratios

2.1 Fineman-Ross method

Fineman-Ross equation: **[(f-1)/ f]F) = r_1 - r_2 F^2/ f**

where: f = myrcene/styrene molar ratios in the polymer (by ^1H NMR analysis)

F = myrcene/styrene molar ratios in the feed

r_1, r_2 = reactivity ratios

Table T1. Copolymerization of M and S with i-Bu_3Al/NaH.

Run [a]	Feed composition		Yield	Copolymer composition		M/S (molar ratio)		F^2/f	(f-1/f)F
	M (*mol*)	S (*mol*)	%	M (*mol%*)	S (*mol%*)	in feed (F)	in copolymer (f)		
1	0.42	0,42	9.1	21	79	1,00	0,26	3,76	-2,76
2	0.42	0,13	8,4	42	58	3,24	0,72	14,47	-1,23
3	0.42	0,11	9,5	45	55	3,81	0,82	17,72	-0,85
4	0.42	0,07	6,8	49	51	5,99	0,96	37,38	0,24
5	0.42	0,04	8,6	66	34	10,5	1,94	56,73	5,09

[a] Reaction conditions: 88 µL, toluene 0.5 mL, tetrahydrofuran 25 µL, 100 °C, 30 min.

Table T2. Reactivity ratio for copolymerization of M and S.

Iniziator	r_1	r_2	$r_1 \bullet r_1$
i-Bu_3Al/NaH	0.13 ± 0.002	3.47 ± 0.91	0.45

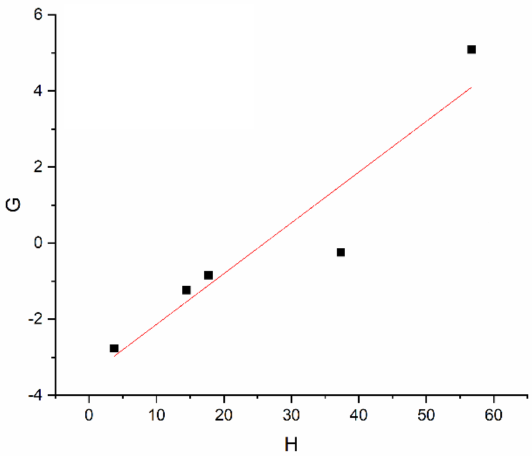

Figure A1. Fineman-Ross plot for copolymerization of myrcene and styrene with i-Bu3Al/NaH as initiating system at 100 °C in toluene and in the presence of THF (F = [Myr]/[Sty] in feed, f = [Myr]/[Sty] in copolymers, r_{Myr} = 0.13 ± 0.002 and r_{Sty} = 3.47 ± 0.91).

2.2 Kelen-Tudos method

The reactivity ratio can also be estimated with Kelen-Tudos equation (**$\eta = (r_1+r_2/\alpha)\xi - r_2/\alpha$**) which variables are expressed as:

G = (f-1/f)F
H = F^2/f
$\eta = G/(\alpha+H)$

$\xi = H/(\alpha+H)$

Where η and ξ are the functions of the parameters G and H, and α is a constant equal to $(H_{max} \times H_{min})^{1/2}$, H_{max} and H_{min} being the lowest and highest H values, respectively.
The intercepts at ξ = 0 and ξ = 1 of the η versus ξ plot gives $-r_1/\alpha$ and r_2

Table T3. FR and KT parameters for PMS copolymers

Sample	$F = M_1/M_2$	$f = m_1/m_2$	H	G	ξ	η
RR1	1,00	0,26	3,76	-2,76	0,20	-0,150
RR2	3,24	0,72	14,4	-1,23	0,50	-0,042
RR3	3,81	0,82	17,7	-0,85	0,55	-0,026
RR4	5,99	0,96	37,4	-0,24	0,72	-0,004
RR5	10,4	1,94	56,7	5,09	0,80	0,071

$\alpha = (H_{min} \times H_{max})^{1/2} = 14,60$.

Table T4. Reactivity ratio for copolymerization of M and S.

Iniziator	r_1	r_2	$r_1 \bullet r_1$
$i\text{-}Bu_3Al/NaH$	0.12 ± 0.003	3.18 ± 0.65	0.38

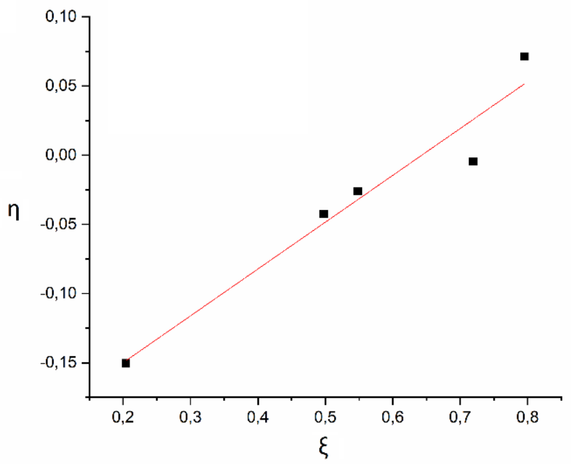

Figure A2. Determination of reactivity ratios using Kelen-Tudos method for PMS copolymers (r_{Myr} = 0.12 ± 0.003 and r_{Sty} = 3.18 ± 0.65).

2.3 Extended Kelen-Tudos method

$Z = \log(1 - S_1)/\log(1 - S_2)$ where S_1 and S_2 are the partial molar conversions:

$S_2 = w(\mu + F)/(\mu + f) \times 100$, w = percentage of conversions, $\mu = M_{wt\ 2}/M_{wt\ 1}$

$S_1 = S_2 f/F$;

They derived an expression, H = F2 / f and G = F (f – 1) / f In this method also, r2 and r1 can be readily obtained either graphically or computation using the least square methods by plotting 1 versus 0. The 1 versus 0 plot gives a straight line between 0 and 1 provided the system can be adequately described by the conventional copolymerization composition equation.

Table T5. exKT parameters for PMS copolymers

Sample	S_1	S_2	Z	H	G	ξ	η
RR1	0,041	0,155	0,249	4,26	-2,93	0,186	-0,129
RR2	0,050	0,225	0,202	17,6	-1,36	0,486	-0,038
RR3	0,059	0,274	0,189	22,8	-0,95	0,550	-0,023
RR4	0,043	0,266	0,140	48,4	-0,28	0,722	-0,004
RR5	0,066	0,358	0,154	81,2	6,09	0,814	0,061

$\alpha = (H_{min} \times H_{max})^{1/2} = 18,60$, $\mu = 0,765$.

Table T6. Reactivity ratio for copolymerization of M and S.

Iniziator	r_1	r_2	$r_1 \bullet r_1$
i-Bu_3Al/NaH	0.10 ± 0.004	3.32 ± 0.68	0.33

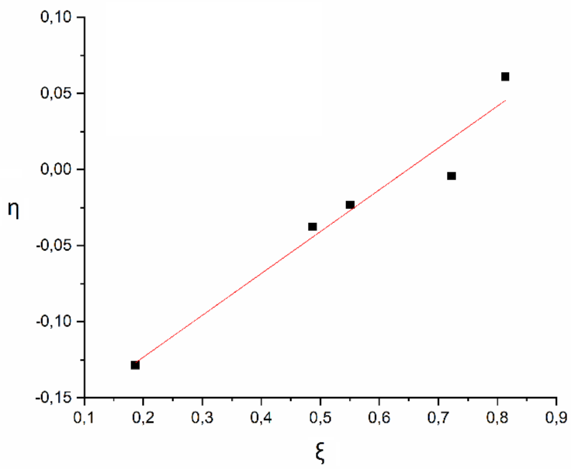

Figure A3. Determination of reactivity ratios using extended Kelen-Tudos method for PMS copolymers (r_{Myr} = 0.10 ± 0.004 and r_{Sty} = 3.32 ± 0.68).

3. NMR Characterizations

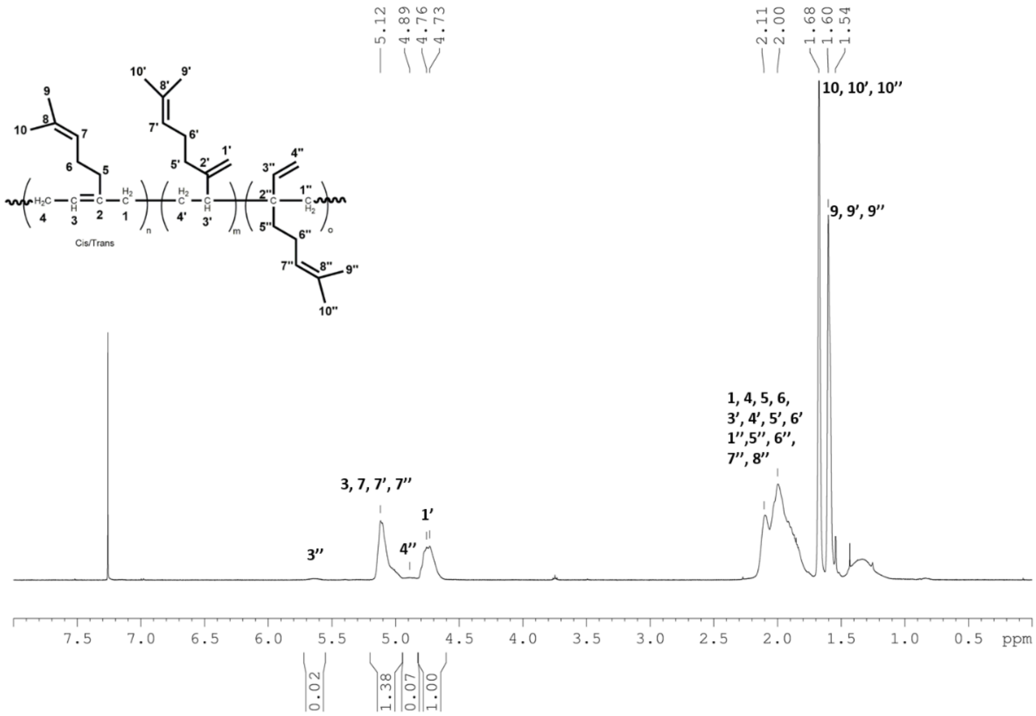

Figure S1. ^{1}H NMR spectrum ($CDCl_3$, 25 °C, 400 MHz) of PM from run 1 of **Table 1**

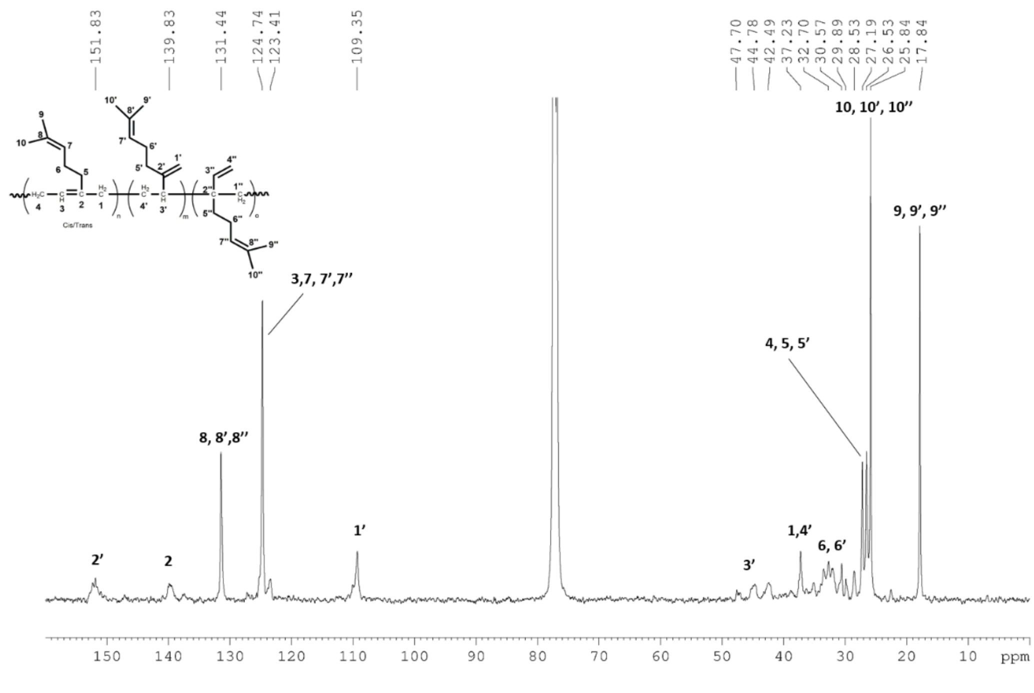

Figure S2. ^{13}C NMR spectrum ($CDCl_3$, 25 °C, 400 MHz) of PM from run 1 of **Table 1**

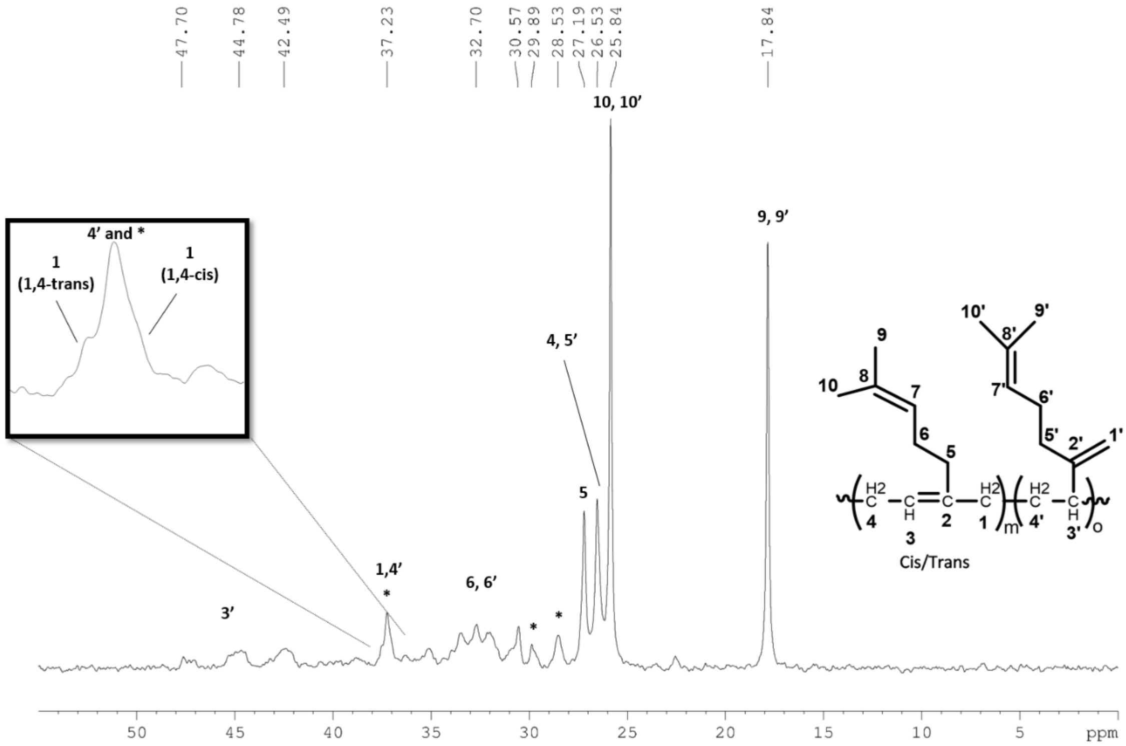

Figure S3. Enlargement of aliphatic region of ^{13}C NMR spectrum ($CDCl_3$, 25 °C, 400 MHz) of PM from run 1 of **Table 1**

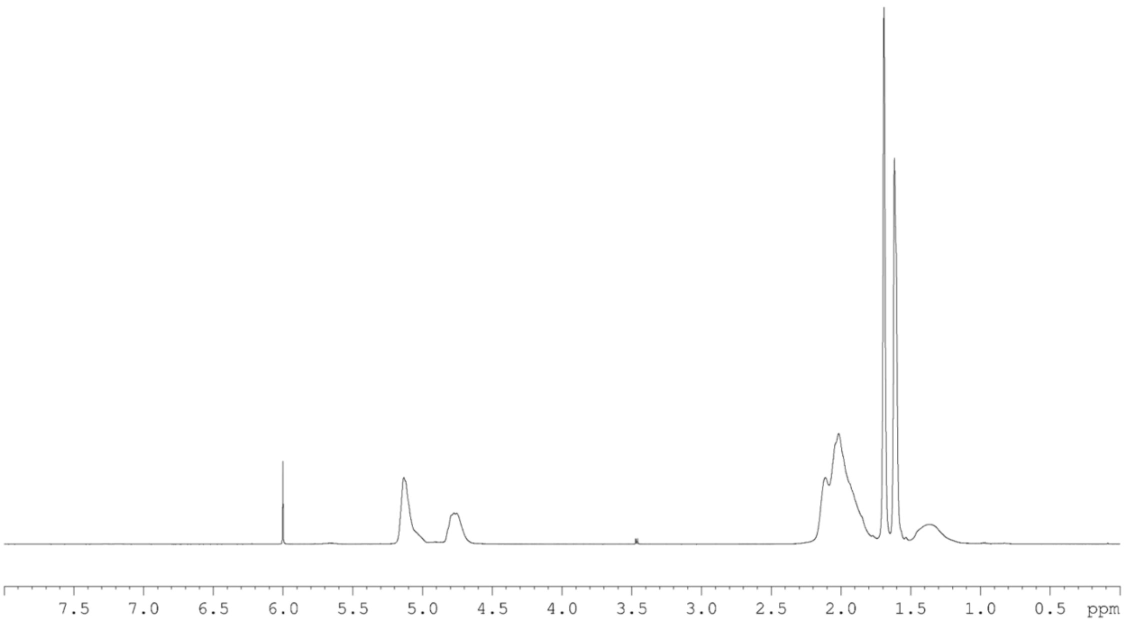

Figure S4. ^{1}H NMR spectrum (TCDE, 25 °C, 400 MHz) of PM from run 4 of **Table 1**

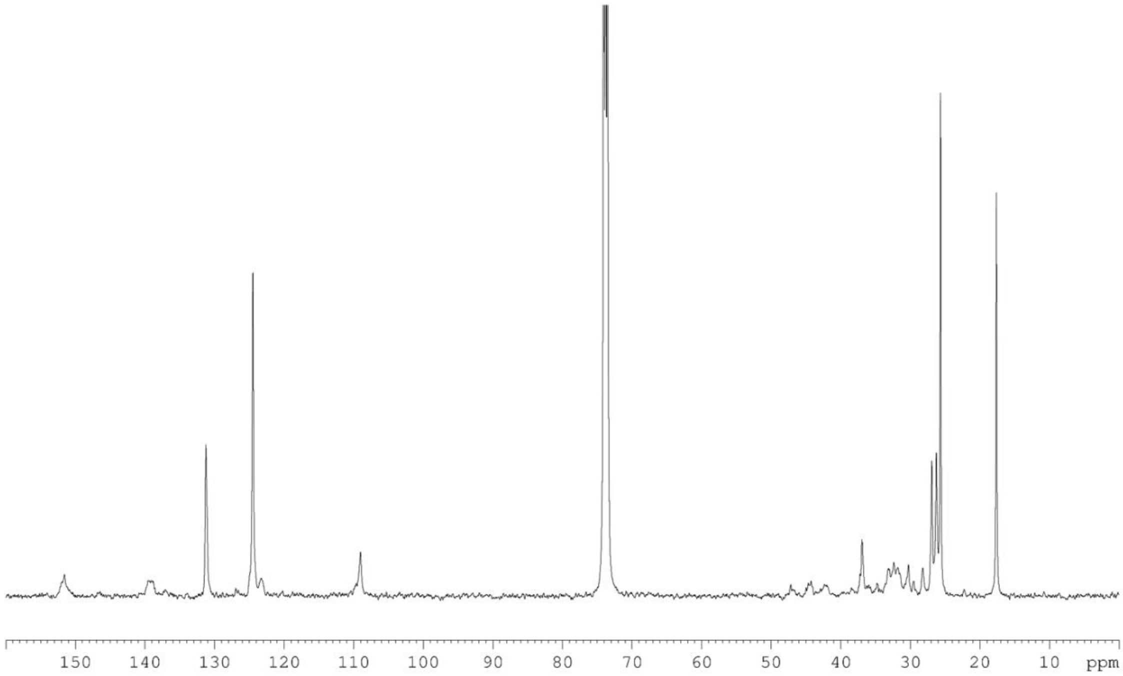

Figure S5. ^{13}C NMR spectrum (TCDE, 25 °C, 400 MHz) of PM from run 4 of **Table 1**

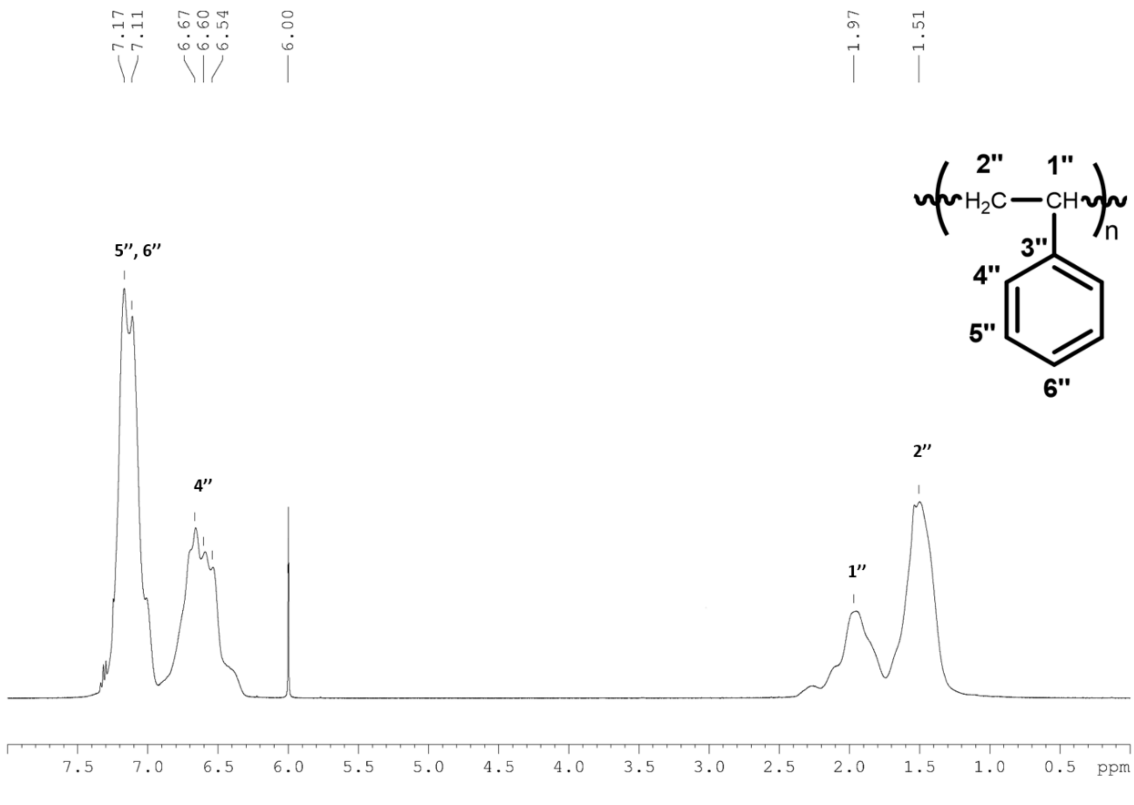

Figure S6. ^{1}H NMR spectrum (TCDE, 25 °C, 400 MHz) of PS from run 5 of **Table 1**

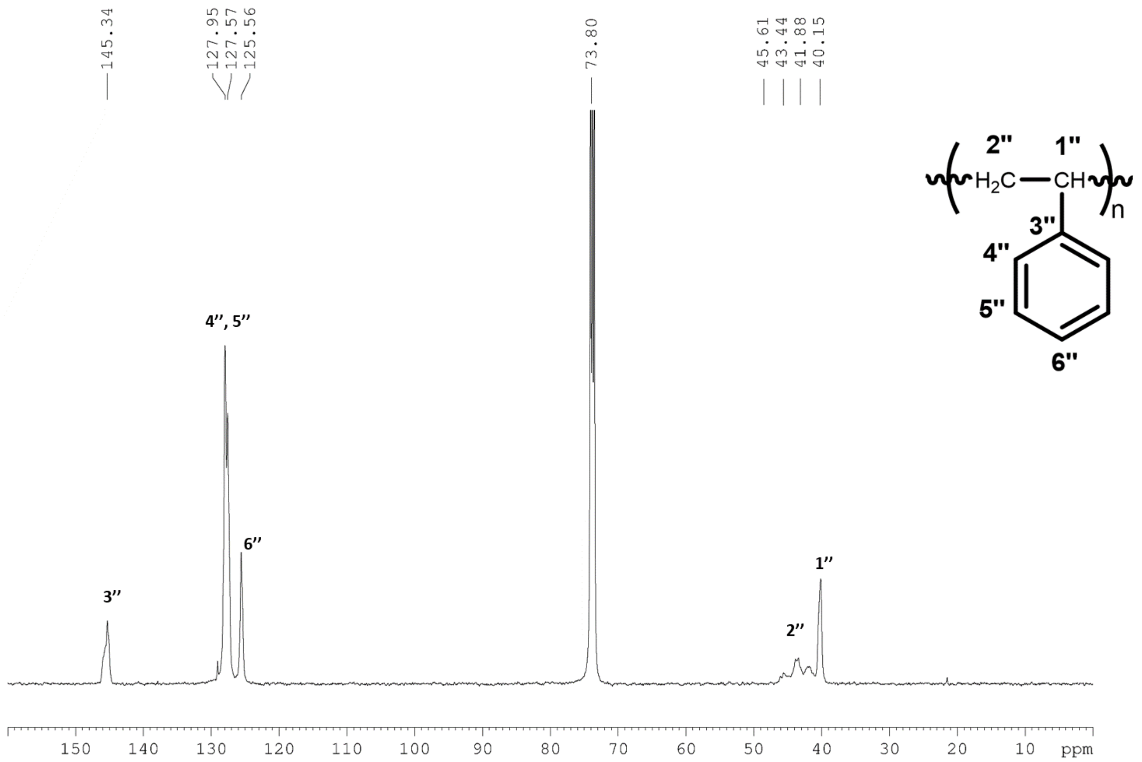

Figure S7. ^{13}C NMR spectrum (TCDE, 25 °C, 400 MHz) of PS from run 5 of **Table 1**

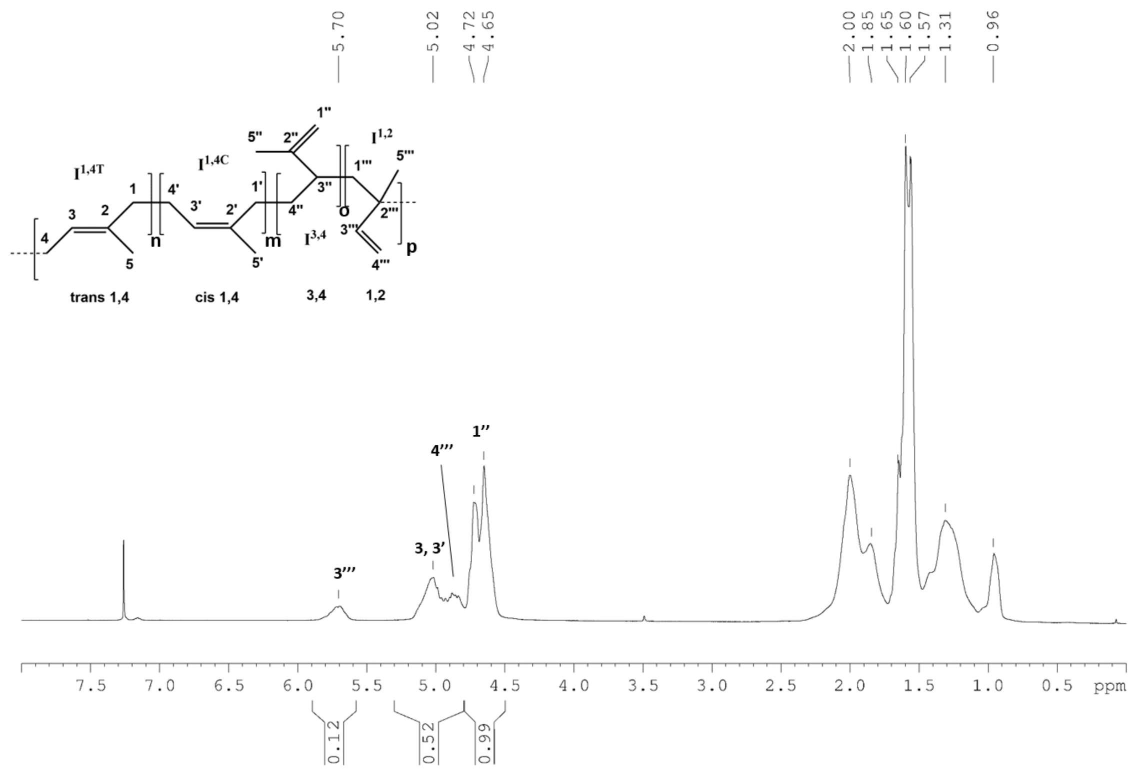

Figure S8. ^{1}H NMR spectrum (TCDE, 25 °C, 400 MHz) of PI from run 7 of **Table 1**

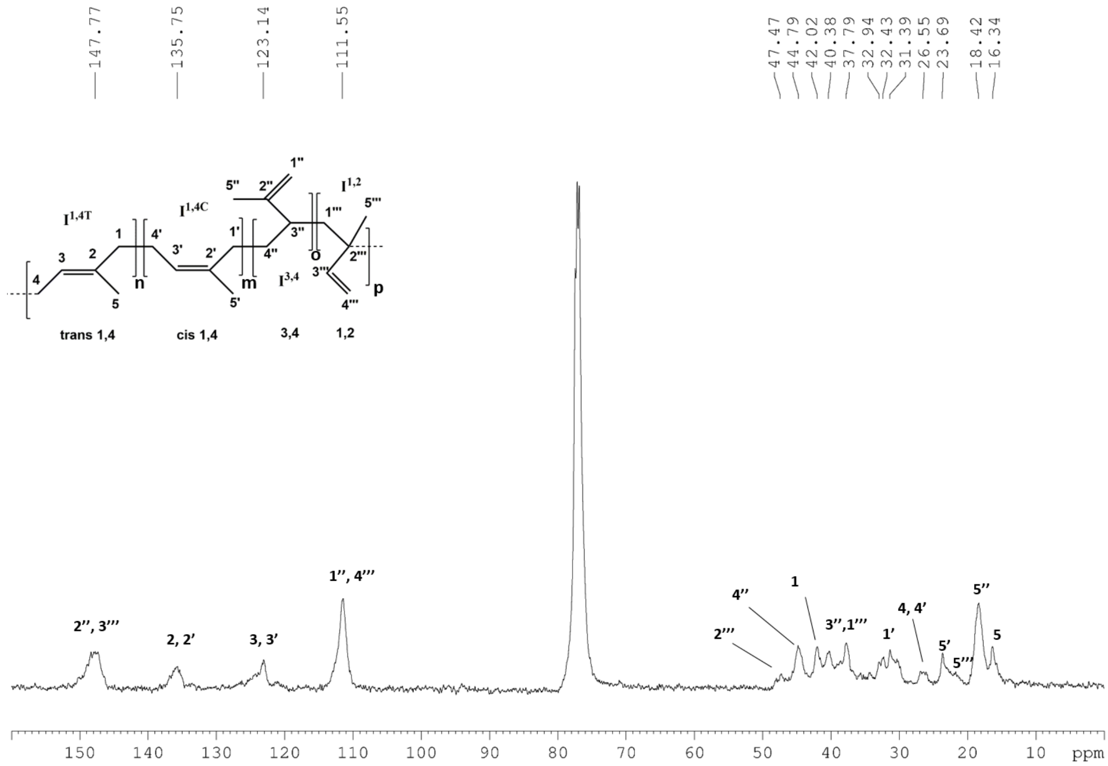

Figure S9. ^{13}C NMR spectrum (TCDE, 25 °C, 400 MHz) of PI from run 7 of **Table 1**

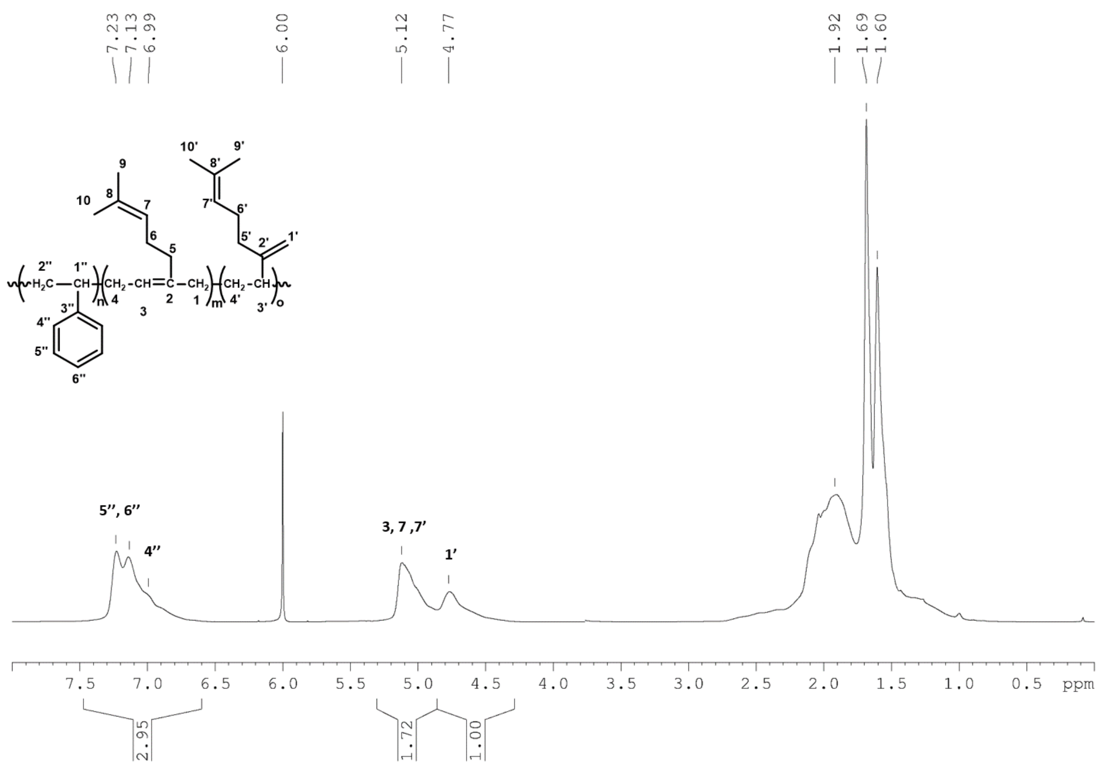

Figure S10. ^{1}H NMR spectrum (TCDE, 25 °C, 400 MHz) of PMS from run 12 of **Table 2**

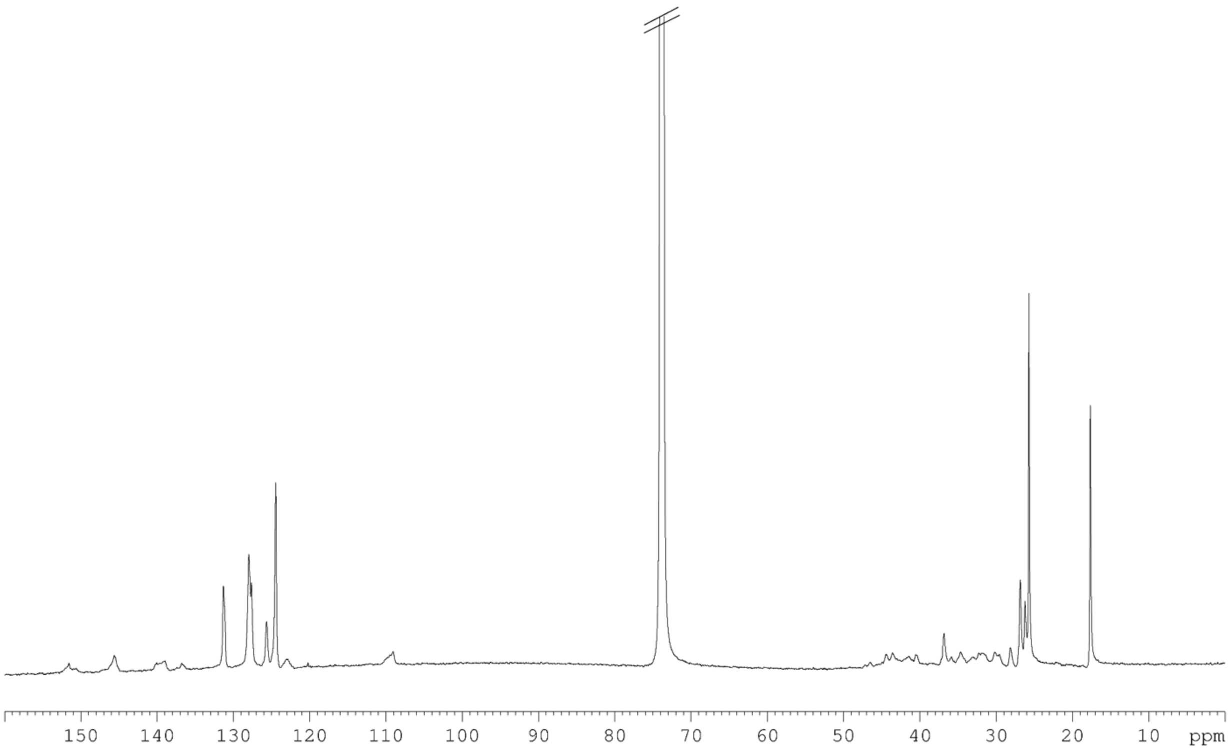

Figure S11. ^{13}C NMR spectrum (TCDE, 25 °C, 400 MHz) of PMS from run 12 of **Table 2**

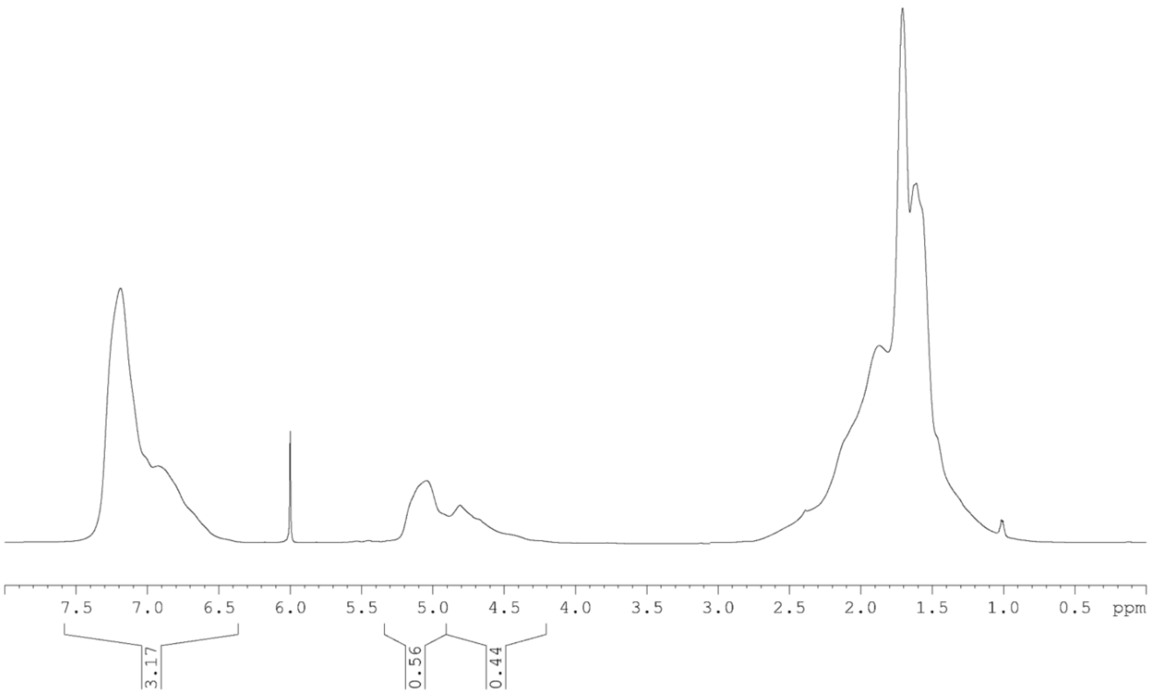

Figure S12. ^{1}H NMR spectrum (TCDE, 25 °C, 400 MHz) of PMS from run 13 of **Table 2**

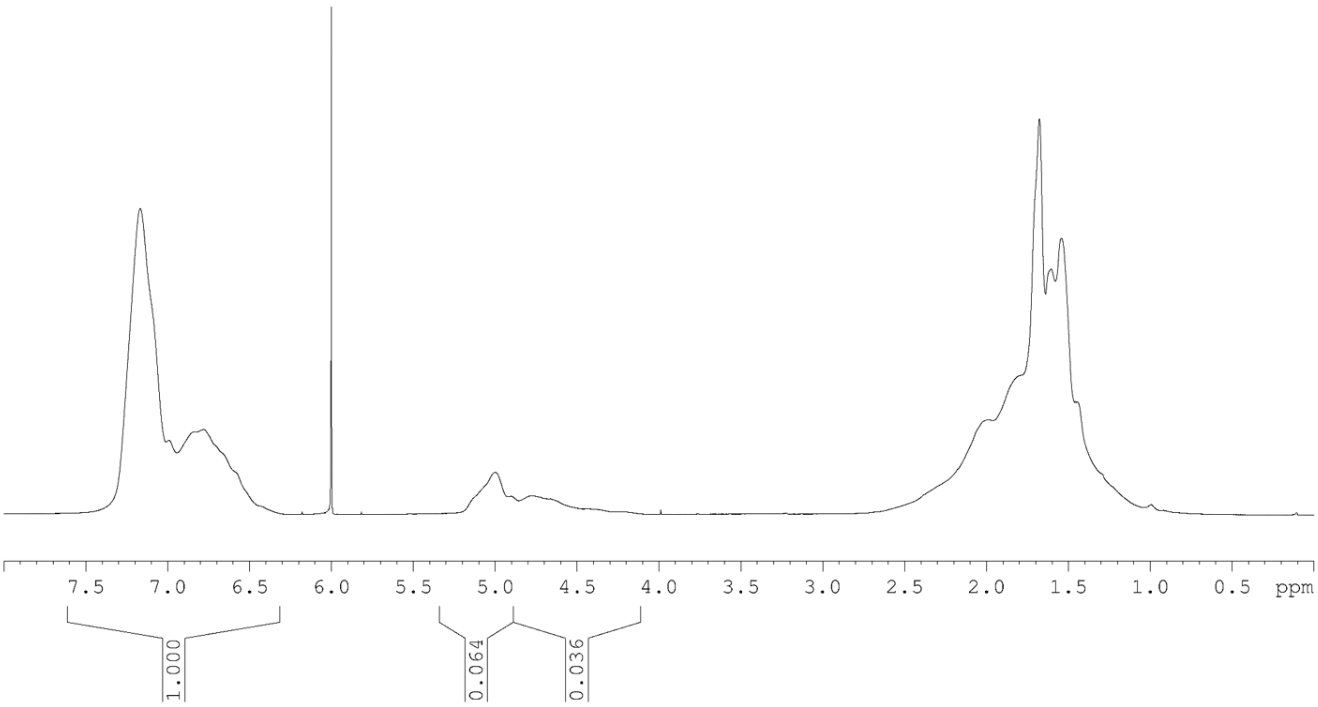

Figure S13. ^{1}H NMR spectrum (TCDE, 25 °C, 400 MHz) of PMS from run 14 of **Table 2**

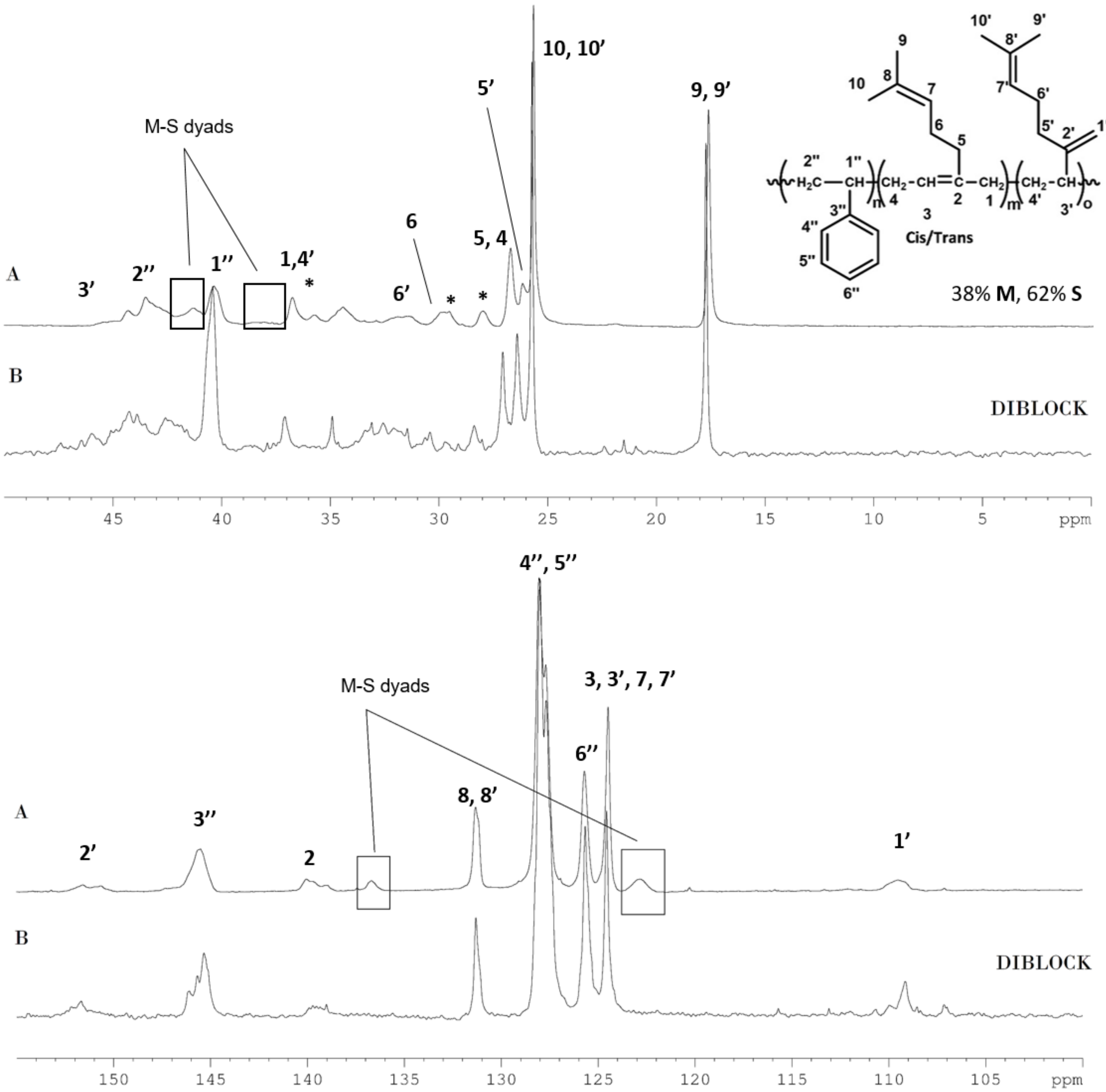

Figure S14. ^{13}C NMR spectra (TCDE, 25 °C, 400 MHz) of PMS copolymer from run 13 (a) and PMS diblock from run 21 (b) of **Table 2**

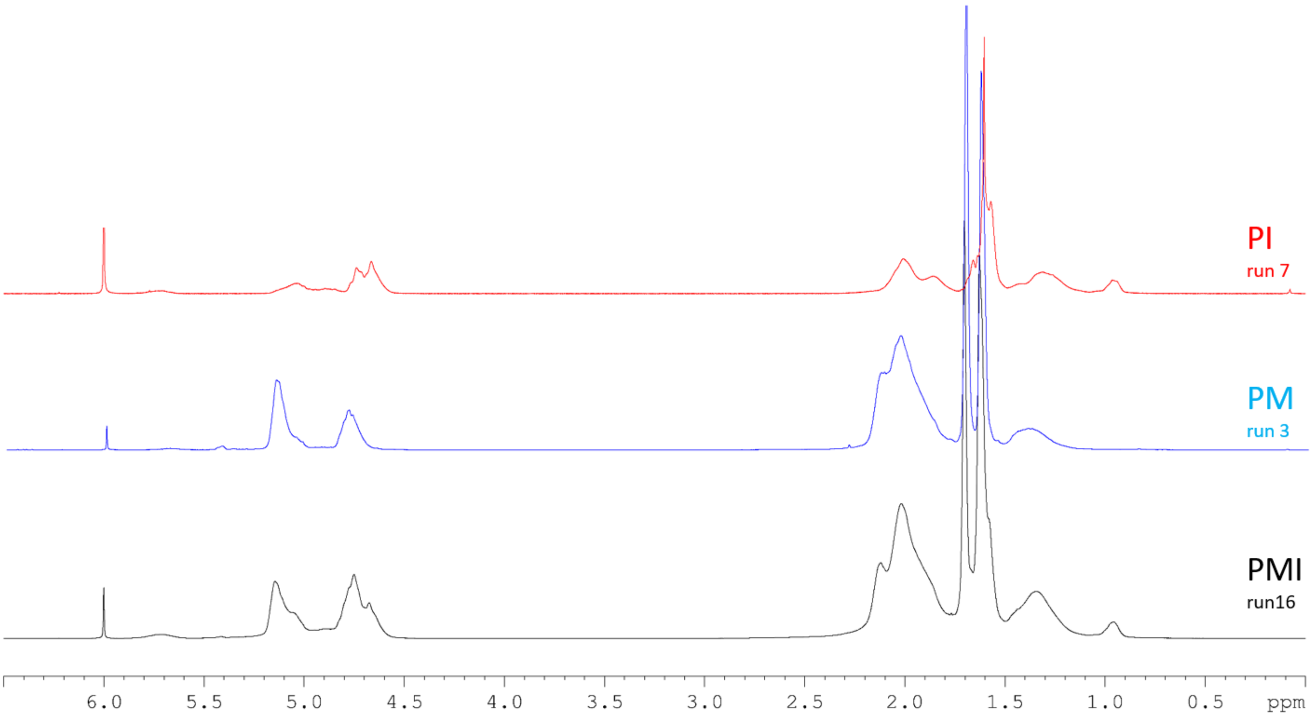

Figure S15. ^{1}H NMR spectra (TCDE, 25 °C, 400 MHz) of PM (run 3), PI (run 7) and PMI (run 16) from **Table 2**

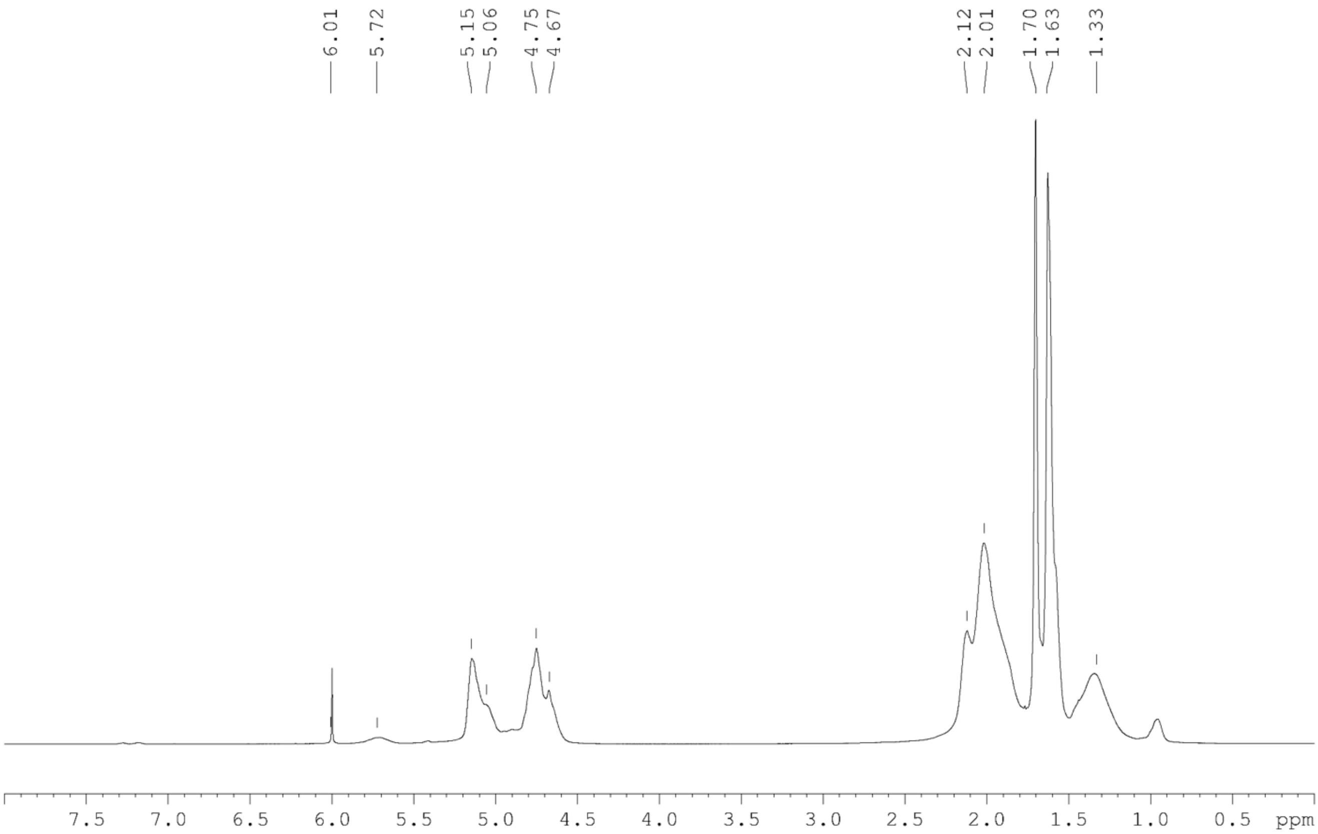

Figure S16. ^{1}H NMR spectrum (TCDE, 25 °C, 400 MHz) of PMI from run 16 of **Table 2**

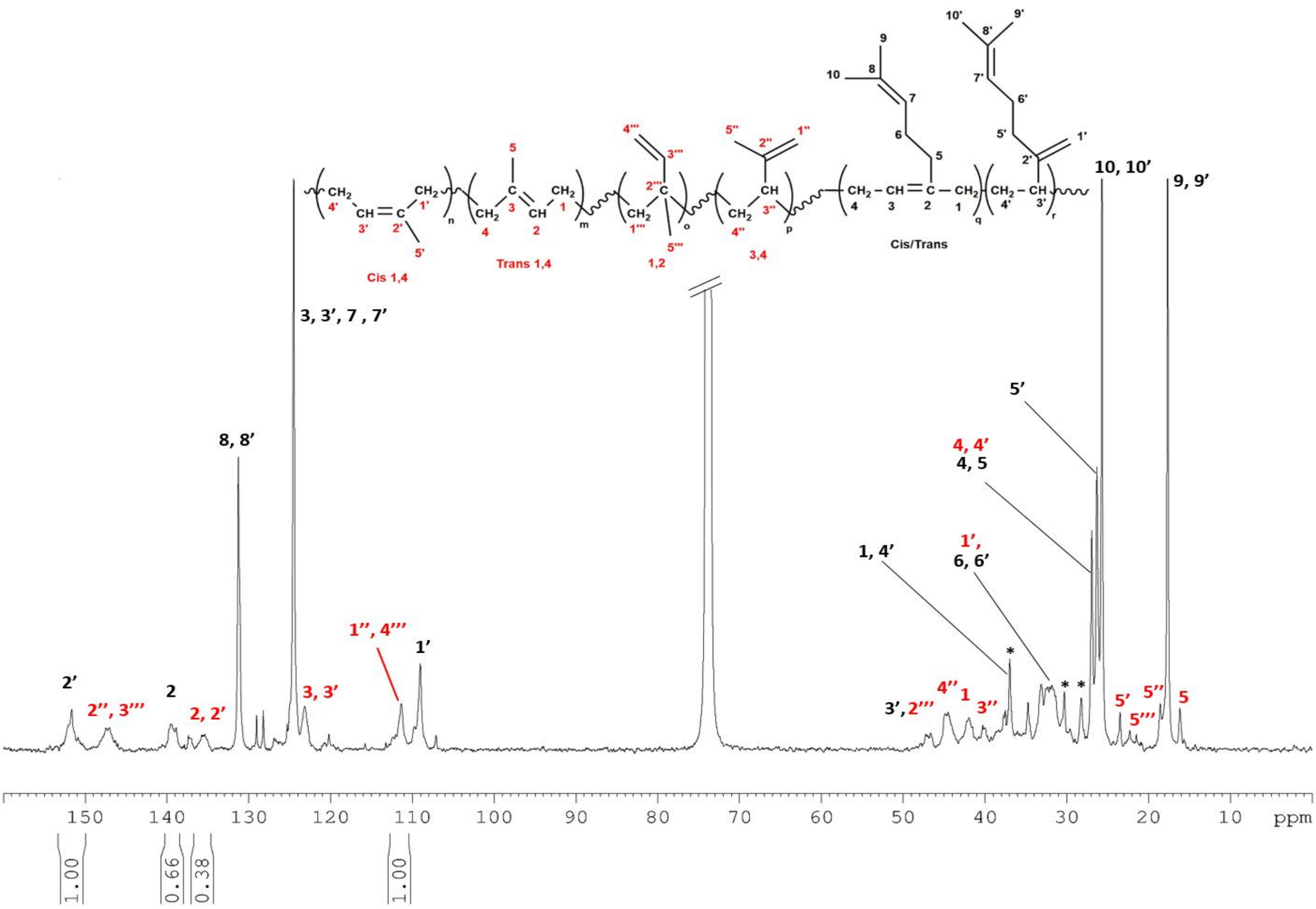

Figure S17. ^{13}C NMR spectrum (TCDE, 25 °C, 400 MHz) of PMI from run 16 of **Table 2**

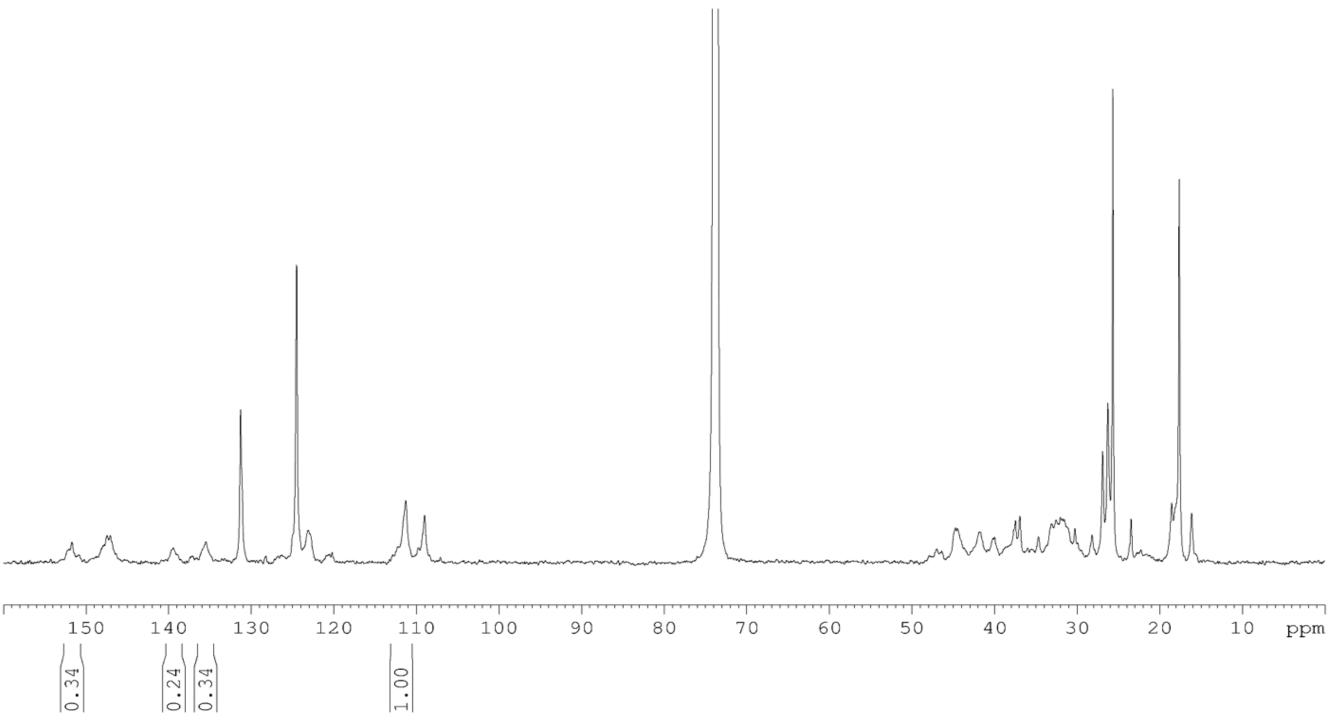

Figure S18. ^{13}C NMR spectrum (TCDE, 25 °C, 400 MHz) of PMI from run 17 of **Table 2**

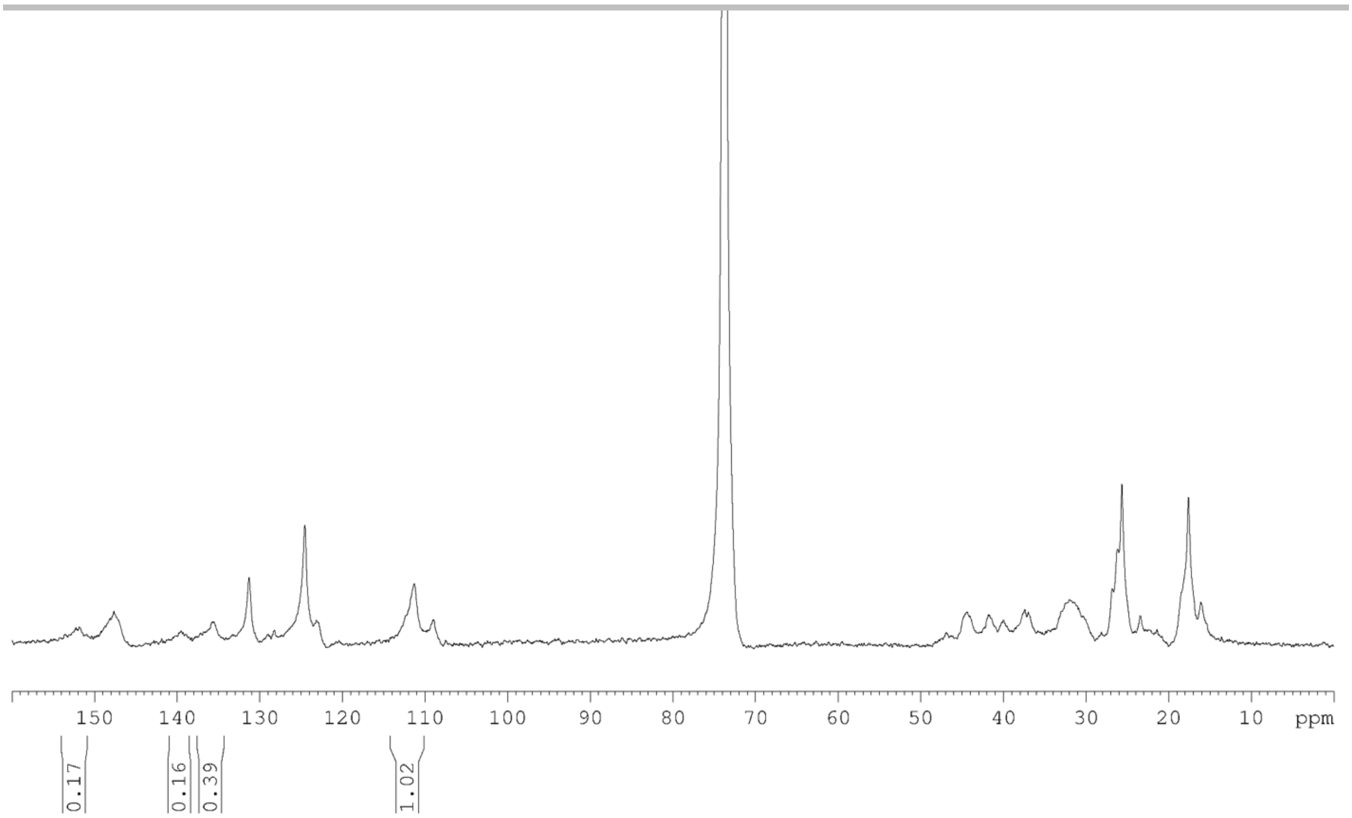

Figure S19. ^{13}C NMR spectrum (TCDE, 25 °C, 400 MHz) of PMI from run 18 of **Table 2**

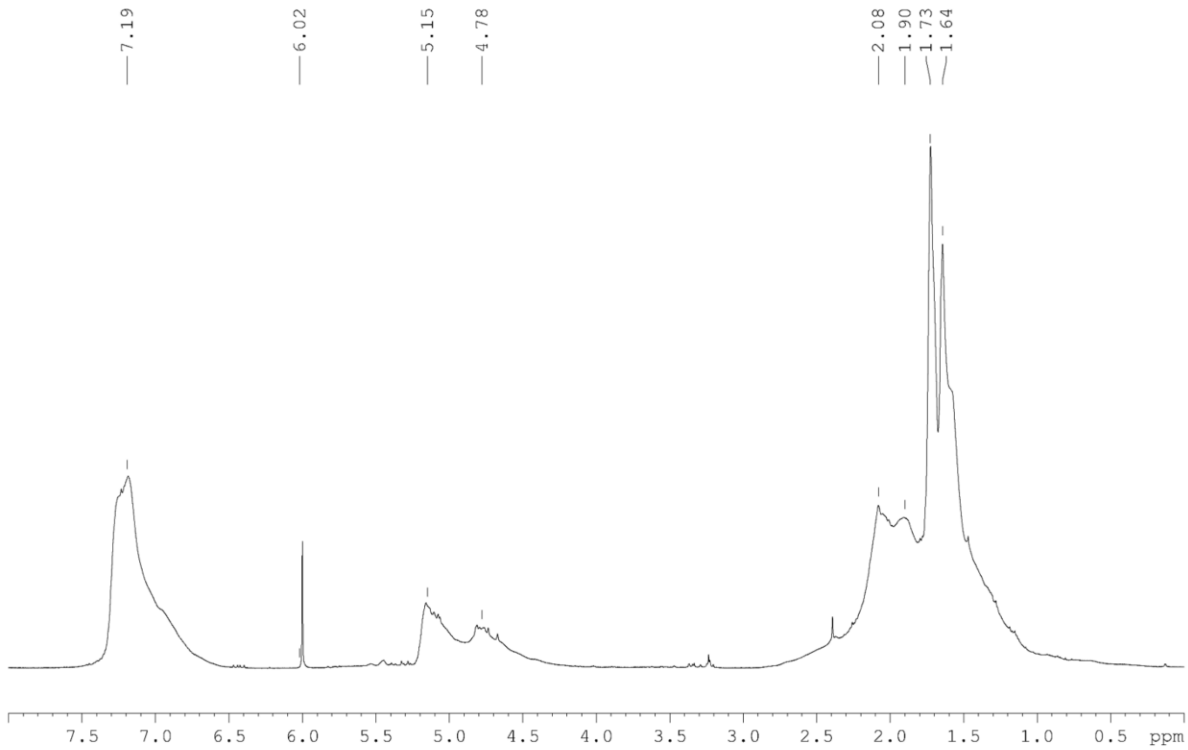

Figure S20. ^{1}H NMR spectrum (TCDE, 25 °C, 400 MHz) of PMSI from run 18 of **Table 2**

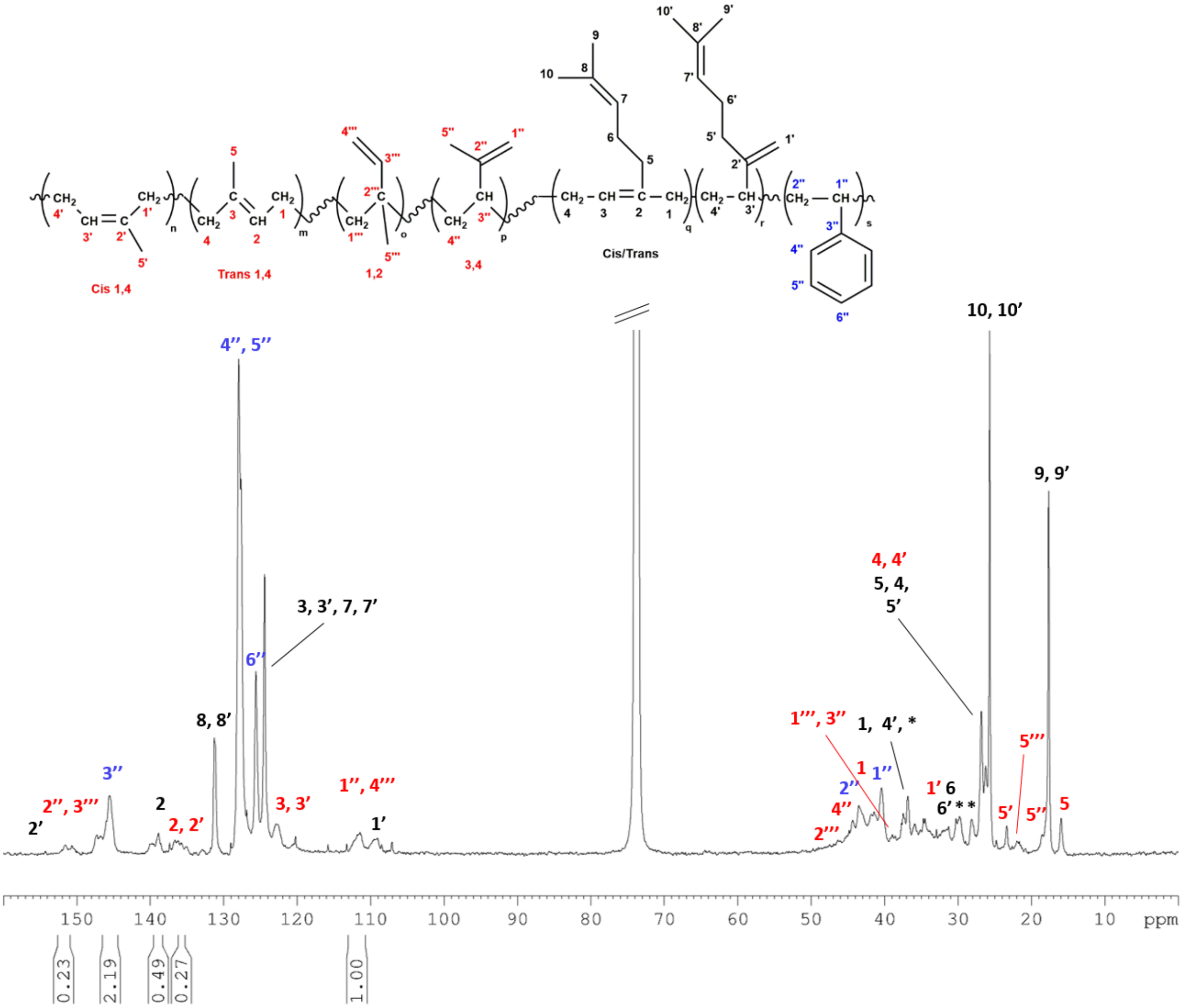

Figure S21. ^{13}C NMR spectrum (TCDE, 25 °C, 400 MHz) of PMSI from run 18 of **Table 2**

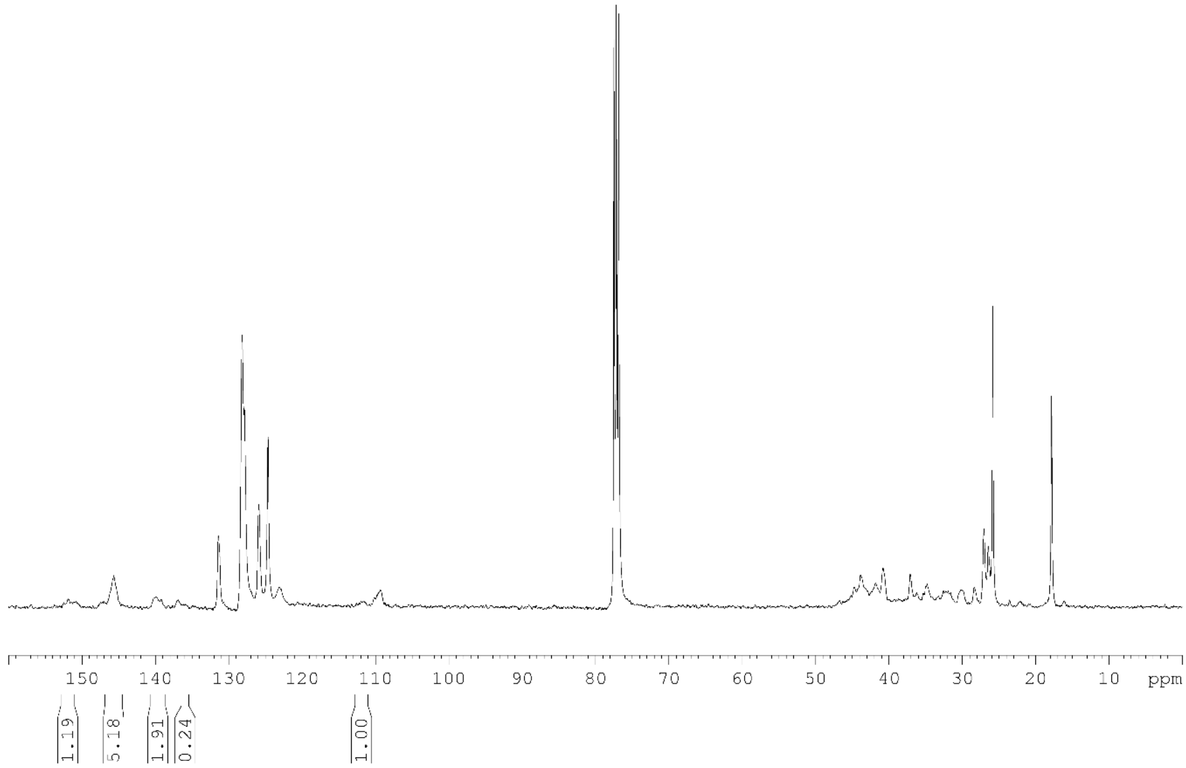

Figure S22. ^{13}C NMR spectrum ($CDCl_3$, 25 °C, 400 MHz) of PMSI from run 19 of **Table 2**

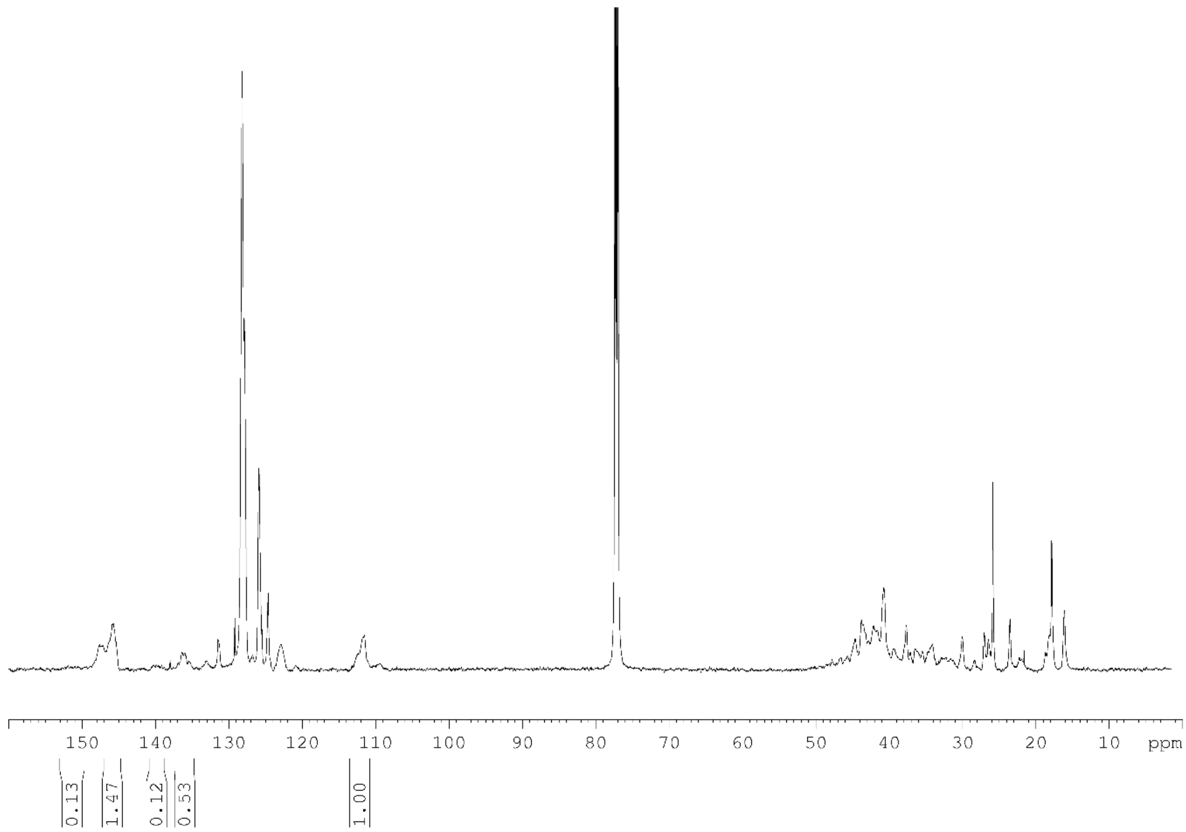

Figure S23. ^{13}C NMR spectrum (TCDE, 25 °C, 400 MHz) of PMSI from run 20 of **Table 2**

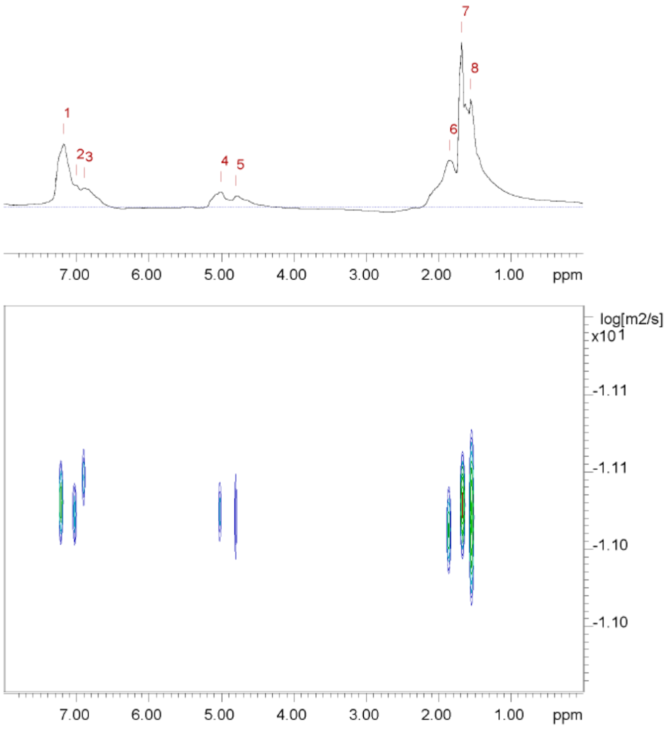

Fitted function:	f (x) = A * exp (-D * x^2 * gamma^2 * littleDelta^2 (bigDelta-littleDelta/3)* 10^4
used gamma:	26752 rad/(s*Gauss)
used little delta:	0.0050000 s
used big delta:	0.14990 s
used gradient strength:	variable
Random error estimation of data:	RMS per spectrum (or trace/plane)
Systematic error estimation of data:	worst case per peak scenario
Fit parameter Error estimation method:	from fit using arbitray y uncertainties
Confidence level:	95%
Used peaks:	automatically picked peaks
Used integrals:	peak intensities
Used Gradient strength:	all values (including replicates) used

Peak name	F2 [ppm]	D [m2/s]	error
1	7.190	8.09e-12	3.034e-13
2	7.008	8.28e-12	3.385e-13
3	6.889	7.89e-12	2.786e-13
4	5.013	8.62e-12	3.627e-13
5	4.795	9.39e-12	7.118e-13
6	1.854	8.84e-12	3.726e-13
7	1.683	8.57e-12	3.458e-13
8	1.558	8.74e-12	6.227e-13

Figure S24. DOSY NMR spectrum ($CDCl_3$, 25 °C, 600 MHz) of PMS copolymers from run 13 of **Table 2**

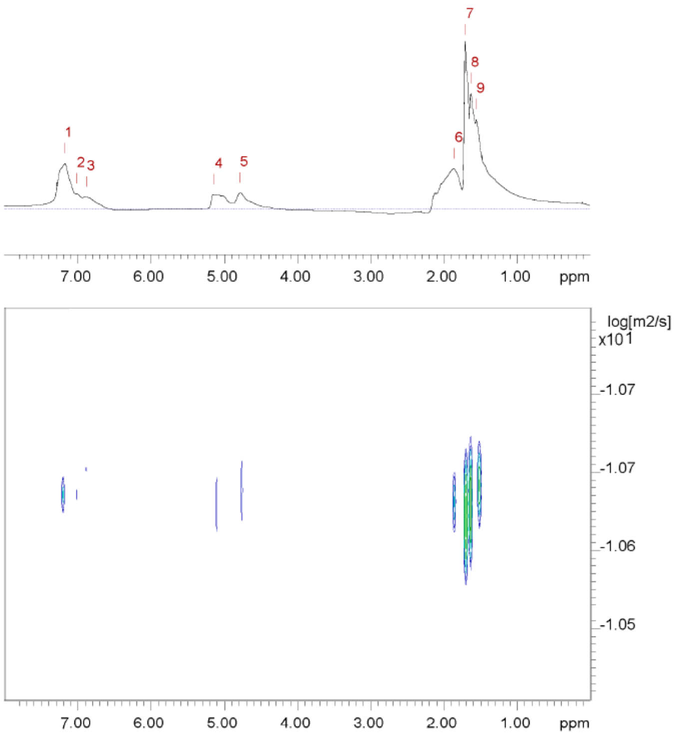

Fitted function:	f (x) = A * exp (-D * x^2 * gamma^2 * littleDelta^2 (bigDelta-littleDelta/3)* 10^4
used gamma:	26752 rad/(s*Gauss)
used little delta:	0.0050000 s
used big delta:	0.14990 s
used gradient strength:	variable
Random error estimation of data:	RMS per spectrum (or trace/plane)
Systematic error estimation of data:	worst case per peak scenario
Fit parameter Error estimation method:	from fit using arbitray y uncertainties
Confidence level:	95%
Used peaks:	automatically picked peaks
Used integrals:	peak intensities
Used Gradient strength:	all values (including replicates) used

Peak name	F2 [ppm]	D [m2/s]	error
1	7.190	2.05e-11	6.259e-13
2	7.018	2.05e-11	5.955e-13
3	6.883	1.97e-11	3.899e-13
4	5.138	2.97e-11	3.340e-12
5	4.790	2.79e-11	2.901e-12
6	1.859	2.29e-11	1.212e-12
7	1.709	2.62e-11	2.167e-12
8	1.636	2.59e-11	2.299e-12
9	1.558	2.20e-11	1.393e-12

Figure S25. DOSY NMR spectrum ($CDCl_3$, 25 °C, 600 MHz) of PMS diblock copolymers from run of 21 **Table 2**

4. DSC Thermal Analysis

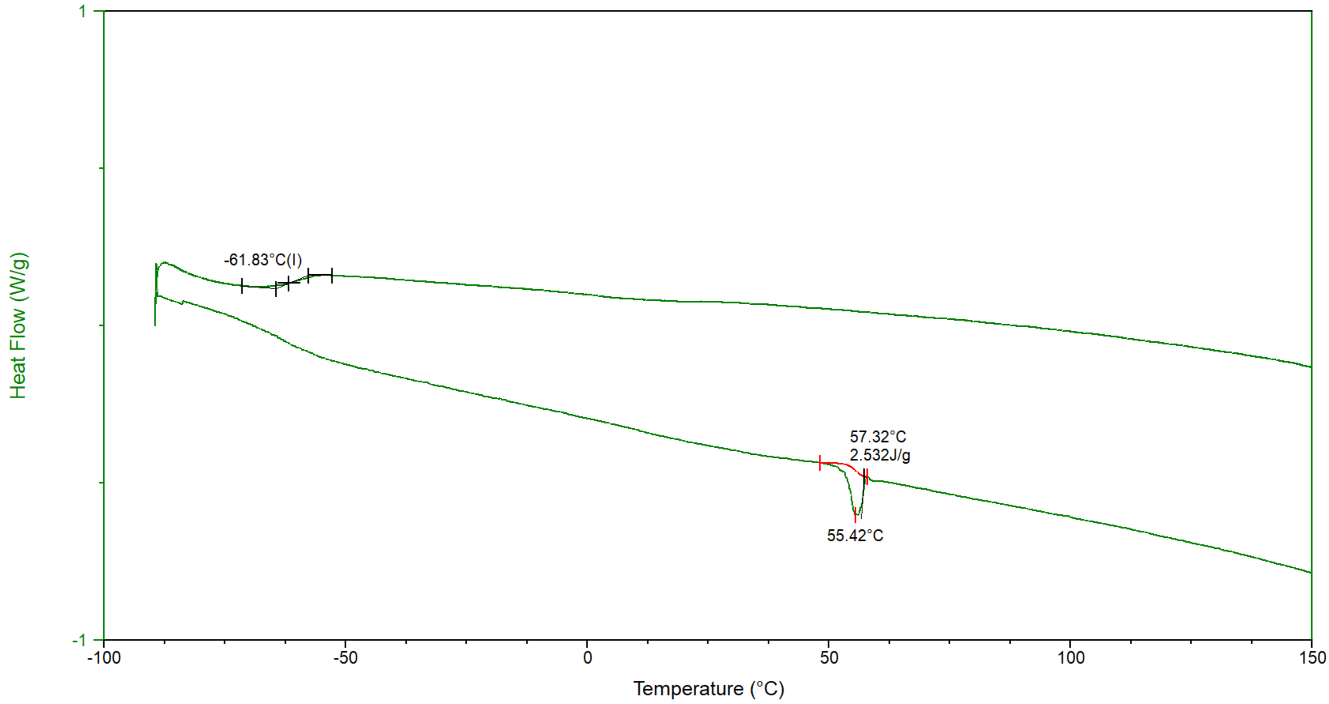

Figure S26. DSC thermogram of PM from run 1 of **Table 1**.

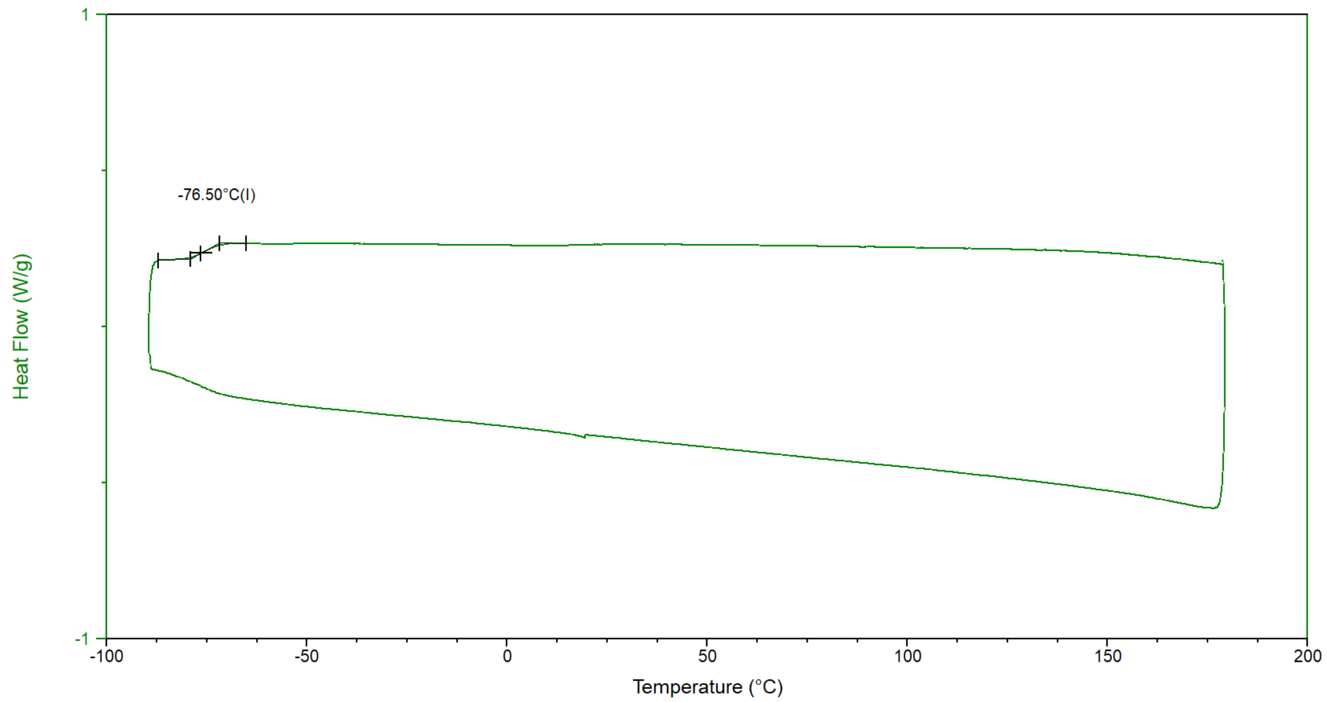

Figure S27. DSC thermogram of PM from run 4 of **Table 1**.

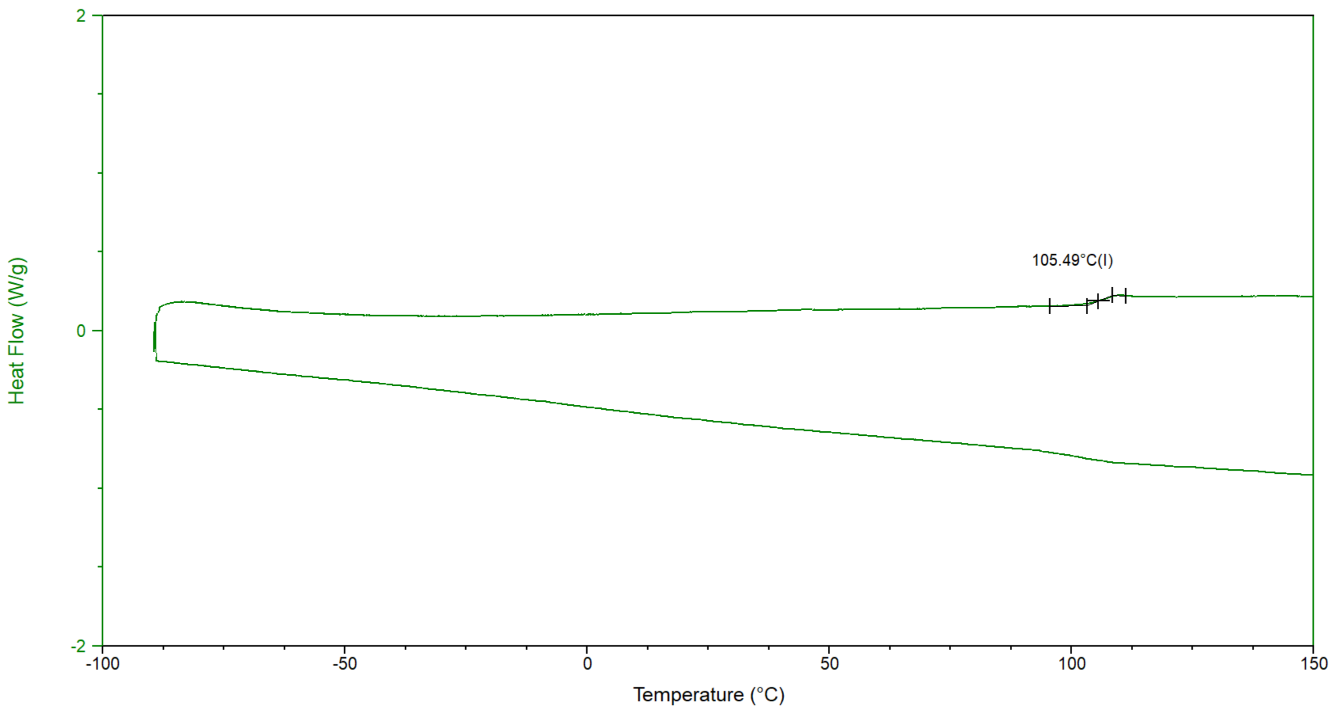

Figure S28. DSC thermogram of PS from run 5 of **Table 1**.

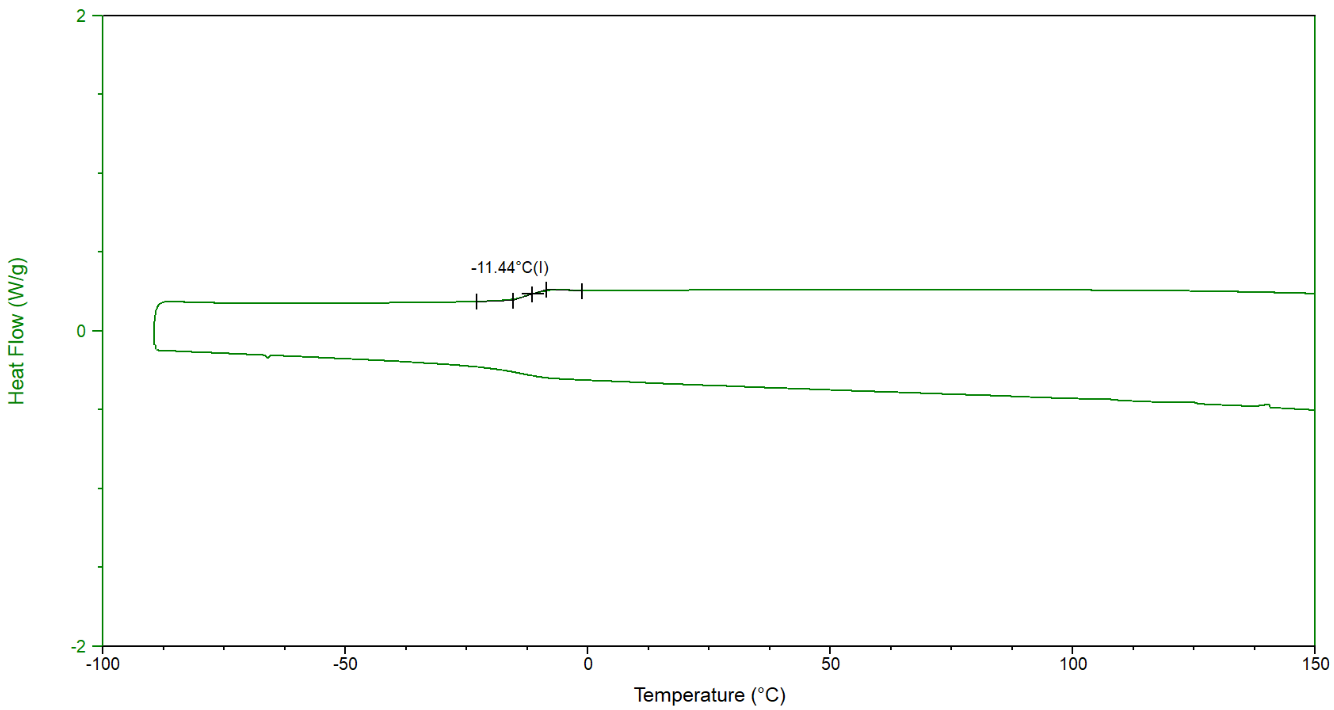

Figure S29. DSC thermogram of PI from run 8 of **Table 1**.

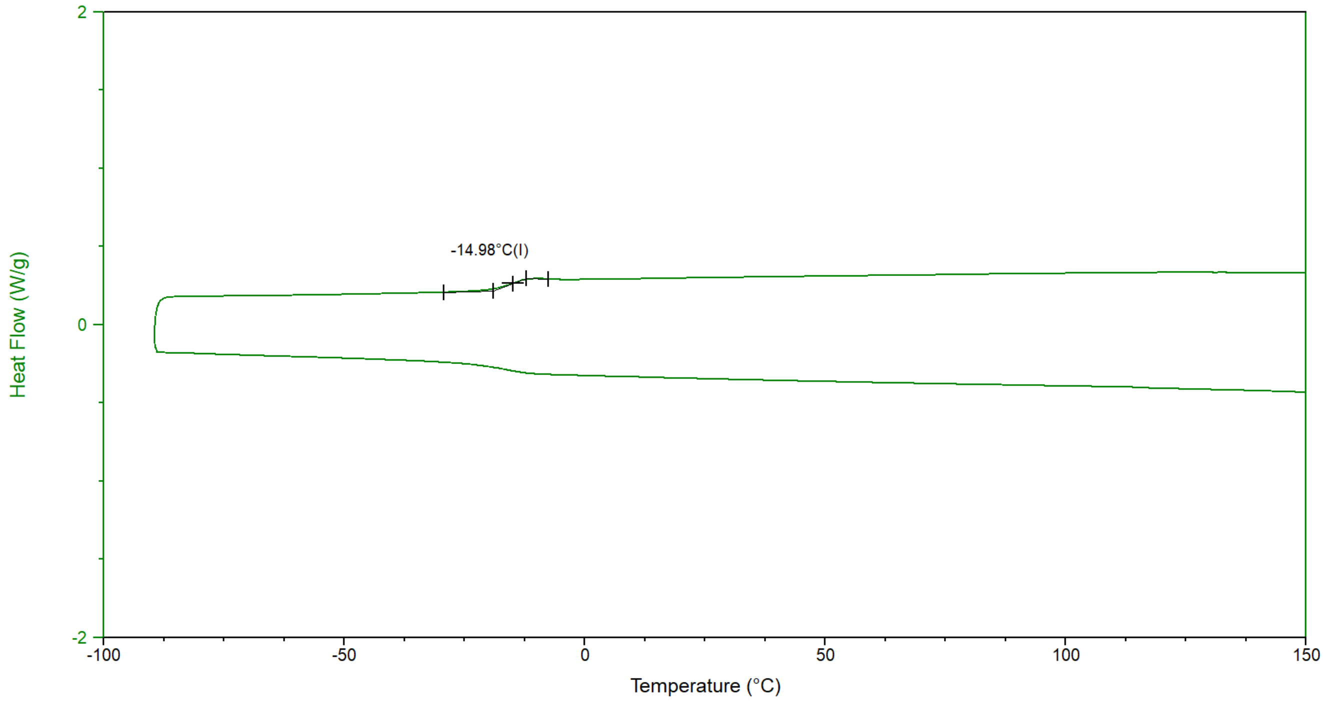

Figure S30. DSC thermogram of PI from run 9 of **Table 1**.

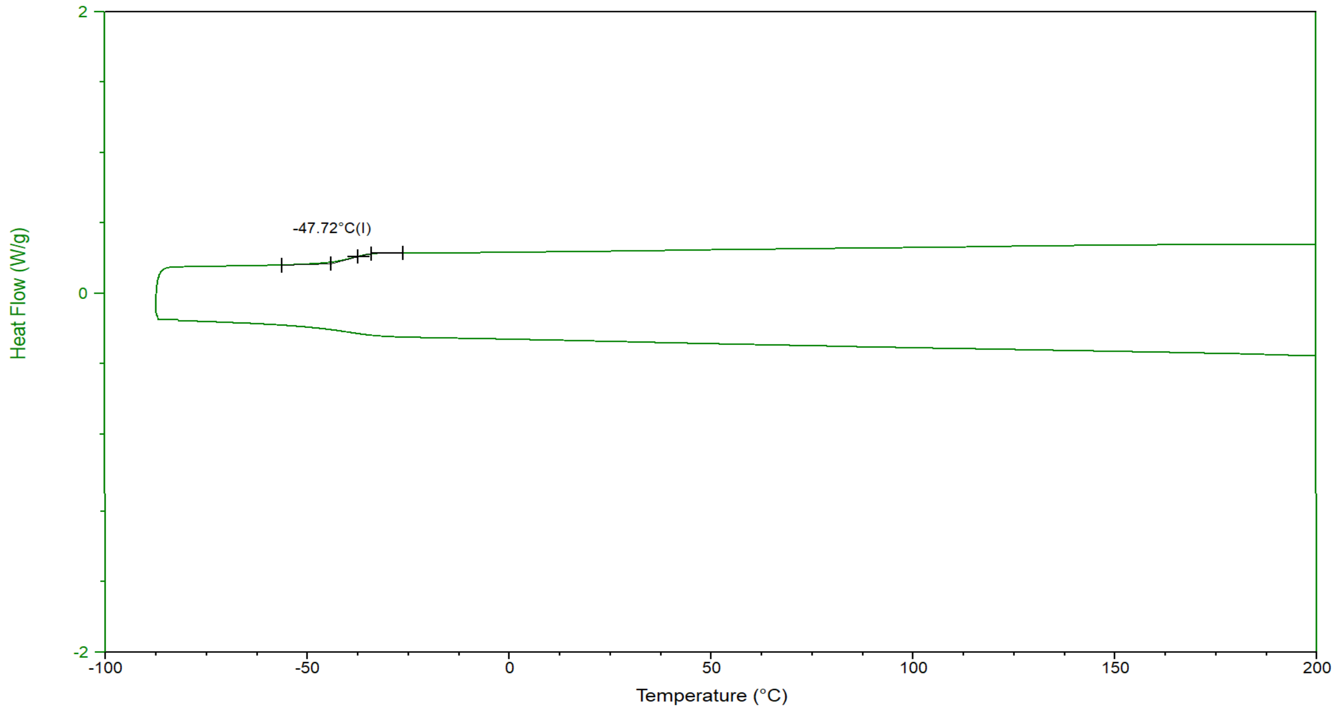

Figure S31. DSC thermogram of PMS from run 10 of **Table 2**.

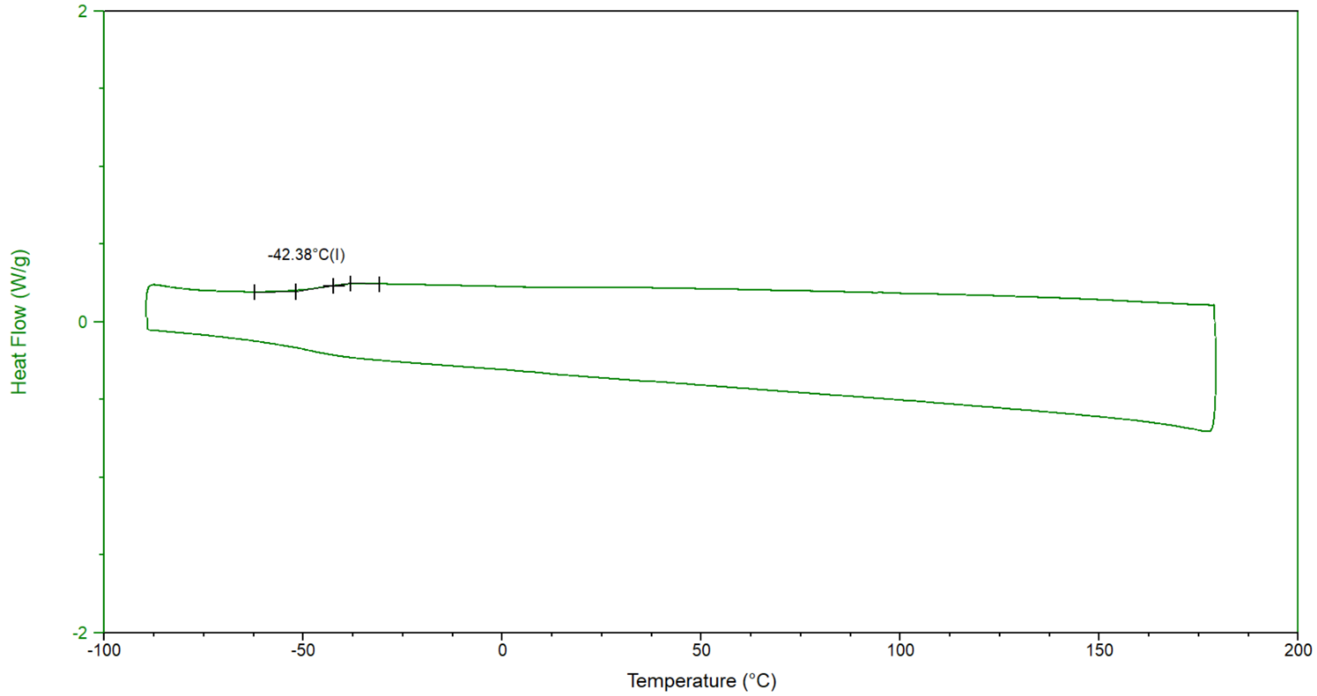

Figure S32. DSC thermogram of PMS from run 12 of **Table 2**.

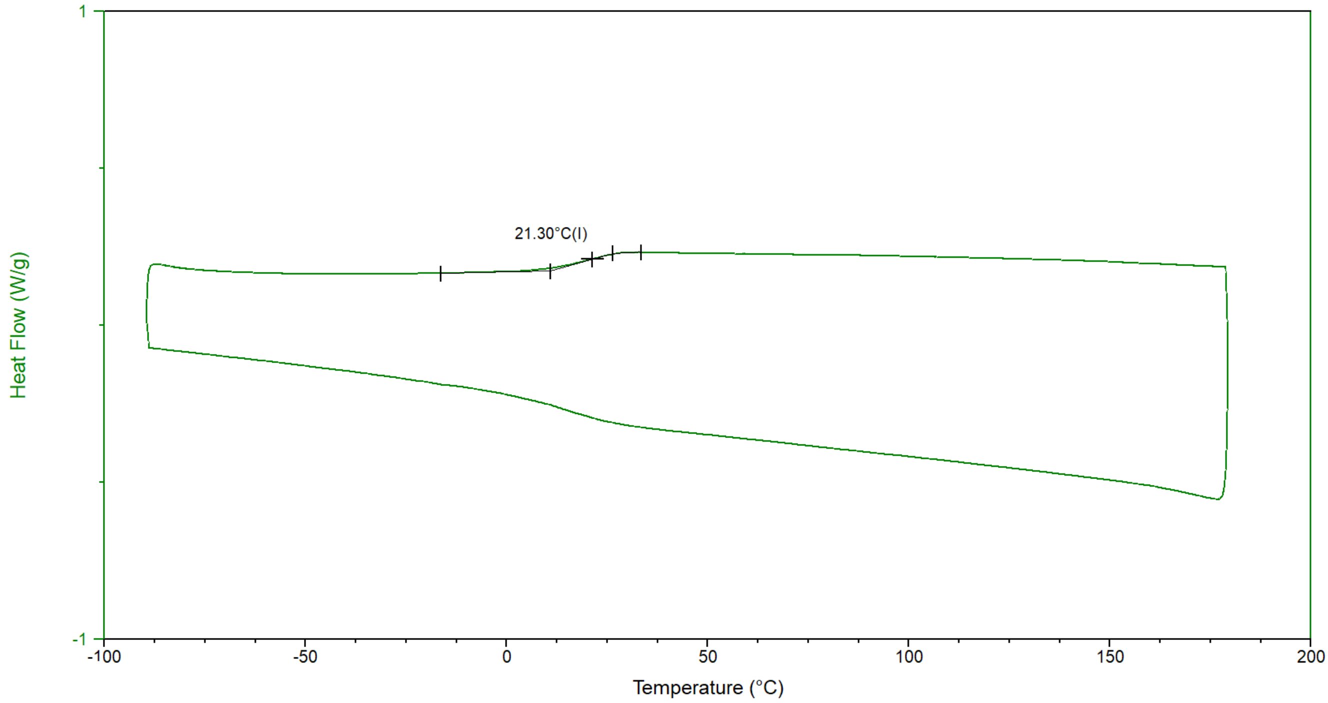

Figure S33. DSC thermogram of PMS from run 14 of **Table 2**.

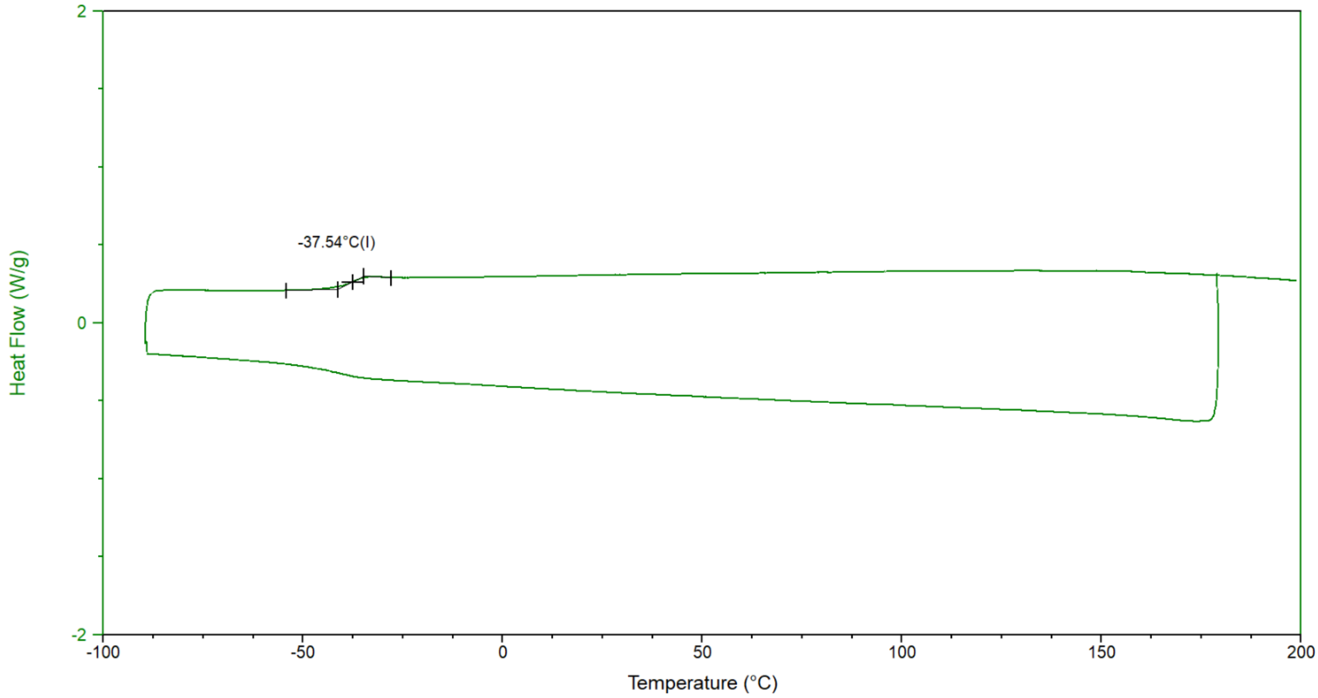

Figure S34. DSC thermogram of PMI from run 16 of **Table 2**.

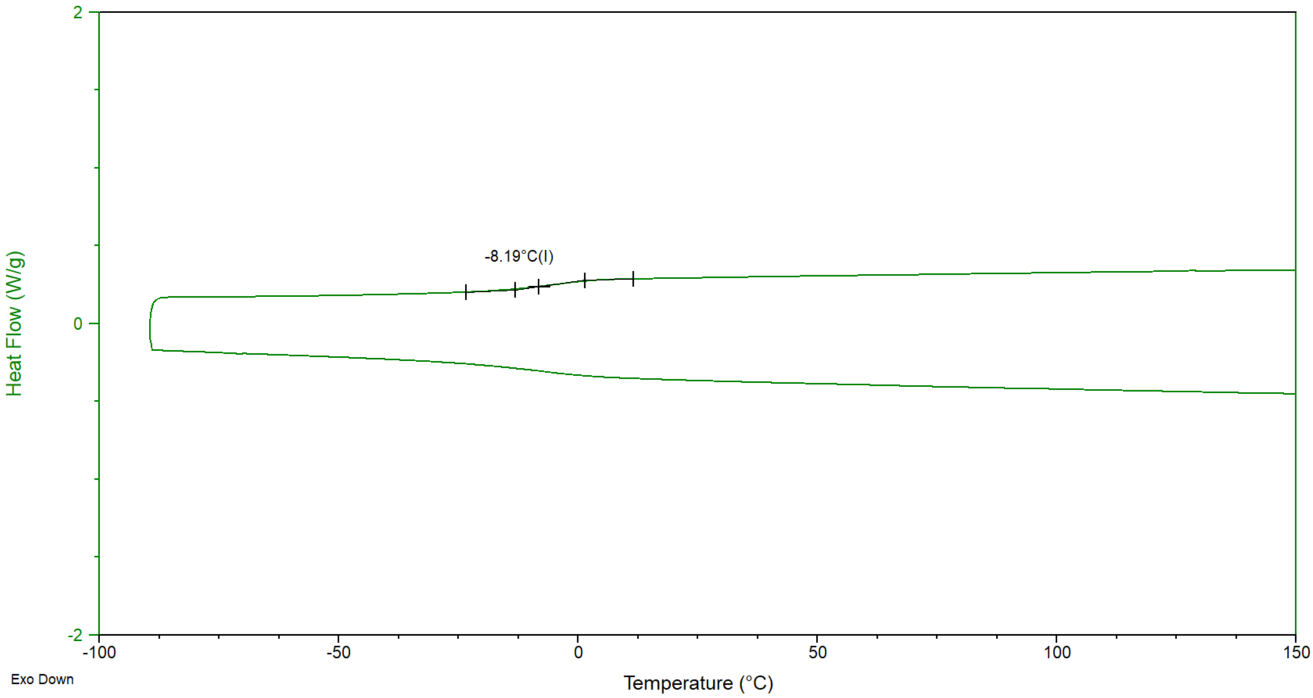

Figure S35. DSC thermogram of PMSI from run 18 of **Table 2**.

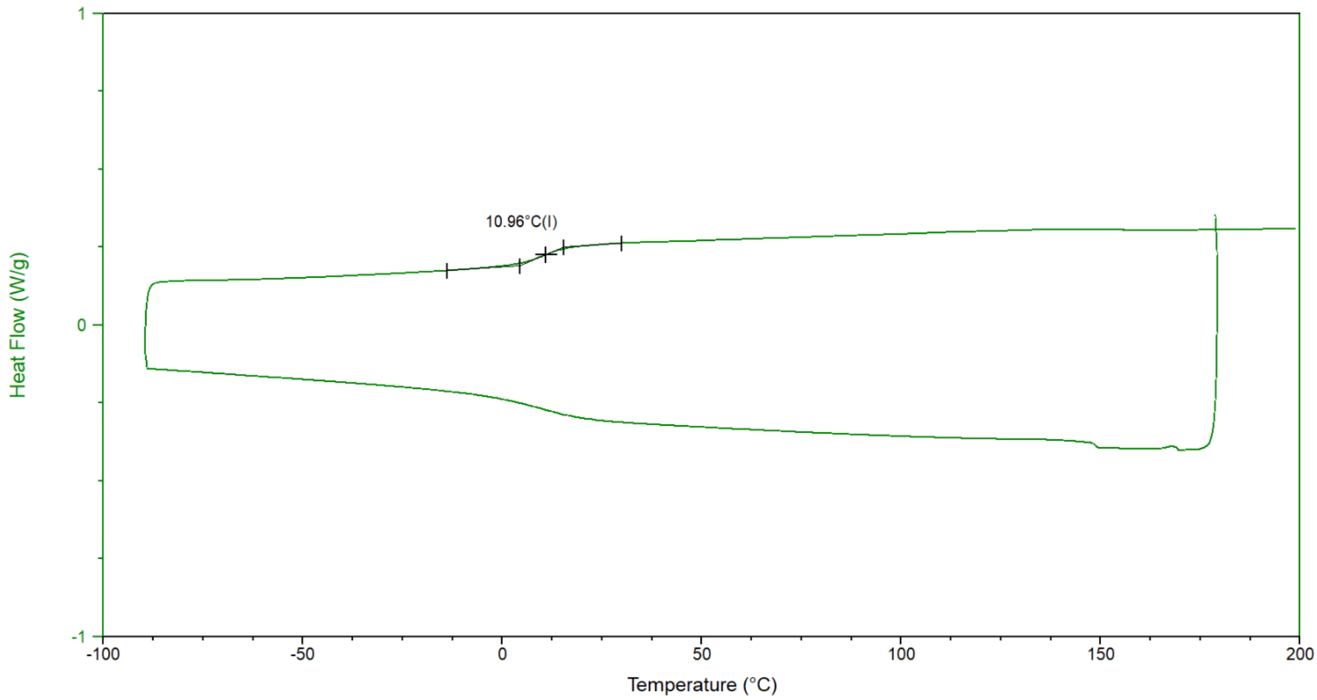

Figure S36. DSC thermogram of PMSI from run 20 of **Table 2**.

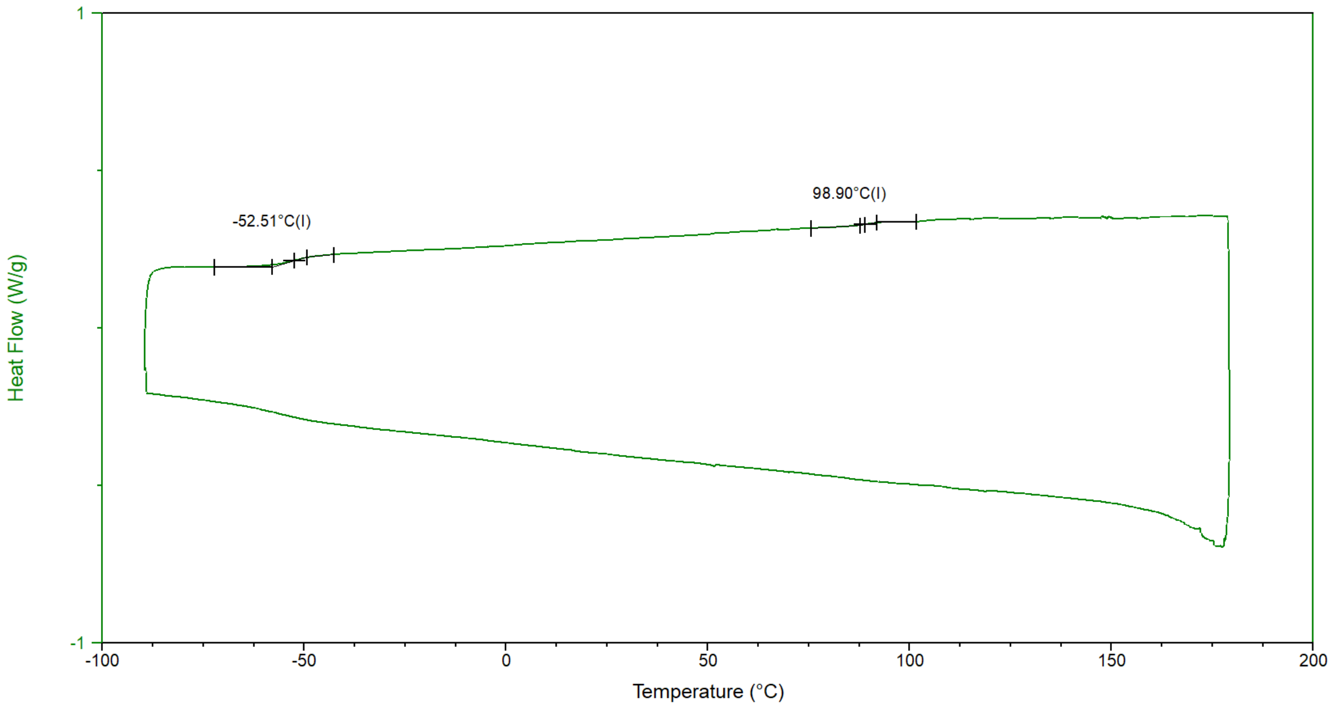

Figure S37. DSC thermogram of diblock PMS from run 21 of **Table 2**.

5. TGA Analysis

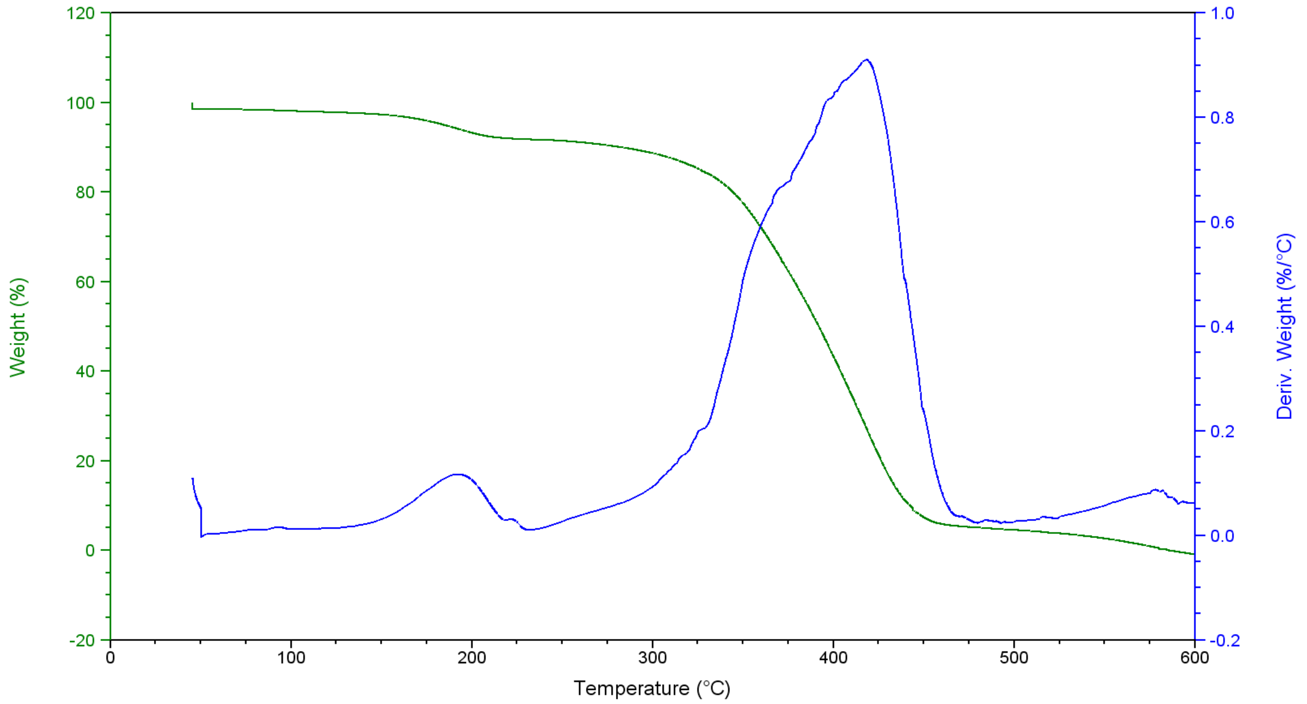

Figure S38. TGA thermogram of PM from run 1 of **Table 1**.

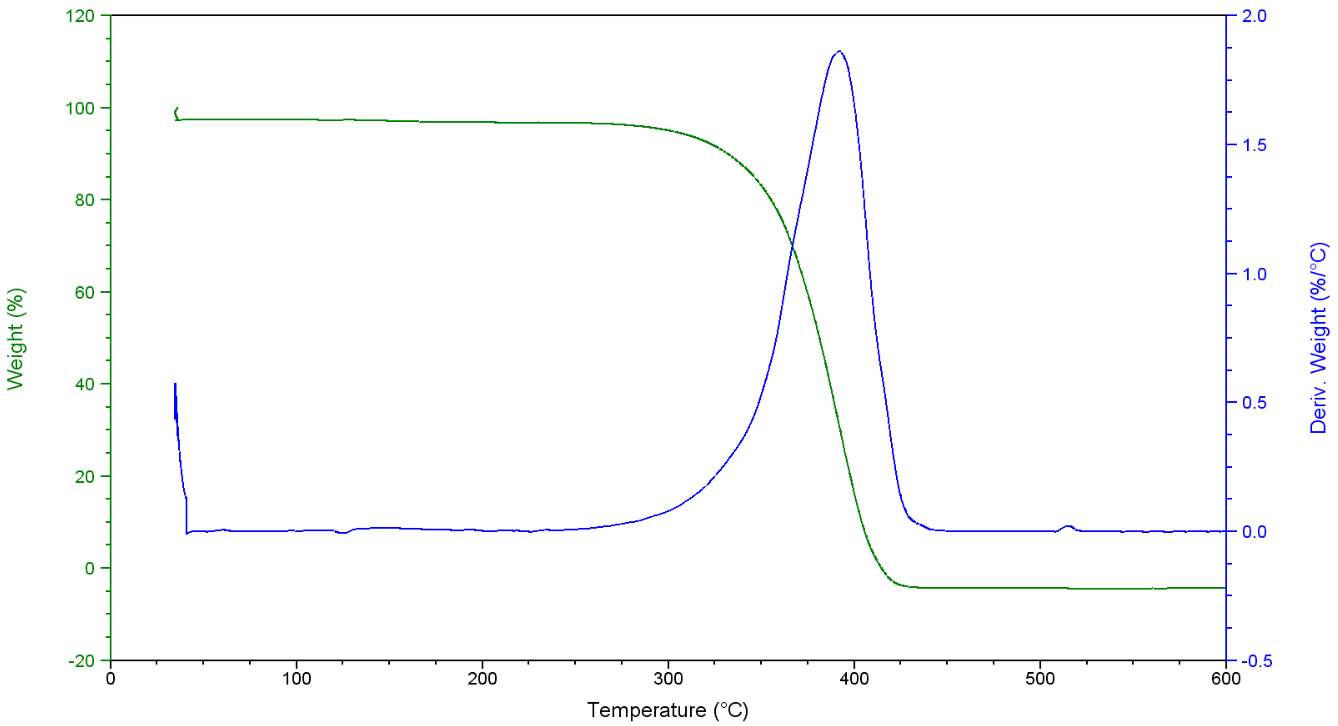

Figure S39. TGA thermogram of PS from run 5 of **Table 1**.

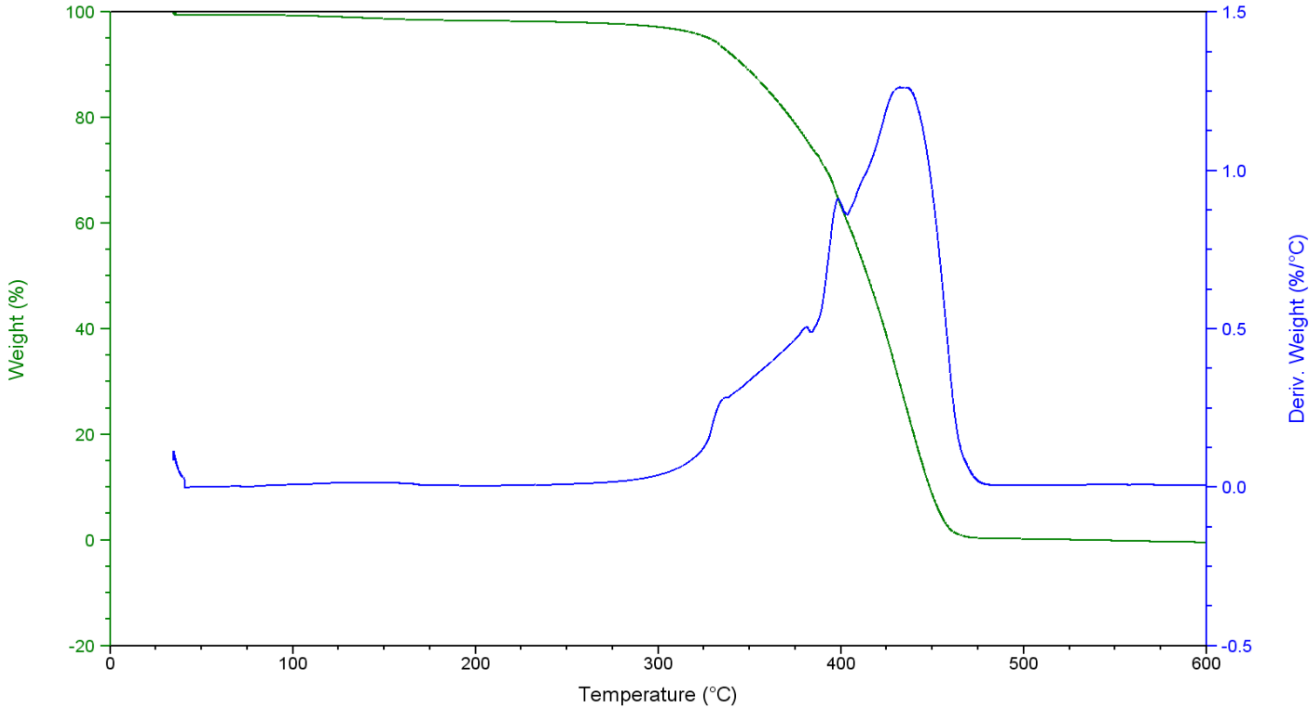

Figure S40. TGA thermogram of PI from run 8 of **Table 1**.

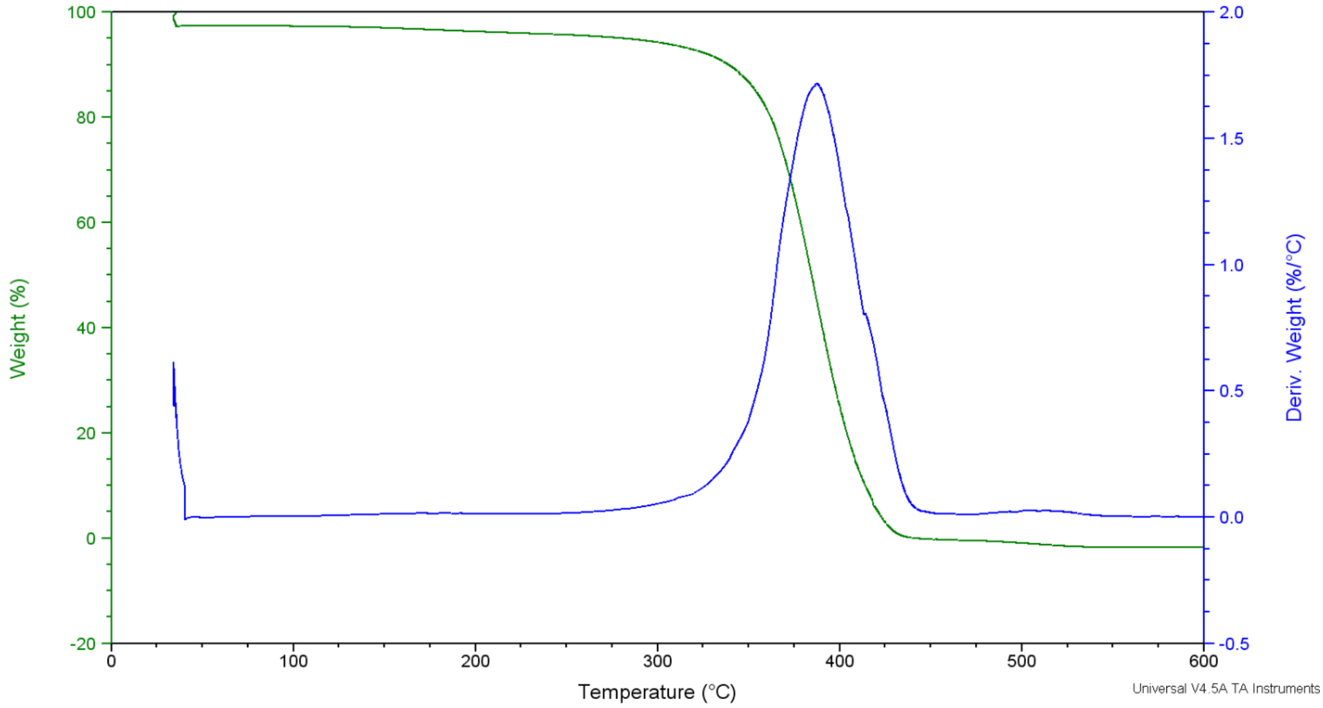

Figure S41. TGA thermogram of PMS from run 12 of **Table 2**.

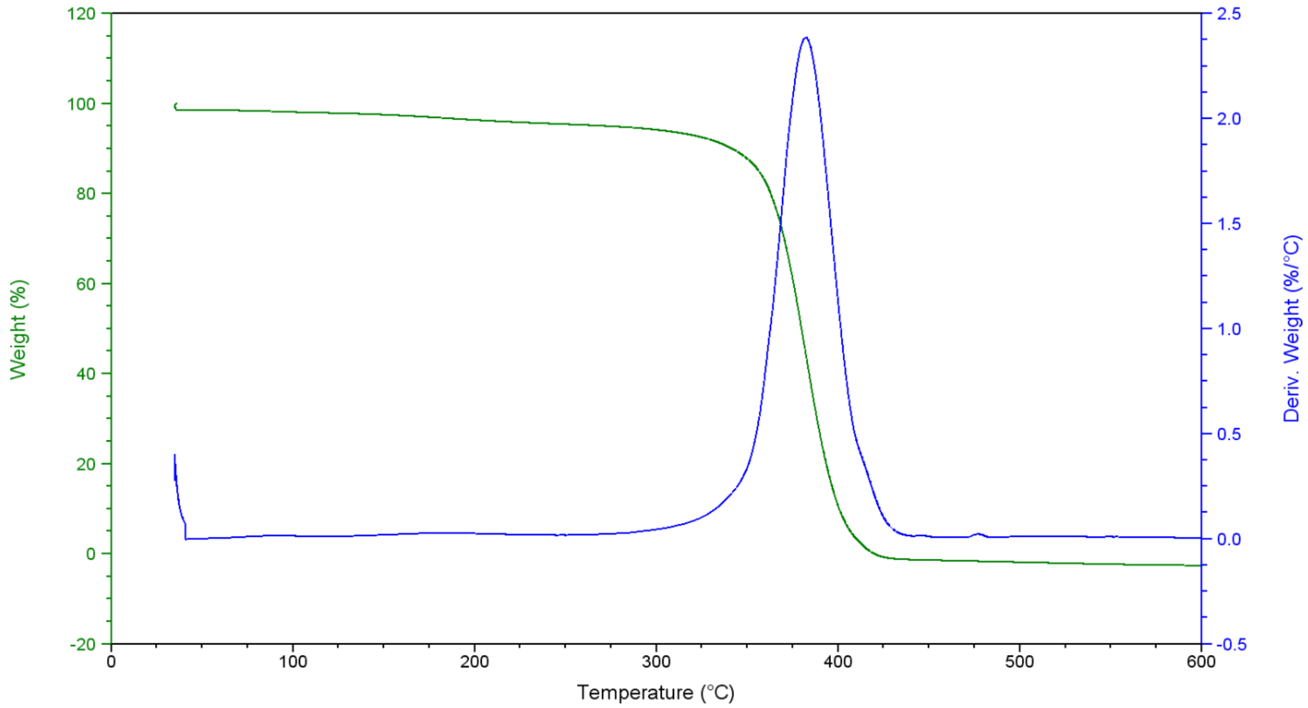

Figure S42. TGA thermogram of PMS from run 14 of **Table 2**.

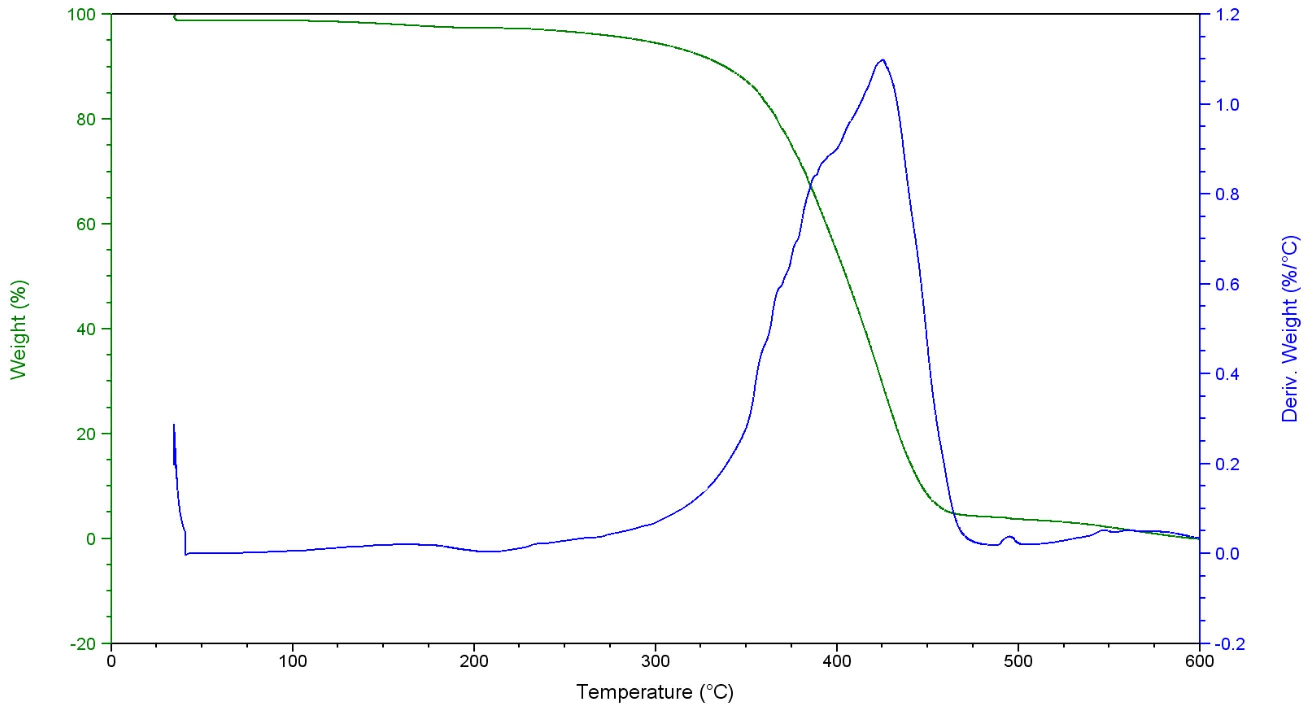

Figure S43. TGA thermogram of PMI from run 15 of **Table 2**.

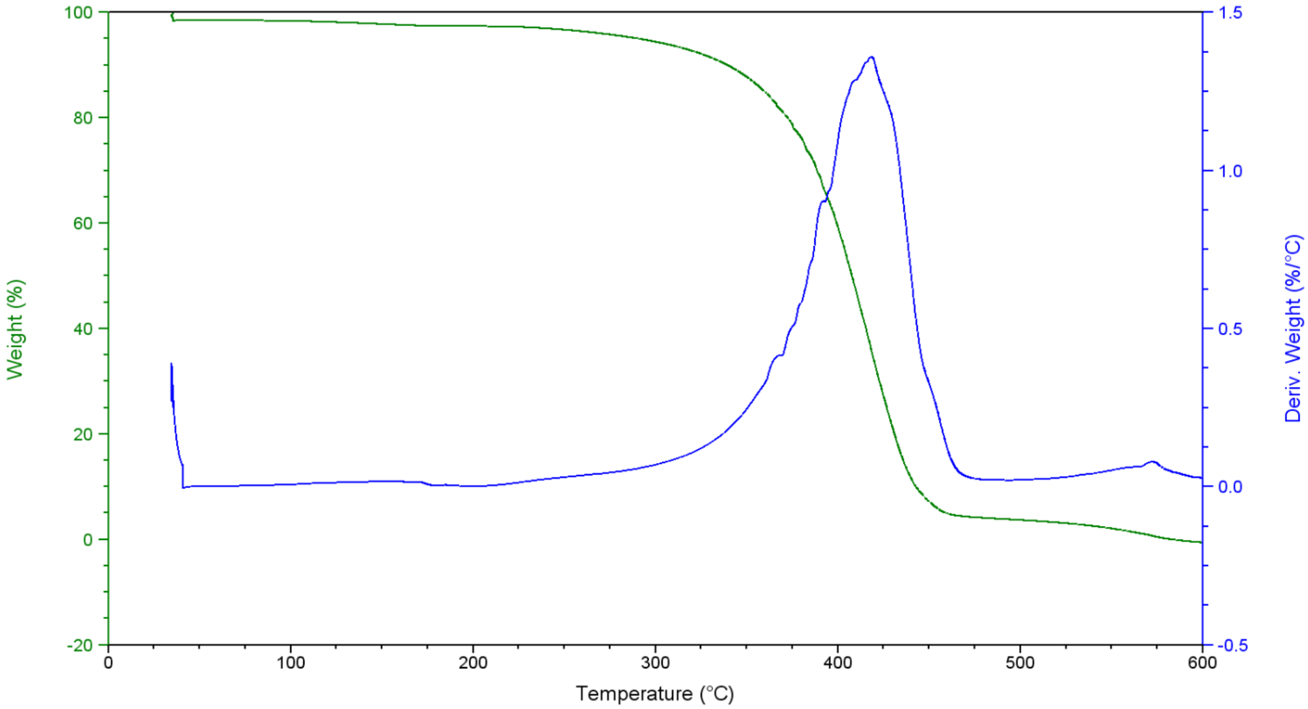

Figure S44. TGA thermogram of PMI from run 16 of **Table 2**.

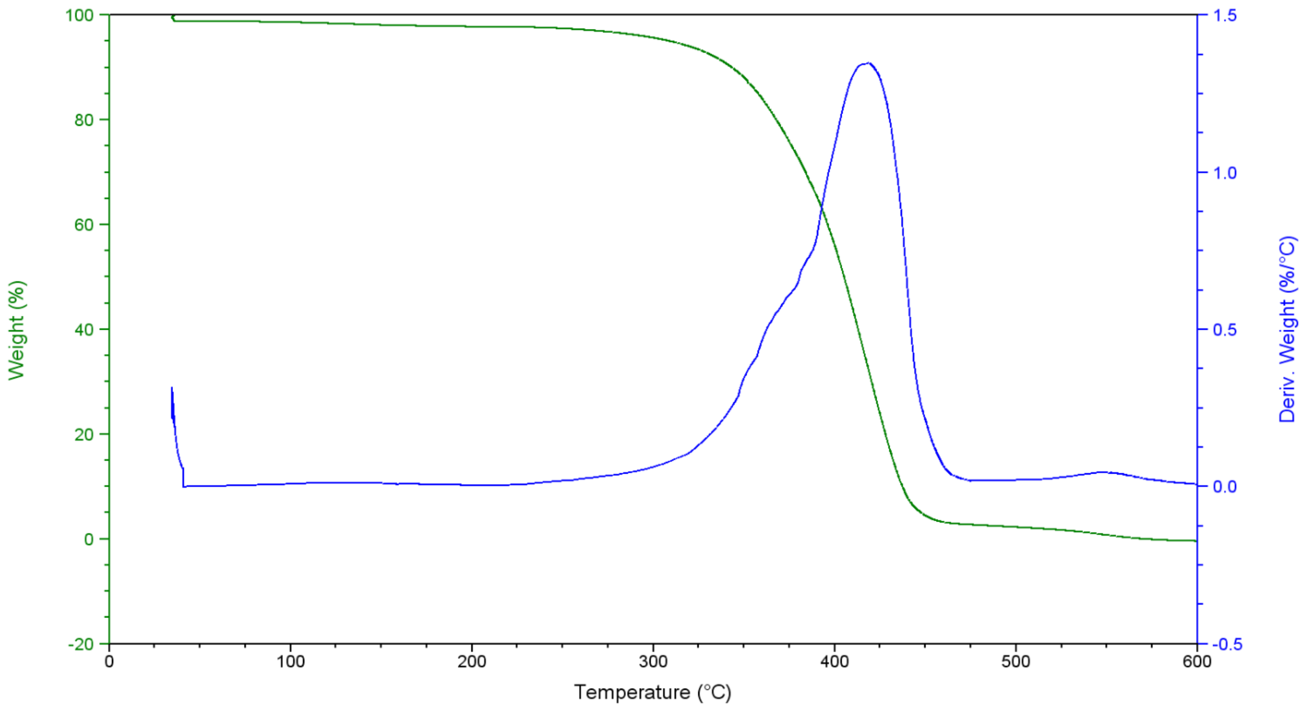

Figure S45. TGA thermogram of PMI from run 17 of **Table 2**.

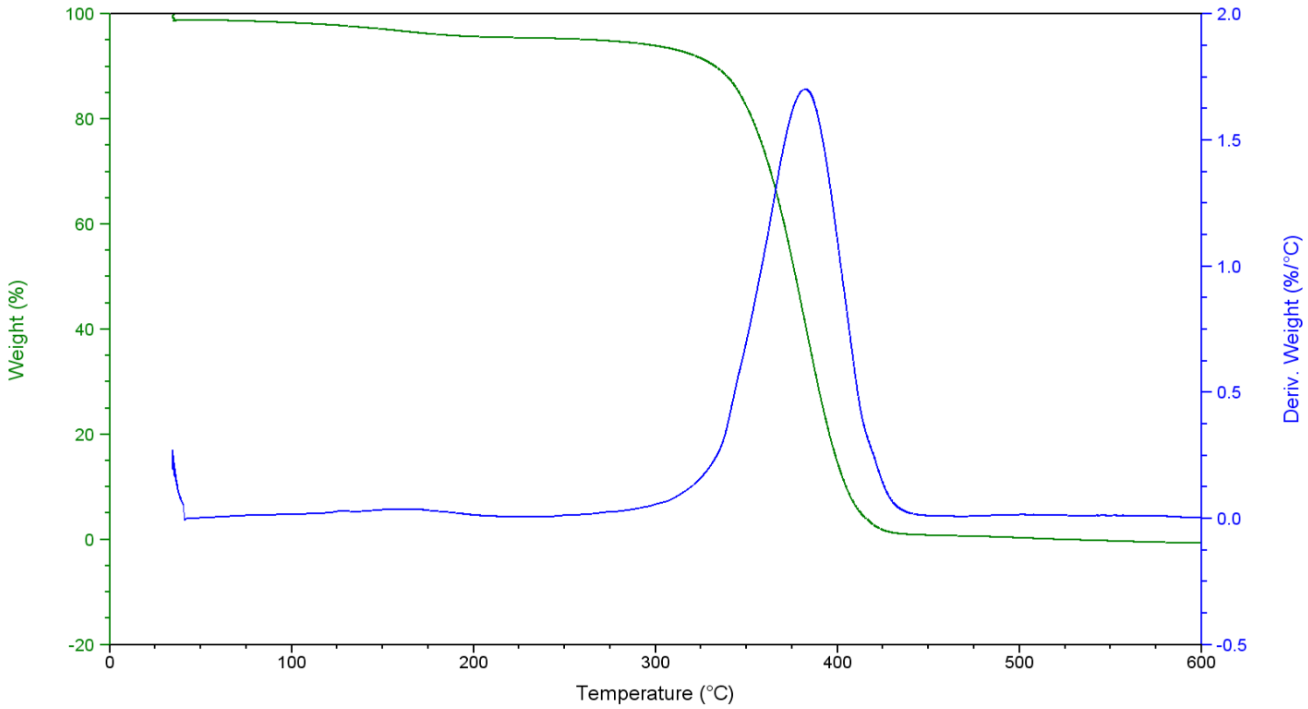

Figure S46. TGA thermogram of PMSI from run 20 of **Table 2**.

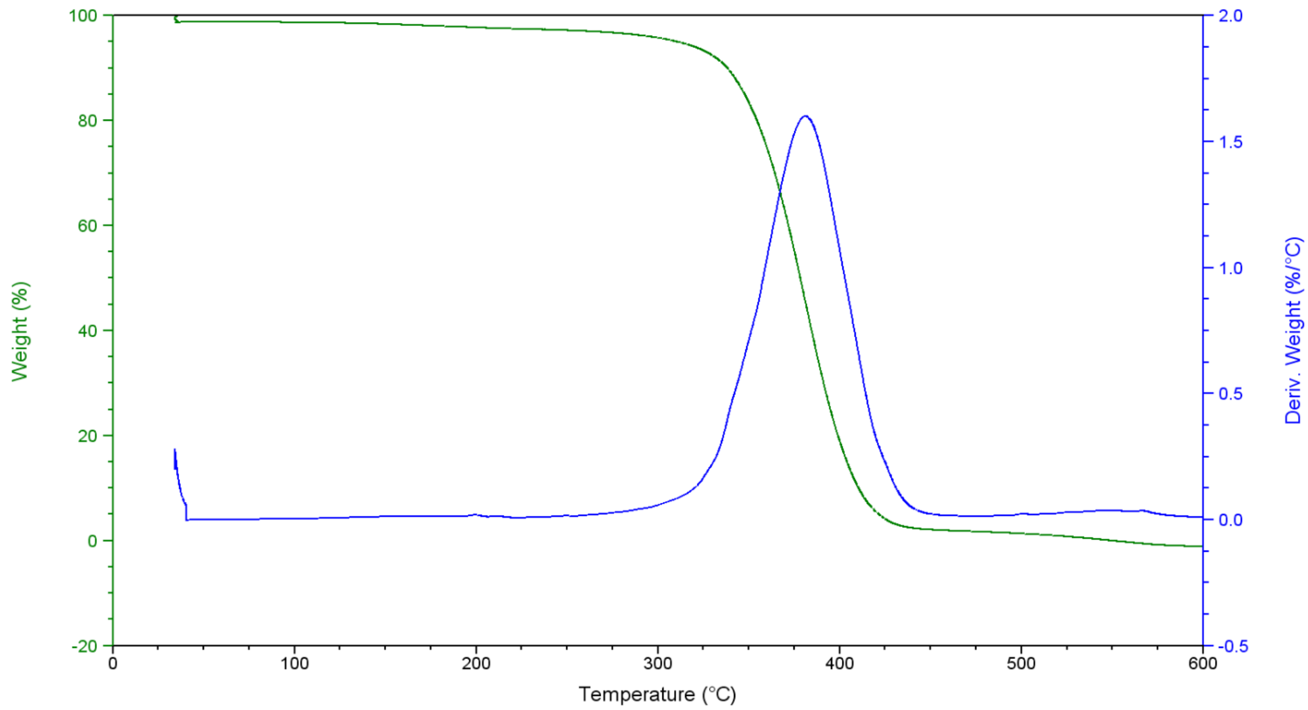

Figure S47. TGA thermogram of diblock PMS from run 21 of **Table 2**.

6. GPC Analysis

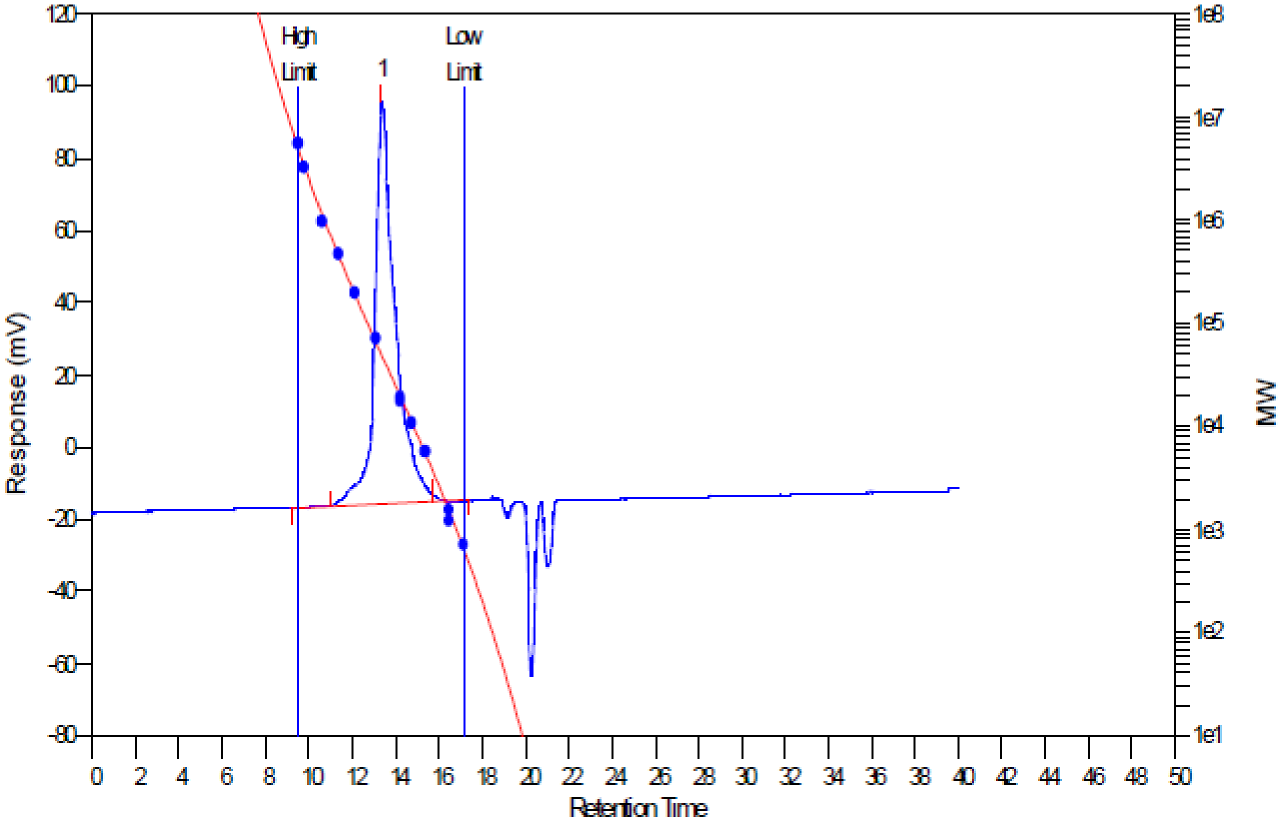

Figure S48. GPC curve of PM from run 1 of **Table 1.**

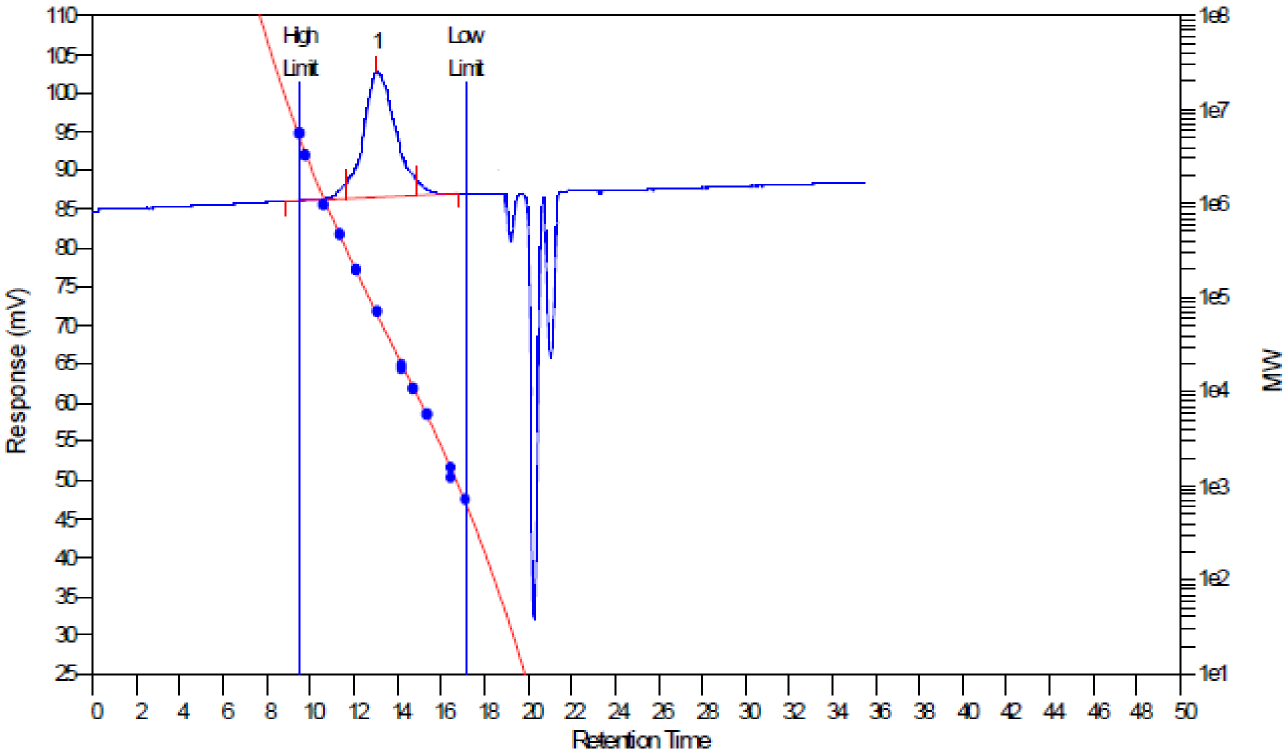

Figure S49. GPC curve of PM from run 2 of **Table 1.**

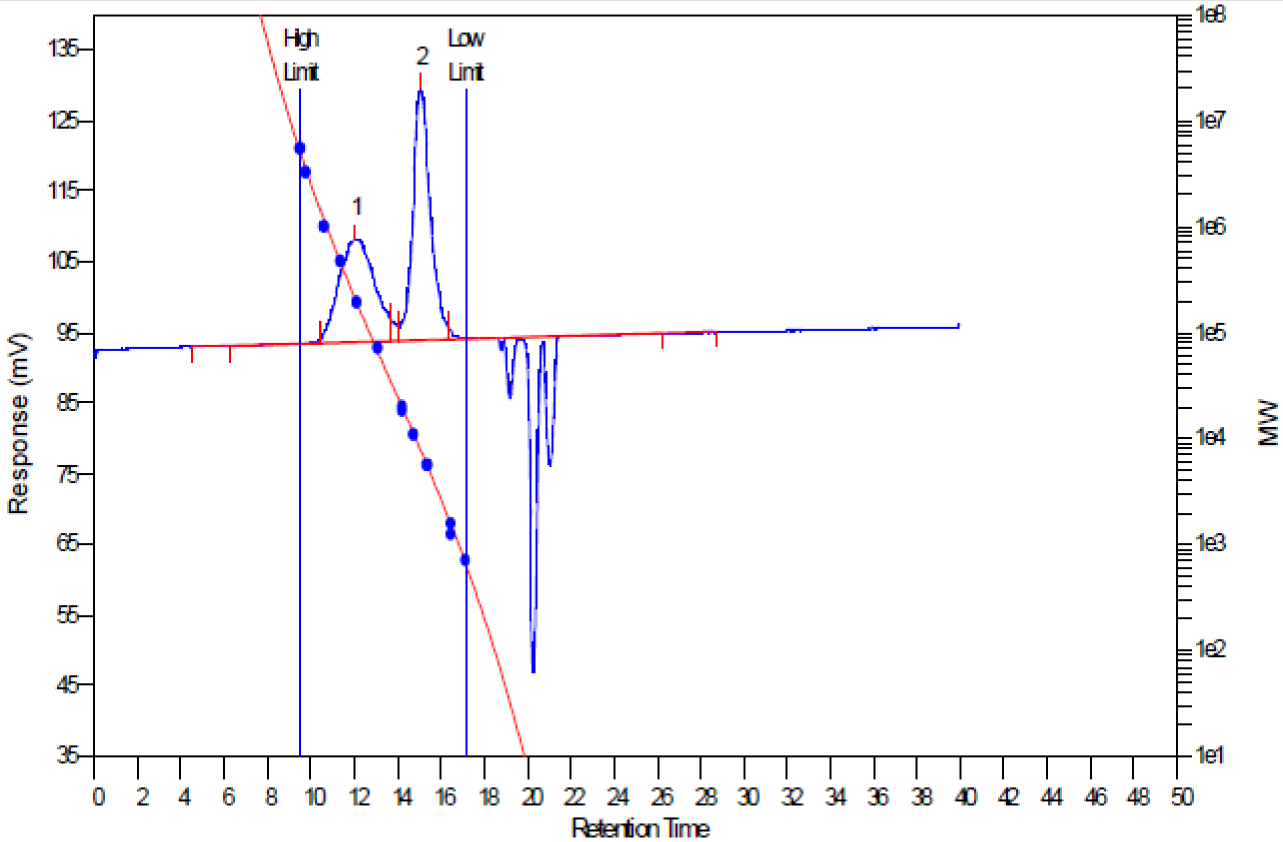

Figure S50. GPC curve of PM from run 3 of **Table 1.**

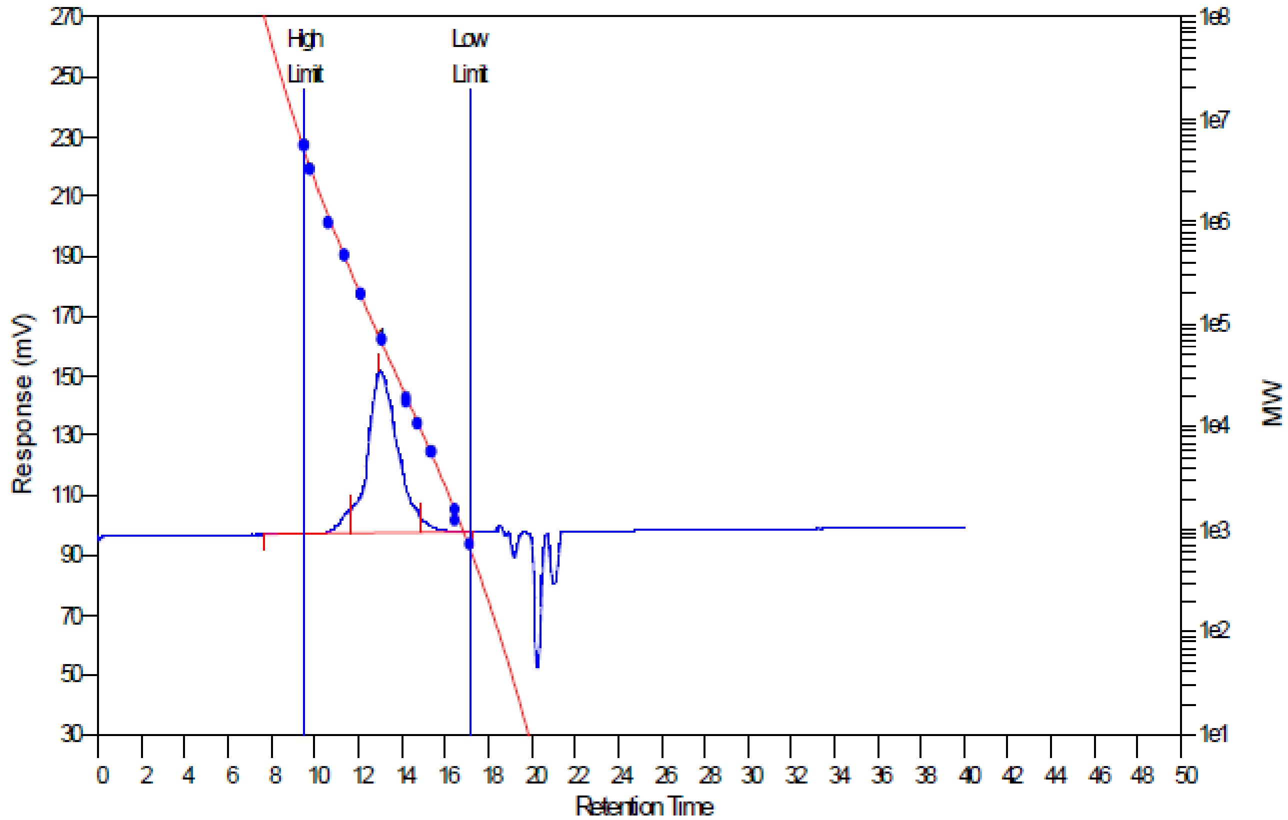

Figure S51. GPC curve of PM from run 4 of **Table 1.**

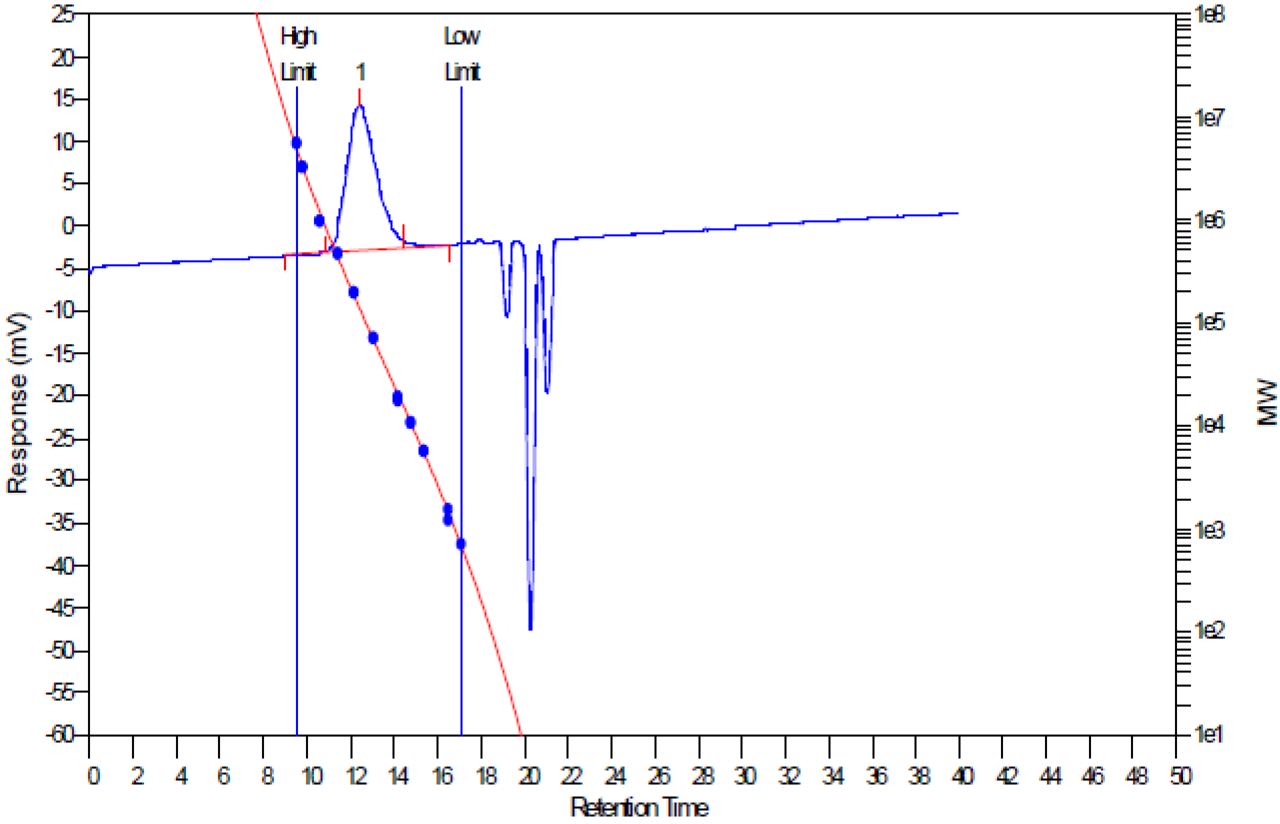

Figure S52. GPC curve of PS from run 5 of **Table 1.**

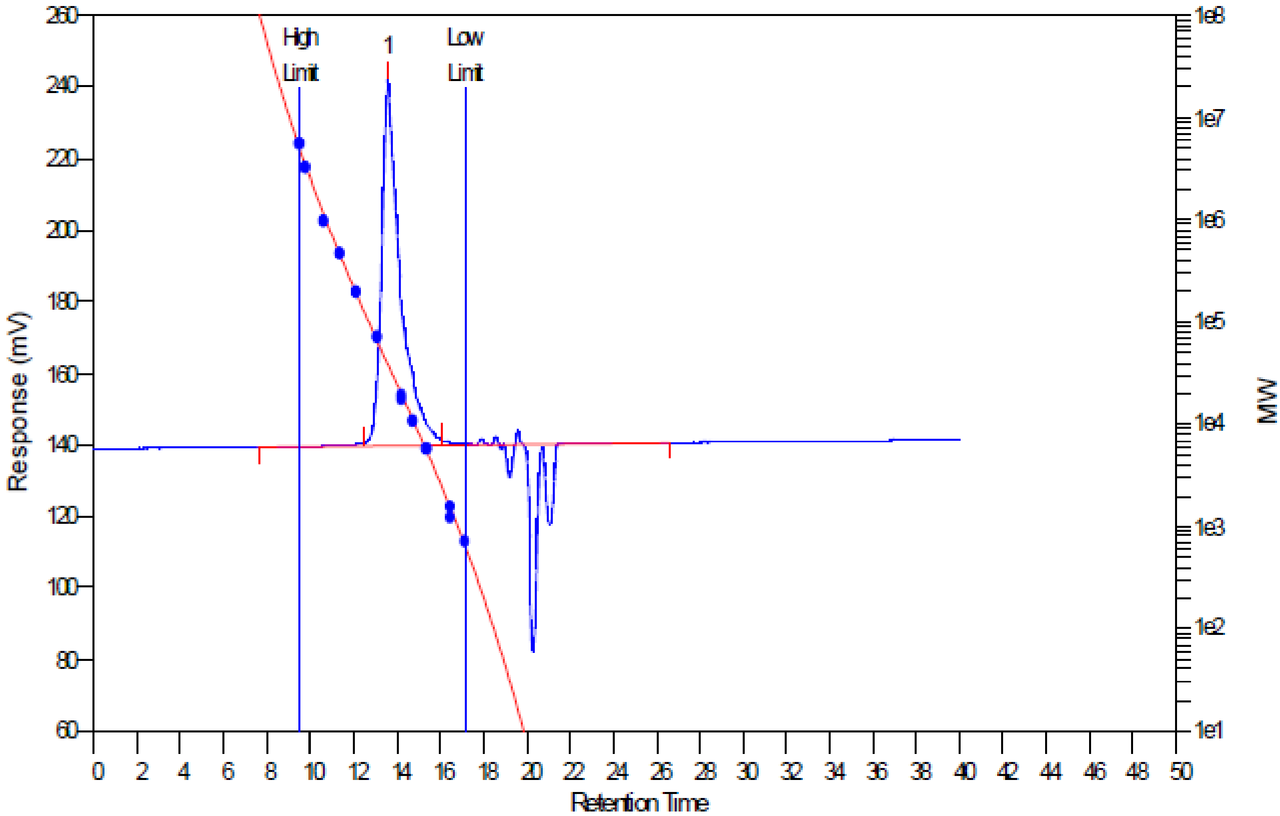

Figure S53. GPC curve of PI from run 8 of **Table 1.**

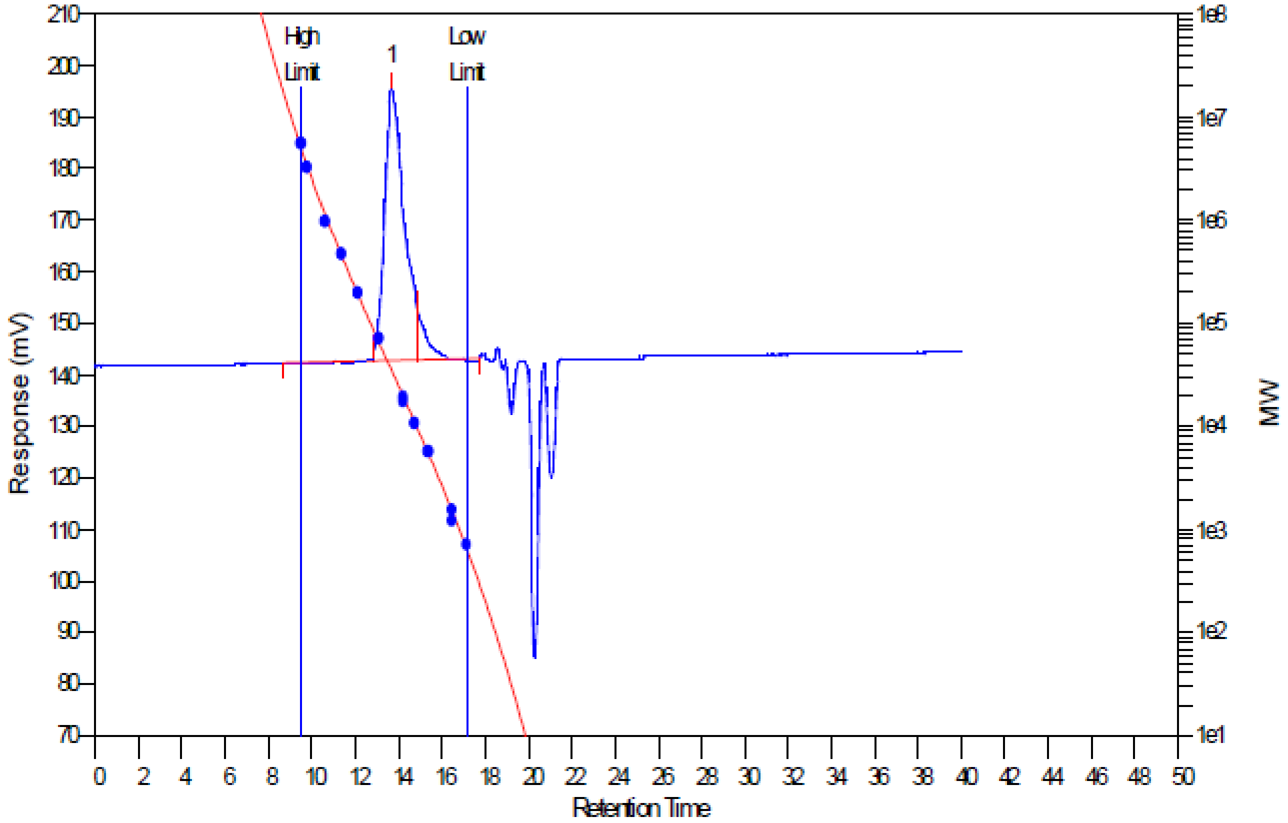

Figure S54. GPC curve of PI from run 9 of **Table 1.**

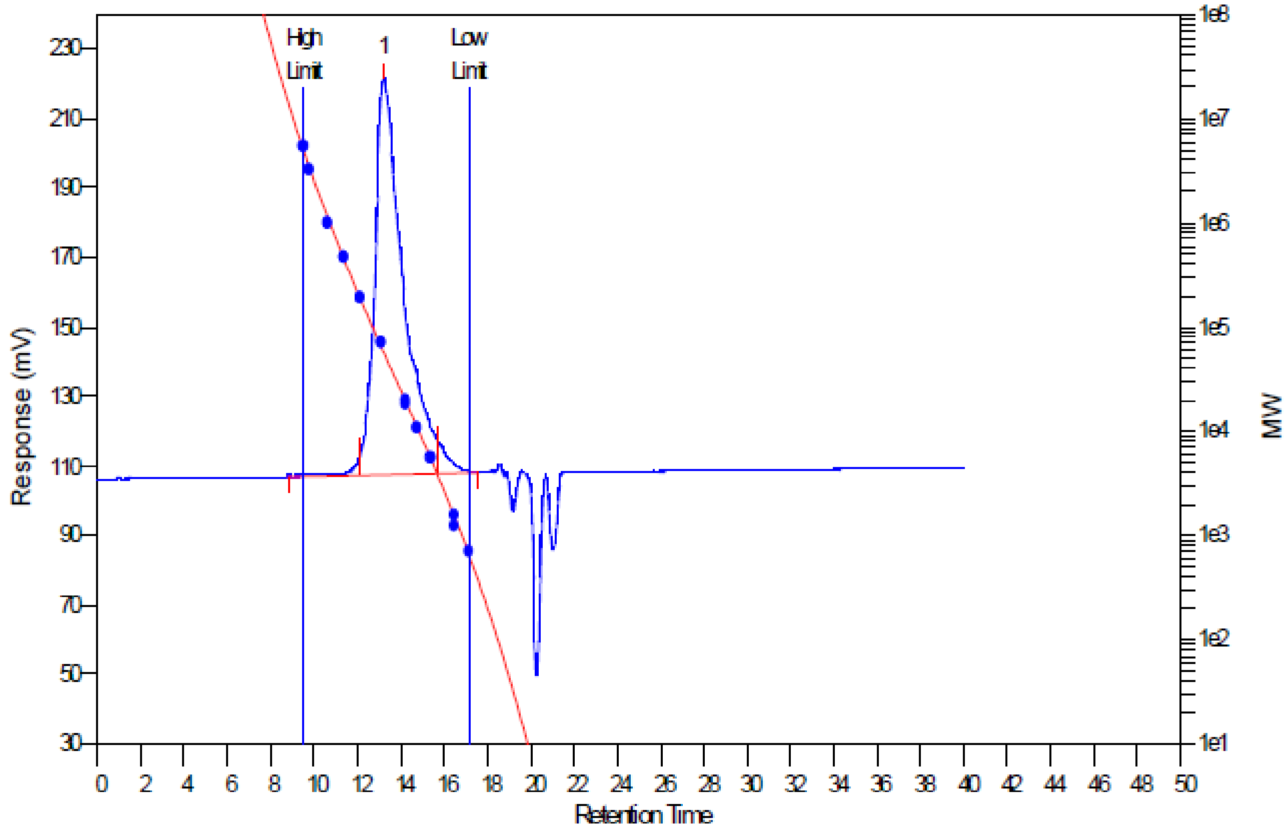

Figure S55. GPC curve of PMS from run 10 of **Table 2.**

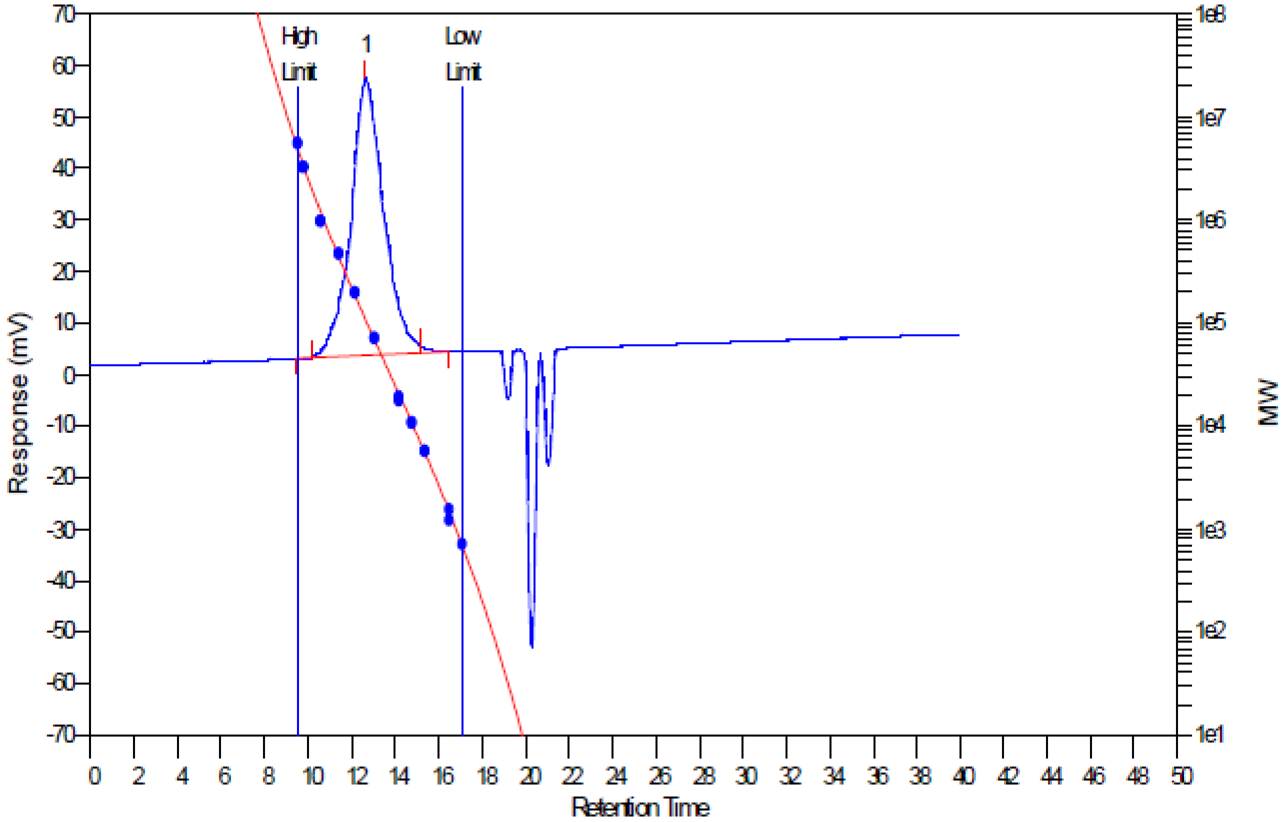

Figure S56. GPC curve of PMS from run 12 of **Table 2.**

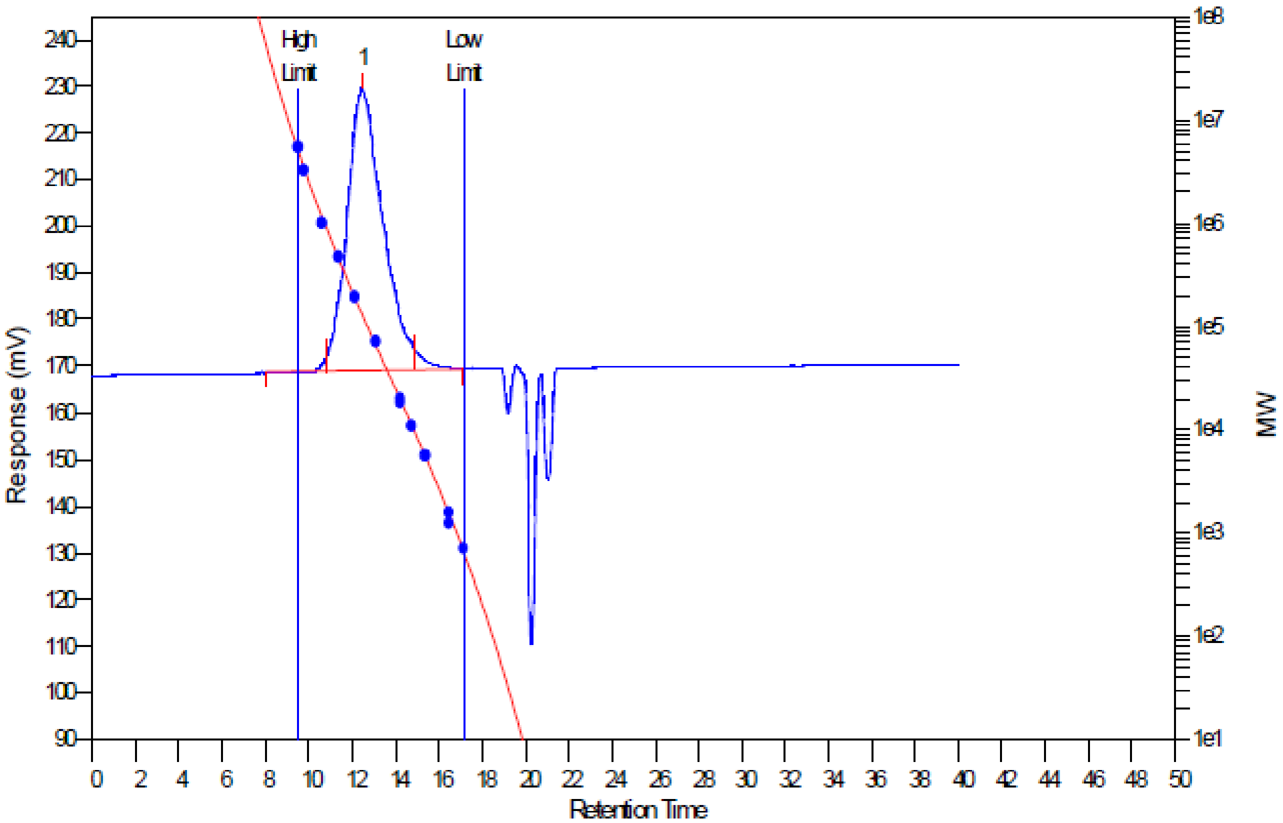

Figure S57. GPC curve of PMS from run 13 of **Table 2.**

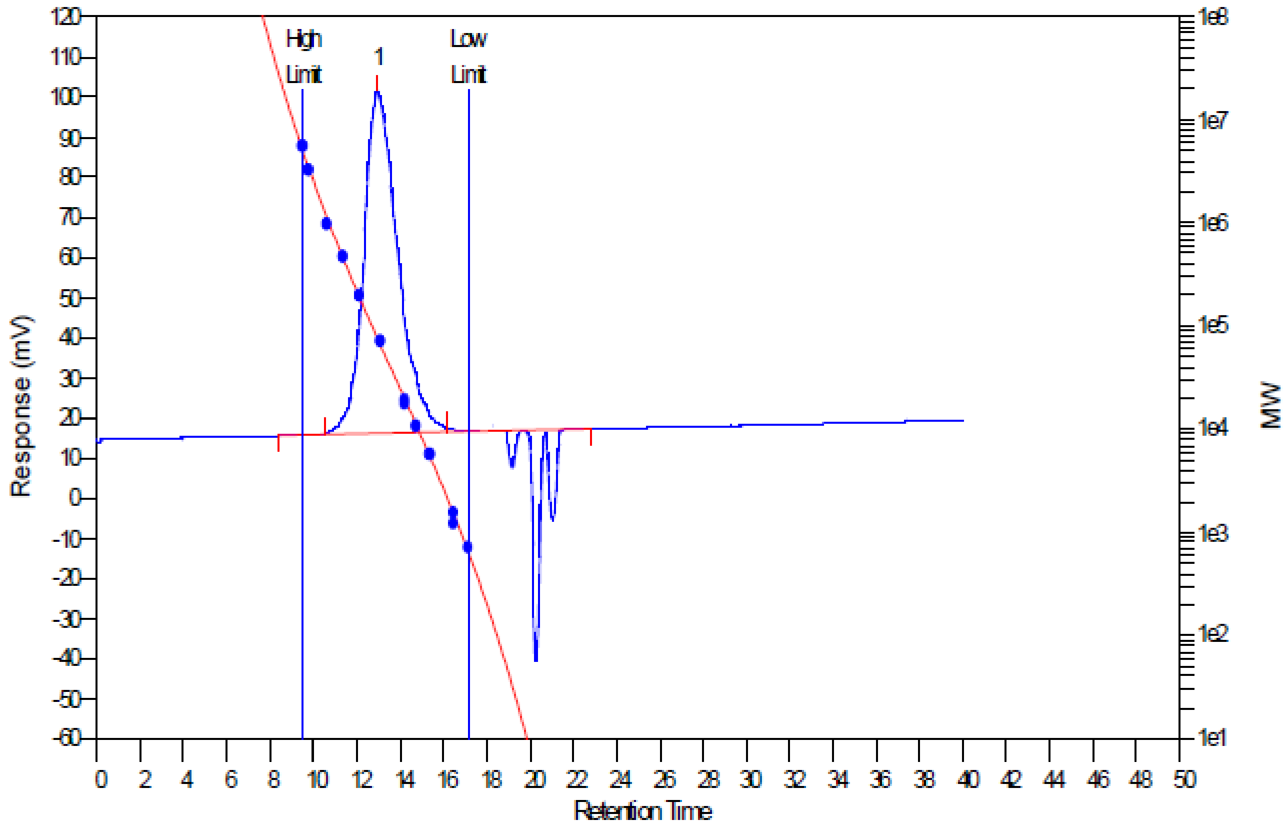

Figure S58. GPC curve of PMI from run 16 of **Table 2.**

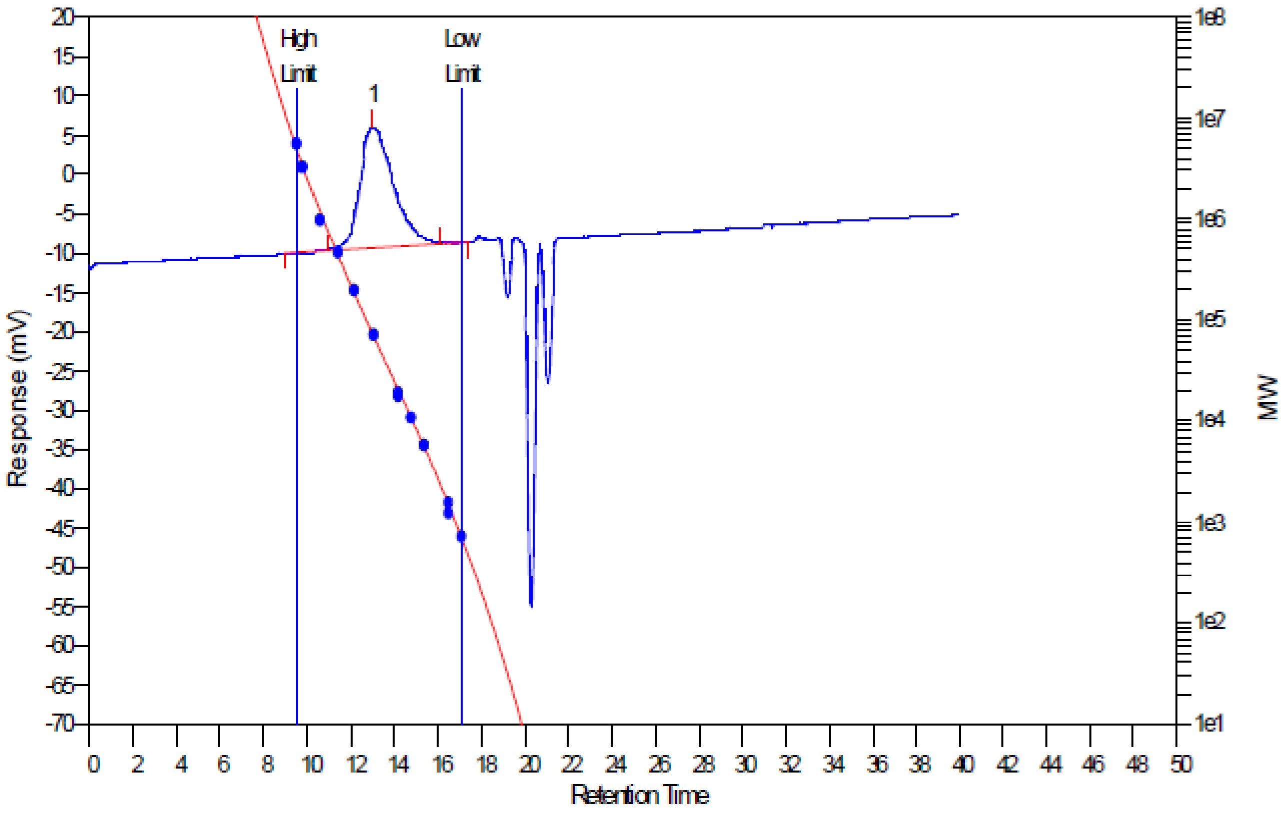

Figure S59. GPC curve of PMI from run 17 of **Table 2.**

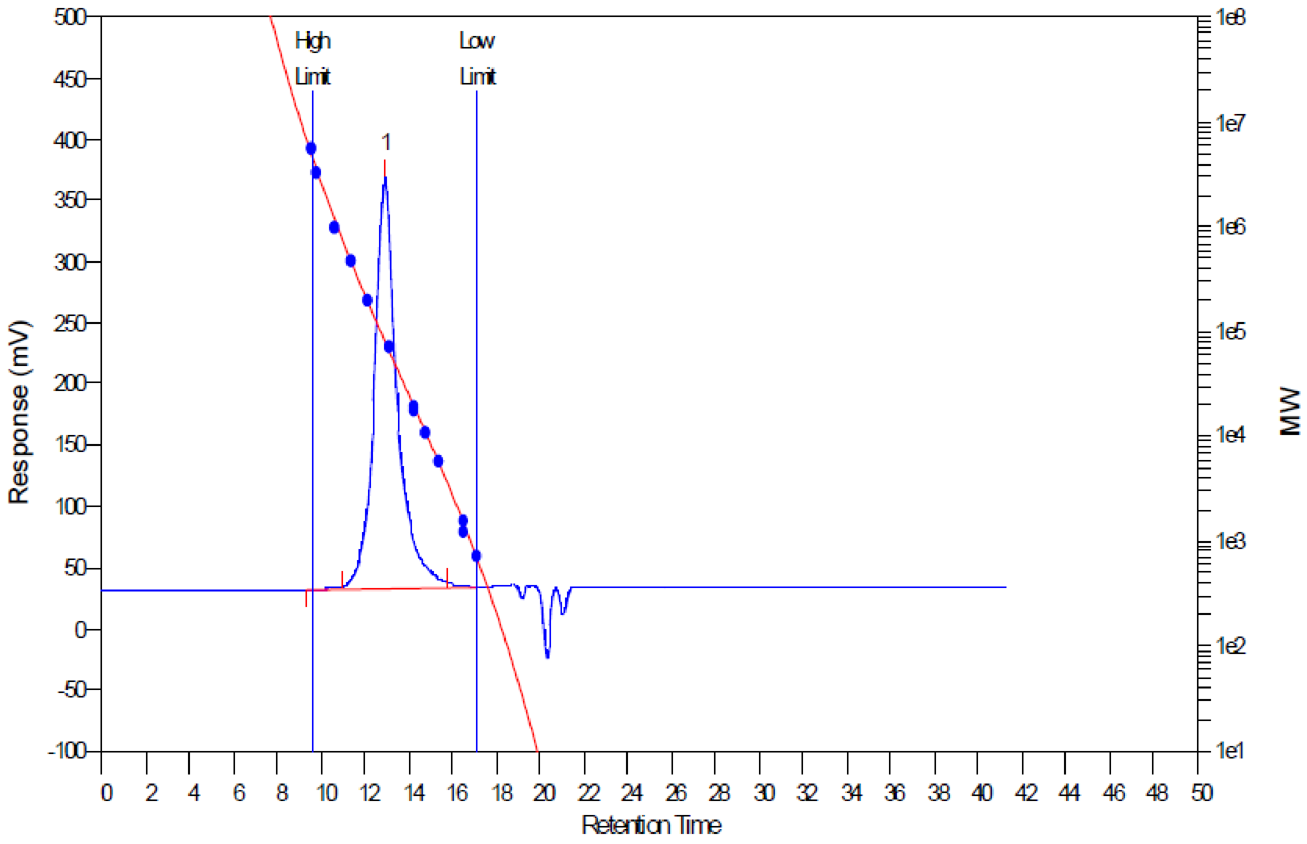

Figure S60. GPC curve of PMSI from run 20 of **Table 2.**

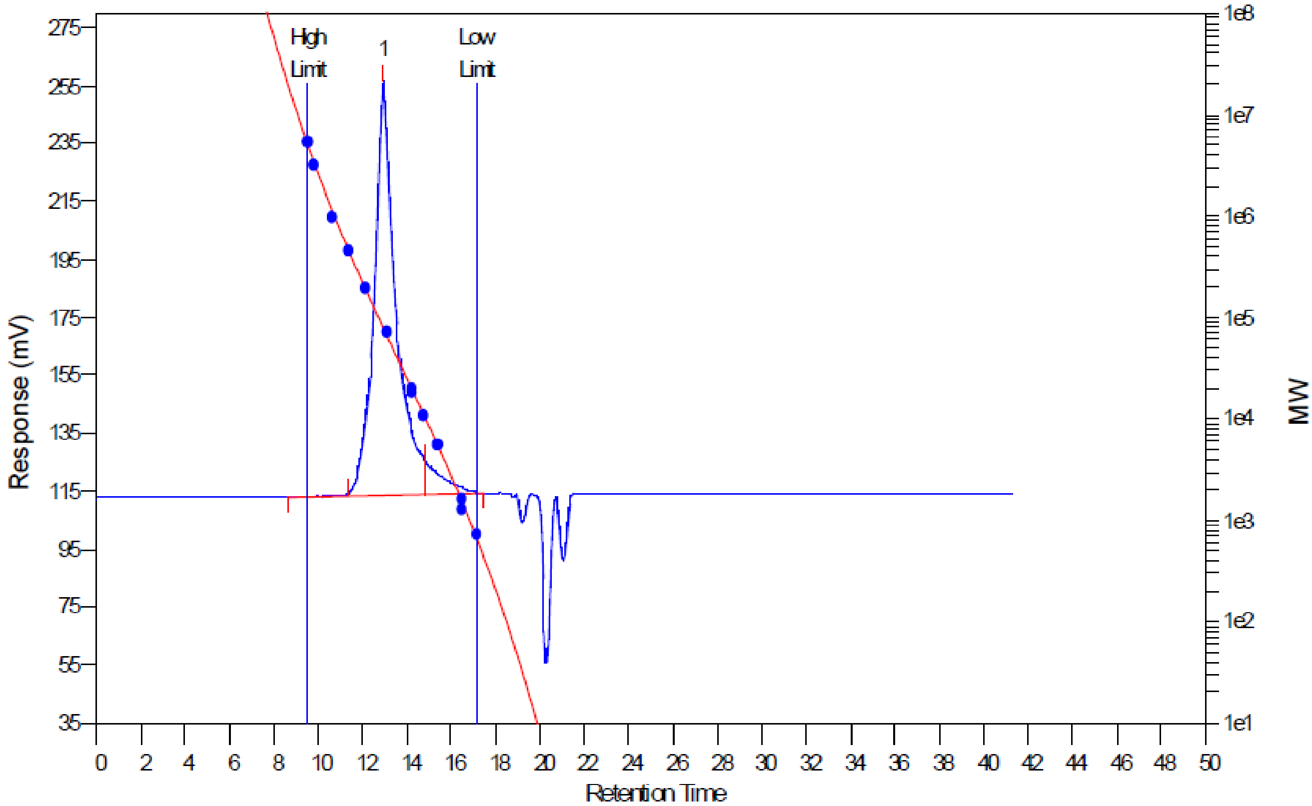

Figure S61. GPC curve of diblock PMS from run 21 of **Table 2.**

7. CAM Analysis

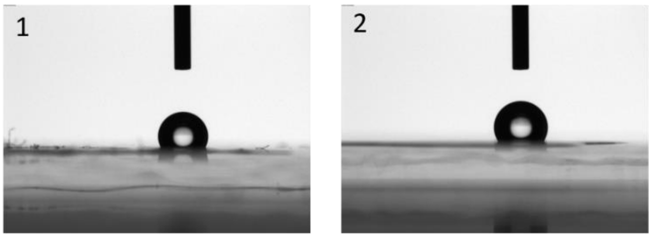

The CAM profiles of PI From run 7 Table 1

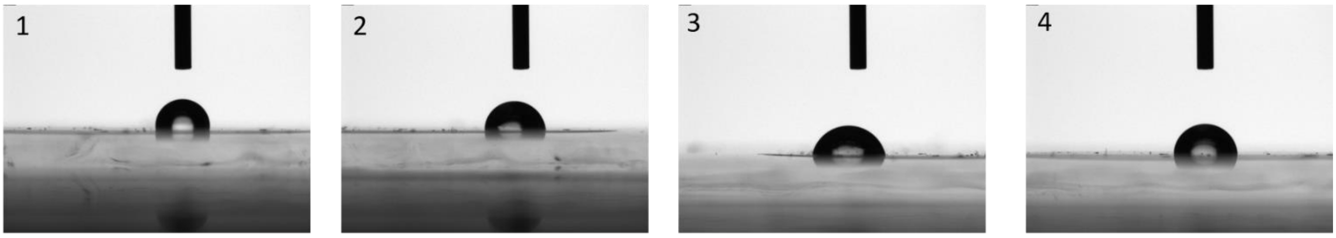

The CAM profiles of PMS From run 14 Table 2

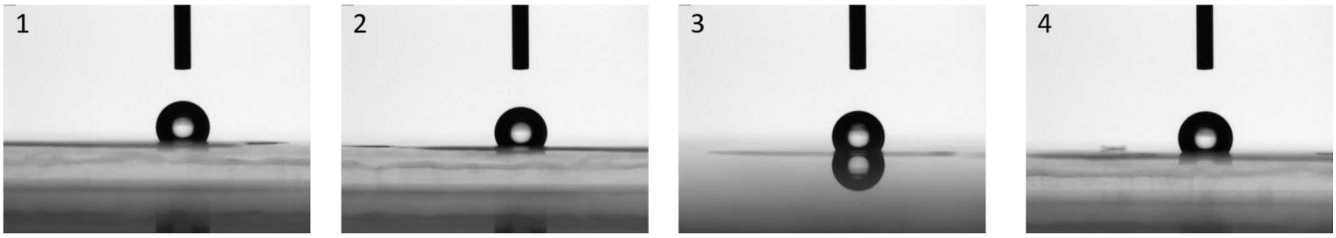

The CAM profiles of PMI From run 17 Table 2

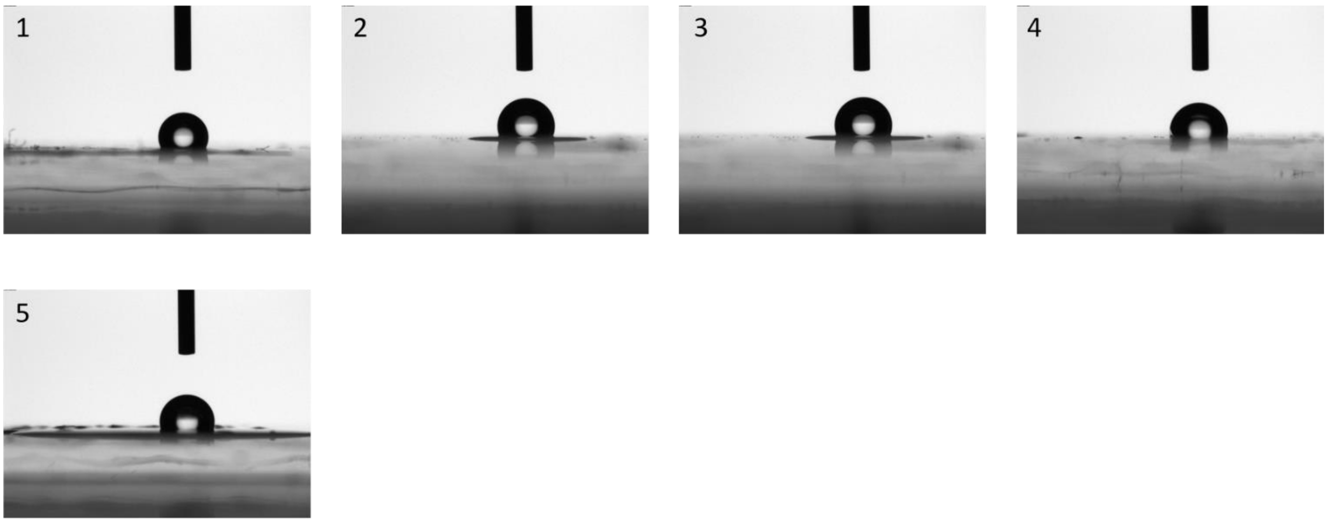

The CAM profiles of PMI From run 19 Table 2

Table T7 – Contact angles for tested samples

Sample	ϴ left	ϴ right	Contact angle
Run 7	114,5	115,6	115,05
"	116,1	112,4	114,25
Run7			**114,85**
Run 14	84,3	84,7	84,5
"	84,1	92,1	88,1
"	77,1	77,8	77,45
"	82,9	86,6	84,75
Run 14			**83,7**
Run 17	125,6	125,8	125,7
"	121	120,2	120,6
"	121,4	120,7	121,05
"	120,8	121,3	121,05
Run 17			**122,1**
Run 19	118,9	120,1	119,5
"	113,7	109,2	111,45
"	108	102	105
"	101,2	110,5	105,85
"	110,8	106,7	108,75
Run 19			**110,11**

8. SEM Analysis

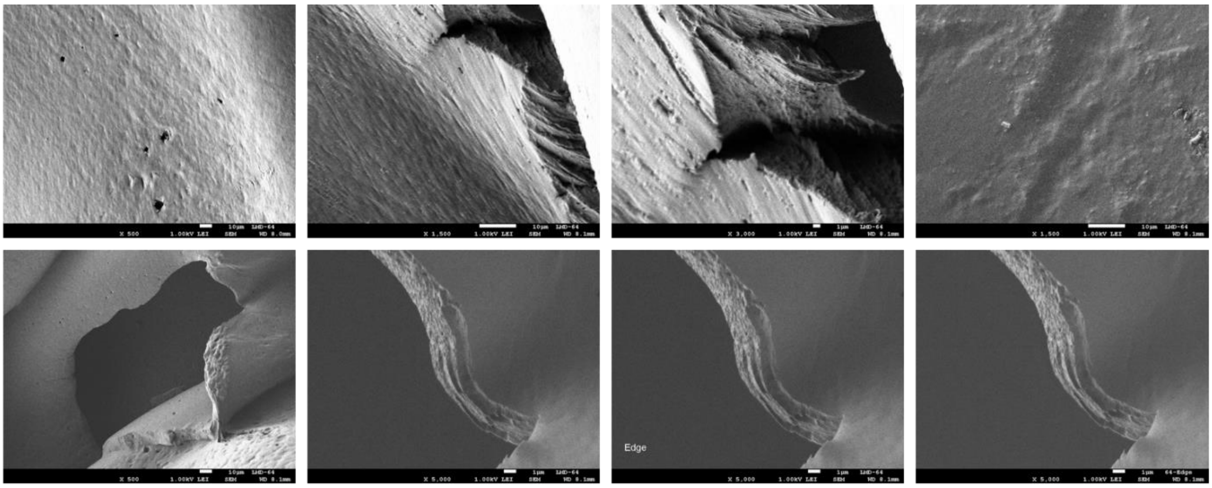

SEM image of PMS from run 14 Table 2

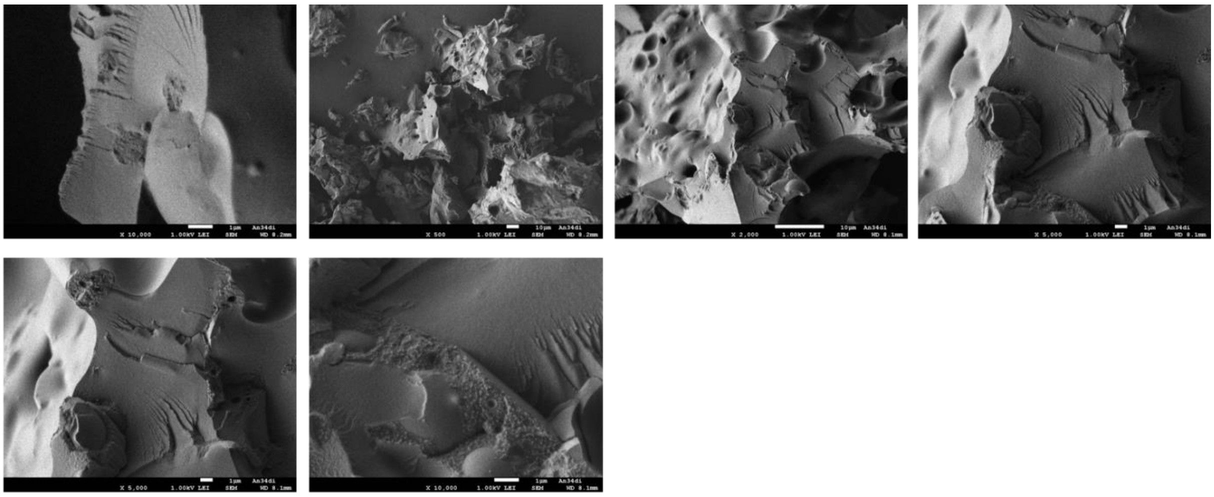

SEM image of PMS from run 21 Table 2

9. Kinetic studies

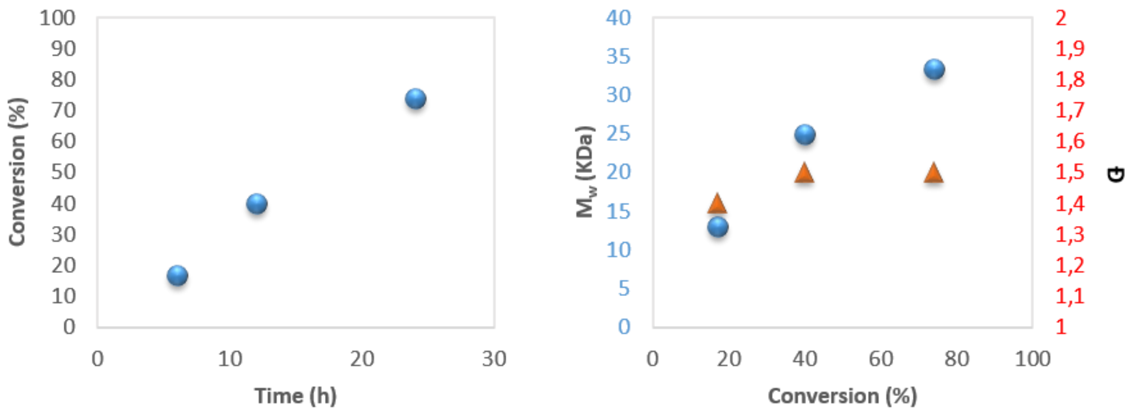

Figure S61. Conversion vs. time plot for isoprene polymerization (on left); plots of M_W (and Đ) vs conversion (on right)

Same experimental conditions of run 7 of **Table 1** (except for time)

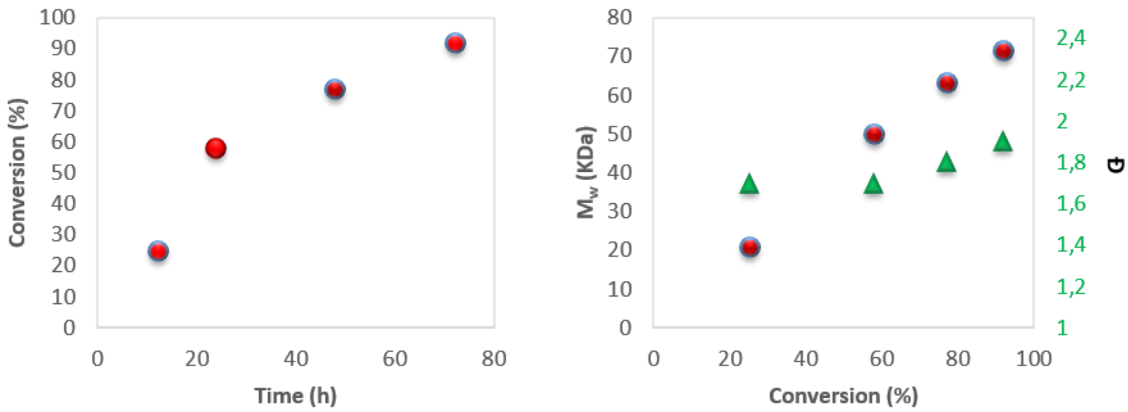

Figure S62. Conversion vs. time plot for myrcene polymerization (on left); plots of M_W (and Đ) vs conversion (on right)

Same experimental conditions of run 1 of **Table 1** (except for time)

10. References

1 M. I. Hulnik, I. V. Vasilenko, A. V. Radchenko, F. Peruch, F. Ganachaud and S. V. Kostjuk, Polym. Chem., 2018, 9, 5690–5700.
2 M. Naddeo, A. Buonerba, E. Luciano, A. Grassi, A. Proto and C. Capacchione, Polymer, 2017, 131, 151–159.
3 X. Jia, X. Zhang and D. Gong, J. Polym. Sci. Part A: Polym. Chem., 2018, 56, 2286–2293.
4 W. Li, J. Zhao, X. Zhang and D. Gong, Ind. Eng. Chem. Res., 2019, 58, 2792–2800.
5 P. Sarkar and A. K. Bhowmick, ACS Sustainable Chem. Eng., 2016, 4, 5462–5474.
6 C. Zhou, Z. Wei, X. Lei and Y. Li, RSC Adv., 2016, 6, 63508–63514.

11. Author Contributions

Conceptualization, M.W., C.C., and D.H.L.; Methodology, M.W. and D.H.L.; Investigation, D.H.L., M.K.; Resources, M.W., C.C.; Data Curation, D.H.L.; Writing—Original Draft Preparation, D.H.L.; Writing—Review and Editing, M.W., C.C., and D.H.L.; Funding Acquisition, M.W., C.C.